Stony Brook University

The role of POFUT2 in gastrulation and axis elongation of the mouse embryo

A Thesis Presented

by

Brian Benz

to

The Graduate School

in Partial Fulfillment of the

Requirements

for the Degree of

Master of Science

in

Biochemistry and Cell Biology

Stony Brook University

December 2015

Stony Brook University

The Graduate School

Brian Benz

We, the thesis committee for the above candidate for the

Master of Science degree, hereby recommend

acceptance of this thesis.

Bernadette C. Holdener – Thesis Advisor
Associate Professor, Biochemistry and Cell Biology

Robert S. Haltiwanger – Second Reader
Adjunct Professor, Biochemistry and Cell Biology

This thesis is accepted by the Graduate School

Charles Taber
Dean of the Graduate School

Abstract of the Thesis

The role of POFUT2 in gastrulation and axis elongation of the mouse embryo

by

Brian Benz

Master of Science

in

Biochemistry and Cell Biology

Stony Brook University

2015

Protein *O*-fucosyltransferase 2 (POFUT2) elongates Thrombospondin Type 1 Repeats (TSR) with an *O*-linked fucose. Forty-nine potential proteins are modified by POFUT2 in the endoplasmic reticulum. Nearly half the POFUT2 targets belong to the A Disintegrin and Metalloprotease with ThromboSpondin type-1 motifs (ADAMTS) or ADAMTS-like family of proteins. One of POFUT2's target proteins, ADAMTS9, contains 15 TSRs and is reported to be embryonic lethal around the same time as our *Pofut2 LoxP* mutants. In this study, we compared the *Pofut2* and *Adamts9* knockout phenotypes and used tissue specific deletion of *Pofut2* to define the role of *Pofut2* during gastrulation. Knockout of *Pofut2* using either the *LoxP* or *RST434* allele, as well as *Adamts9* knockout resulted in a disorganized epithelia, compressed visceral and parietal endoderm, and reduction of mesoderm production during gastrulation. *Adamts9* was expressed in the trophoblast giant cells, the parietal endoderm, a ring of proximal visceral endoderm near the ectoplacental cone, and the anterior primitive streak. To determine whether gastrulation defects in *Pofut2* mutants resulted from abnormalities in the epiblast or from defects in the extra-embryonic tissues, we used *Sox2::Cre* to delete of *Pofut2* in the epiblast. In contrast to the *Pofut2* knockout, *Sox2::Cre Pofut2* epiblast mutants formed mesoderm demonstrating the necessity of POFUT2 function in the extra-embryonic tissues for gastrulation. A shortened axis in the epiblast mutants implied a function of POFUT2 in the epiblast for axial elongation as well. Given the similarity between the *Adamts9* and *Pofut2* knockout phenotypes, and the expression of *Adamts9* in the extra-embryonic tissues, we propose that the gastrulation defects in the *Pofut2* knockout results from a defect in ADAMTS9 function in the trophoblast, parietal endoderm, or proximal visceral endoderm. Similarly, we propose that defects in axis elongation in the *Pofut2* epiblast mutants could result from disruption of ADAMTS9 function in the anterior primitive streak.

Dedication Page

To my family, thank you for the years of support as I continued my education.

Table of Contents

Supplemental Material

List of Figures

List of Tables

List of Abbreviations

POFUT2	Protein *O*-fucosyltransferase
TSR	Thrombospondin Type-1 Repeat
GDP	Guanidine Di-phosphate
ER	Endoplasmic Reticulum
ECM	Extracellular matrix
B3GLCT	β3-glucoslytransferase
ES	Embryonic stem
EMT	Epithelial to mesenchymal
H&E	Hematoxylin and eosin
DVE	Distal visceral endoderm
AVE	Anterior visceral endoderm
ADAMTS	A Disintegrin and Metalloprotease with Thrombospondin Type 1 Repeats
ADAMTSL	ADAMTS-like
CCN	named for its members Cyr61, CTGF, and Nov
BAI	Brain-specific Angiogenesis Inhibitor
MABT	Malic acid buffer with tween
NTMT	Alkaline Phosphate buffer
µL	Microliter
NBT	nitro blue tetrazolium
BCIP	5-bromo-4-choloro-3-indolyl-phosphate
mL	Milliliter
PFA	paraformaldehyde
ºC	Degrees Celsius
bp	Base pairs
PCR	Polymerase Chain Reaction
RT-PCR	Reverse Transcriptase PCR
RNA	Ribonucleic Acid
DNA	Deoxyribonucleic acid
PBS	Phosphate buffered saline
TBE	Tris/ Borate/ EDTA buffer
mV	Millivolts

Acknowledgments

Thank you to Dr. Bernadette Holdener and Dr. Robert Haltiwanger for your guidance and patience over the past year and giving me the opportunity to learn and grow as a scientist in your labs. Thank you to Richard Grady and Megumi Takeuchi for your instruction and support in the lab, teaching me the techniques and providing assistance in the project throughout my time in the lab. I would also like to acknowledge Rich for his maintenance of the mouse colonies and Megumi for her work with the *Adamts9* project. I would like to thank the rest of the Haltiwanger lab for their support as well, including Michael Schneider for showing me the cell culture procedures. Lastly I would like to acknowledge Dr. Neta Dean for her guidance and support as director of the Biochemistry and Cell Biology Master's program.

Chapter 1

Introduction

POFUT2 and its function in early mouse embryogenesis

Protein *O*-fucosyltransferase 2 (POFUT2) is the enzyme responsible for addition of fucose to a serine or threonine residue within a Thrombospondin Type-1 Repeats (TSR). The POFUT2 protein transfers fucose from GDP-fucose to the serine or threonine in the consensus sequence (CXX(S/T)CXXG) located within the properly folded TSR (Figure 1) (Luo et al., 2006; Vasudevan and Haltiwanger, 2014). The TSR is a sixty amino acid motif with a distinct conformation formed by six conserved cysteine residues forming three disulfide bonds (Luther and Haltiwanger, 2009). *O*-fucosylation functions as a quality control mechanism in the endoplasmic reticulum (ER), where POFUT2 only recognizes and modifies properly folded TSRs. In cell culture, siRNA silencing of *Pofut2* blocks secretion of several POFUT2 targets (Luther and Haltiwanger, 2009; Vasudevan et al., 2015). POFUT2 has approximately fifty target proteins (based on database searches with the above consensus sequence) that are localized to the cell surface or secreted into the extracellular matrix (ECM) (Figure 4) (Du et al., 2010; Vasudevan and Haltiwanger, 2014).

The fucosylated TSR becomes the target of another enzyme β3-glucoslytransferase (B3GLCT) that elongates the fucose with an *O*-linked glucose (Kozma et al., 2006). Mutations of the *B3GLCT* gene in humans is the cause of a rare autosomal recessive genetic disorder, Peter's Plus Syndrome (Aliferis et al., 2010; Lesnik Oberstein et al., 2006). The hallmarks of this disease include Peter's anomaly of the eye, mental delay, and short stature. Other less common phenotypes may also

manifest; including a cleft palate, broad neck and prominent forehead (Maillette de Buy Wenniger-Prick and Hennekam, 2002). As with *POFUT2,* the silencing of the *B3GLCT* gene in culture results in defects in secretion of target proteins; however, defects are not as severe (Vasudevan et al., 2015).

In early mouse development, POFUT2 is important in the formation of the three distinct germ layers of the mouse during gastrulation (Du et al., 2010). The *Pofut2 RST434* gene-trap insertion (Figure 2) results in a non-functional allele, demonstrated by a 50% reduction in POFUT2 activity in lysates of heterozygous ES cells, thereby generating a tool for understanding the role of *Pofut2* in mouse embryogenesis. In homozygous *Pofut2 RST434* gene-trap mutants, enhanced epithelial to mesenchymal transition (EMT) was observed in H&E (hematoxylin and eosin) stained sections of the embryos as evidenced by the expansion of mesodermal markers detected by *in situ* hybridization. We hypothesized that signaling from the extra-embryonic ectoderm, required for EMT, was also enhanced during gastrulation in the *Pofut2 RST434* mutants. Loss of *Pofut2* in gene-trap embryos results in embryonic lethality before embryonic day (E) 10.5 (Du et al., 2010). Presumably, this lethality is due to loss of function of one or more POFUT2 targets.

Events during early mouse development affected by POFUT2

Pofut2 RST434 mutants significantly increased EMT, expanding mesoderm formation during gastrulation (Du et al., 2010). The formation of three distinct germ layers—ectoderm, mesoderm, and endoderm—begins with the onset of gastrulation at embryonic day (E) 6.5 (Arnold and Robertson, 2009; Lim and Thiery, 2012). Prior to gastrulation, the extra-embryonic ectoderm develops at the proximal end of the egg

cylinder and the epiblast is located adjacent to this tissue at the distal end. The visceral endoderm forms a layer surrounding these tissues (Figure 3) (Arnold and Robertson, 2009; Lu et al., 2001).

Reciprocal signaling between the epiblast and extra-embryonic tissues drives the formation of the anterior-posterior axis. *Nodal* expression in the epiblast drives the expression of *Bmp4* in the extra-embryonic ectoderm. BMP4 signaling the extra-embryonic ectoderm adjacent to the epiblast will enhance *Wnt3* expression, further enhancing the expression of *Nodal* in the epiblast. This positive feedback signaling loop establishes a gradient of *Nodal* expression in the epiblast, decreasing toward the distal tip (Arnold and Robertson, 2009; Beck et al., 2002; Robertson et al., 2003). As a result of the gradient of *Nodal* expression, the distal visceral endoderm (DVE) forms at the distal tip of the embryo. The DVE will then migrate to the anterior, and be termed the anterior visceral endoderm (AVE). The AVE is an important signaling center specifying the anterior cell fate through the signals DKK1, LEFTY and CERBERUS which inhibit BMP4, NODAL, and WNT3 signals. The primitive streak forms in the posterior epiblast opposite the AVE (Arnold and Robertson, 2009).

The mesodermal and endodermal contributions to the embryo are derived from the primitive streak during gastrulation. The primitive streak extends toward the distal tip before regressing as gastrulation proceeds. Positioning and time of ingression through the streak plays an important role in the fate of the mesodermal precursors. In the anterior primitive streak, mesodermal precursors contributes to the lateral plate mesoderm, paraxial mesoderm, and heart and cranial mesoderm in mid streak stage embryos (Kinder et al., 1999). Migrating mesoderm from the posterior primitive streak

gives rise to the extra-embryonic mesoderm and allantois. This mesoderm will migrate from the posterior toward the anterior, displacing the extra-embryonic ectoderm in the proximal direction to form the exocoelomic cavity (Pereira et al., 2011).

Late in gastrulation, the node forms at the anterior end of the primitive streak. Indicated by an indentation at the distal tip, the node is comprised of two adjacent layers of columnar epithelia. Cells of the ventral side of the node each contain primary cilia (Sulik et al., 1994). The node is important in specification of the axial mesendoderm and the definitive endoderm that will eventually become part of the notochord and gut endothelium. These layers of mesoderm and endoderm ultimately displace the visceral endoderm that surrounds the epiblast tissue. The cilia of the node generates a leftward flow of signaling giving rise to the left/right patterning of the embryo (Beddington and Robertson, 1999).

POFUT2 targets and functions of those targets

POFUT2 is predicted to modify approximately fifty targets, including members of the ADAMTS (A Disintegrin and Metalloprotease with Thrombospondin Type 1 Repeats) and ADAMTS-like family, the CCN (named for its members Cyr61, CTGF, and Nov) family, the BAI (Brain-specific Angiogenesis Inhibitor) family, and several other proteins that interact with the ECM (Figure 4). The CCN family of proteins interacts with ECM components for cell adhesion and migration. Adhesion is mediated through interactions with fibronectin and heparin. These proteins can also interact with integrins and growth factors, playing a role in cell signaling (Holbourn et al., 2008). The BAI family of proteins are G-protein coupled receptors that regulate signaling cascades within the cell and have anti-angiogenic functions (Cork and Van Meir, 2011). All ADAMTS and

ADMATS-like family members are secreted into the extracellular matrix where they function. The ADAMTS's are a family of proteases that cleave collagen, aggrecan, and versican. One exception is ADAMTS13, which is the von Willebrand Factor protease (Apte, 2004). Proteoglycans, such as versican, can complex with hyaluronic acids and link to other components of the ECM such as fibronectin and signaling molecules. Cleavage of versican by several ADAMTS's plays an important role in development of limb and cardiac tissues. (Nandadasa et al., 2014) Several ADAMTS's have known developmental effects. The *gon-1* gene in *C.elegans*, an orthologue of ADAMTS, plays a role in cell migration (Blelloch et al., 1999b). ADAMTS9 is a *gon-1* orthologue and *Adamts9* homozygous mutants are embryonic lethal around the same time as *Pofut2* mutants (Enomoto et al., 2010) suggesting that ADAMTS9 may be a major target of POFUT2 during mouse embryogenesis.

Goals of this Project

Our study focused on the role of *Pofut2* in mouse embryonic development. Previously, our lab looked at the *Pofut2 RST434* gene-trap allele which increased mesoderm formation during gastrulation, leading to embryonic lethality. We generated a new mouse *Pofut2* knockout allele and addressed the question that the *RST434* gene-trap and the *LoxP* knockout were identical. In our study, we demonstrated that the *Pofut2 LoxP* allele and the *Pofut2 RST434* allele were identical in elimination of POFUT2 function. Our next goal was to understand which target of POFUT2 was responsible for the *Pofut2* phenotype. Comparing *Pofut2 LoxP* mutants and *Adamts9* null mutants, we determined that ADAMTS9 function, dependent on POFUT2 *O*-fucosylation, was responsible for the defects in gastrulation. Lastly, we determined that

Adamts9 was expressed in the extra-embryonic tissues and questioned what role of POFUT2 in the extra-embryonic tissues. Using epiblast conditional mutants, we demonstrated that POFUT2 in the extra-embryonic tissues rescued gastrulation defects but presented defects in axial elongation. This study gives a greater insight as to the importance of *O*-fucosylation and ECM interactions in mouse development.

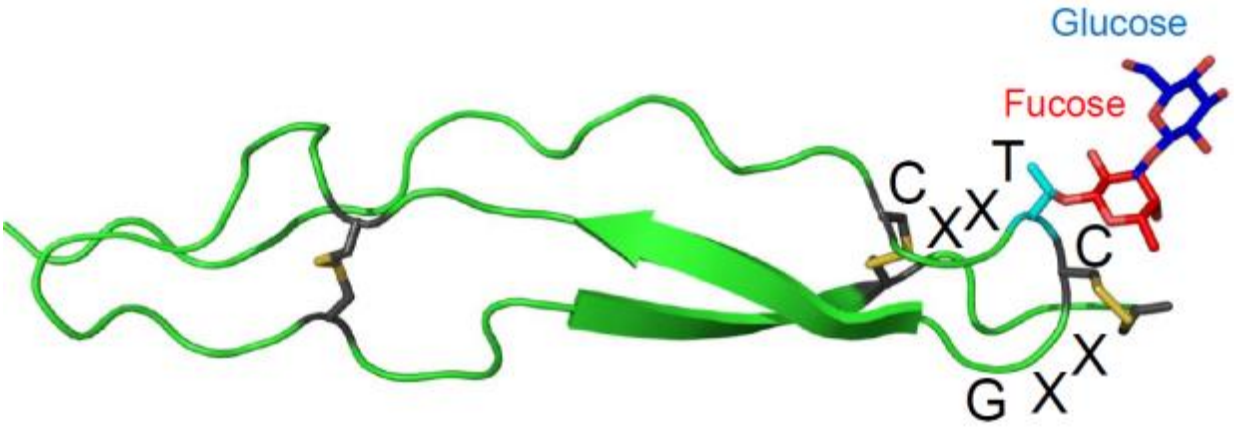

Figure 1: Consensus Sequence of TSR
The properly folded TSR (green) contains 3 disulfide bonds (grey). The Threonine residue (light blue) is modified with an *O*-linked fucose (red) by POFUT2 and glucose (blue) by B3GLCT. (Tan et al., 2002) modified by Christina Melief-Leonard using Sweet software provided by www.glycosciences.de.

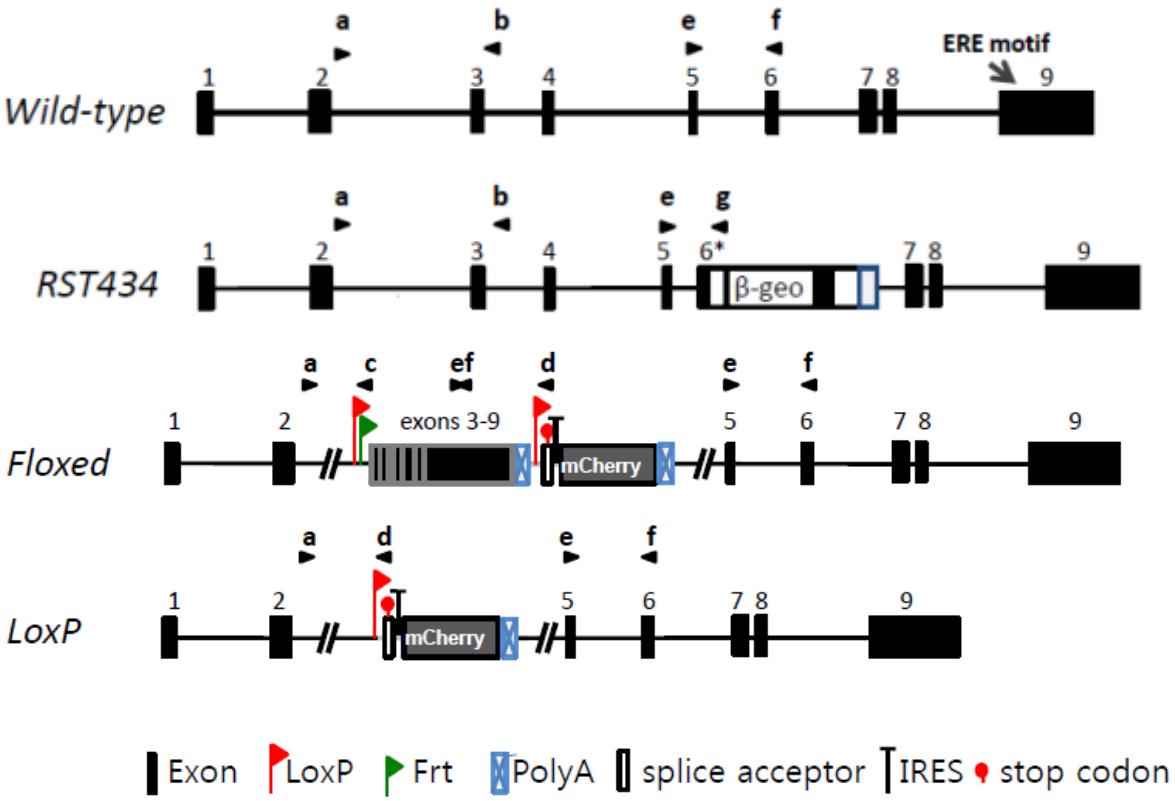

Figure 2: *Pofut2* alleles and primer sites
The *Pofut2* wild-type allele contained 9 exons and the ERE motif was found within exon 9. The *Pofut2 RST434* allele had the β-geo gene-trap inserted into exon 6 of the *Pofut2* allele. The *Pofut2 Floxed* allele had *LoxP* sites flanking the cDNA of exons 3-9 between exon2 and a mCherry construct. The *Pofut2 LoxP* allele had a stop codon after exon 2 was followed by mCherry. Wild-type allele determined by ensemble, *RST434* allele (Du et al., 2010), *Floxed* and *LoxP* allele –unpublished data from B. Holdener and R. Haltiwanger.

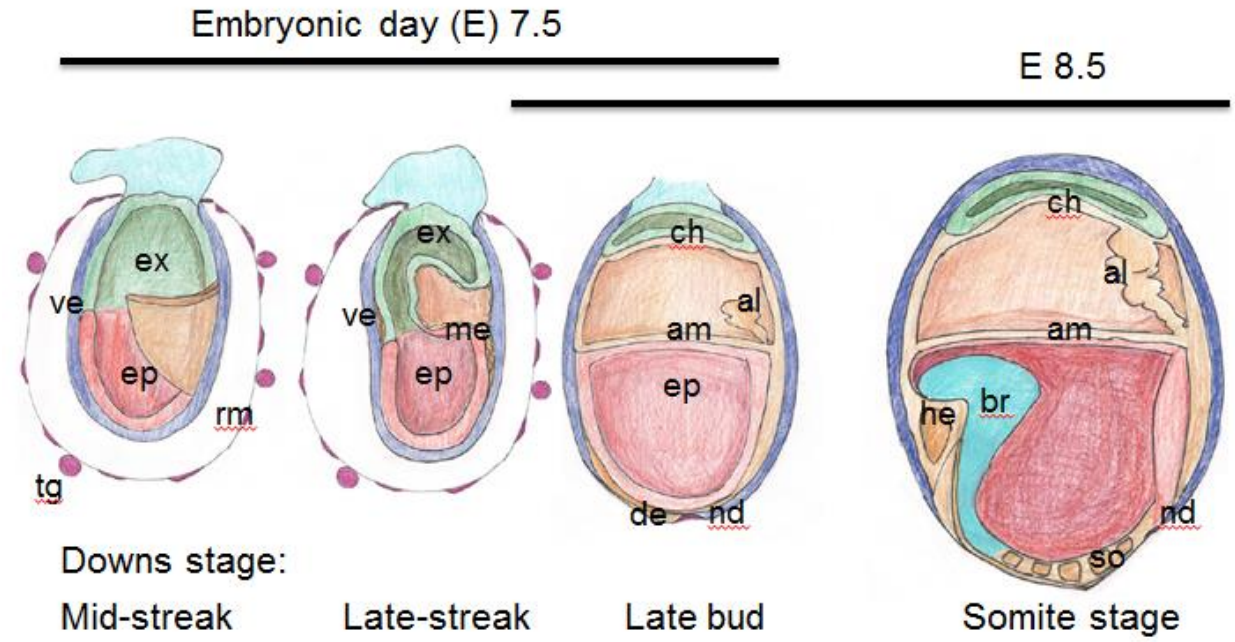

Figure 3: Development of the mouse embryo during gastrulation
In the mid-streak stage embryo (Early E 7.5), gastrulation is underway and the wings of mesoderm form in the posterior epiblast (ep) migrate toward the anterior in between the epiblast and the visceral endoderm (ve). By the late-streak stage (E 7.5), mesoderm from the posterior primitive streak displaces the extra-embryonic ectoderm toward the proximal end creating the extra-embryonic membranes (lateral wings not shown). In the late bud stage (late E 7.5), the extra-embryonic membranes have completely formed forming the exocoelom cavity. The amnion (am) consists of a layer of epiblast and mesoderm cells and the chorion (ch) is comprised of the extra-embryonic ectoderm and mesoderm cells. The allantois (al) forms in the posterior exocoelom cavity. In the distal tip of the embryo, a distinct population of cells forms the node (nd). The node is a signaling center that allows for the specification of definitive endoderm (de) which displaces the surround visceral endoderm. In the somite stage (E 8.5), the allantois has fused with the chorion. The primitive streak has regressed and the notochord has extended toward the anterior. The heart (he) and brain (br) have formed and somites are visible along the anterior posterior axis.
Proximal is up and anterior is left. Epiblast (ep), extra-embryonic ectoderm (ex), visceral endoderm (ve), Reichert's membrane (rm), trophoblast giant cells (tg), mesoderm (me), chorion (ch), amnion (am), node (nd), definitive endoderm (de),brain (br), heart (he), somites (so).
Gastrulation Development (Arnold and Robertson, 2009; Lim and Thiery, 2012)
Downs staging (Downs and Davies, 1993).

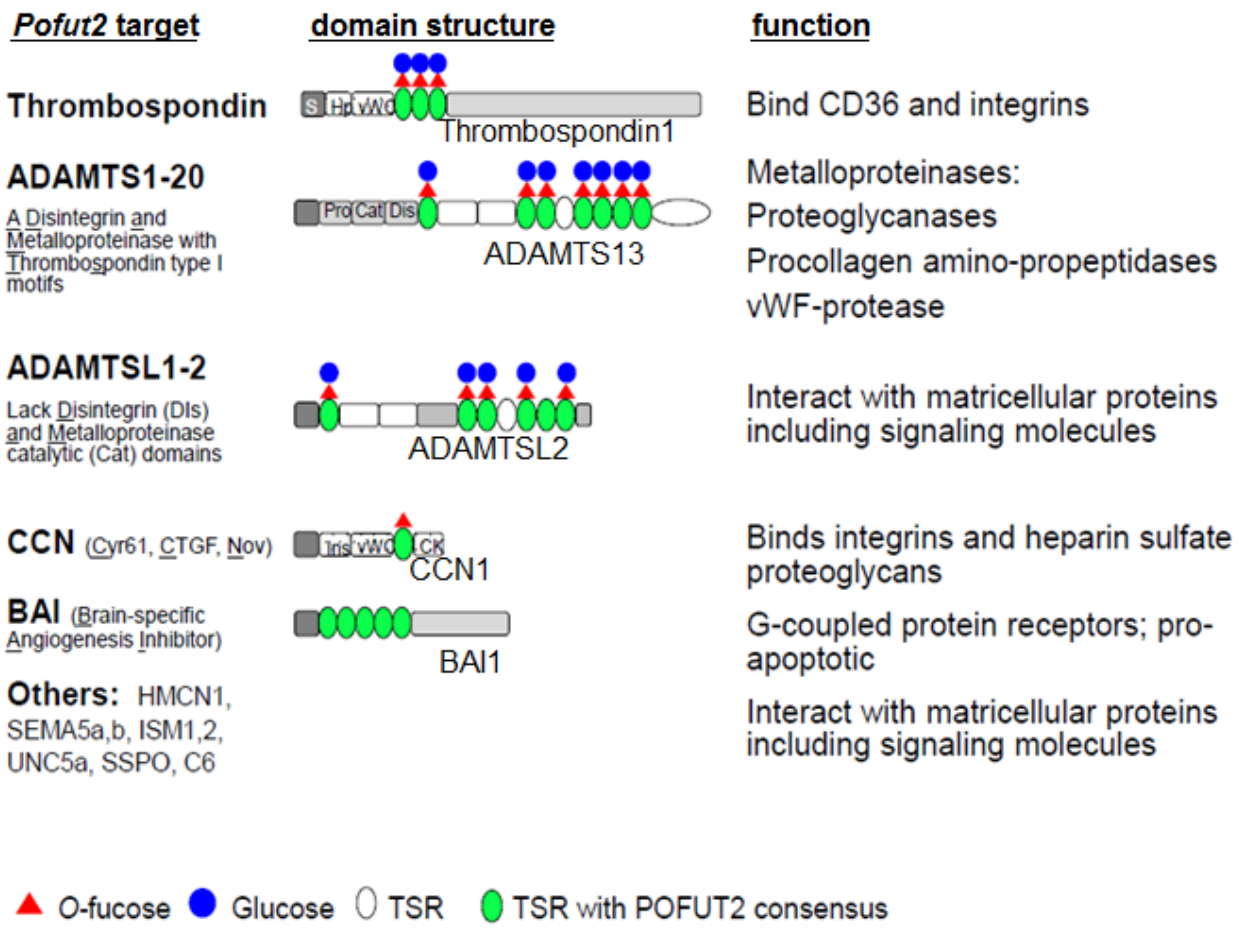

Figure 4: Potential Targets containing the TSR consensus sequence of POFUT2
A list of potential targets of POFUT2 that may lead to the defects seen in *Pofut2* null mutants. Fucose and glucose have been added to TSRs that were confirmed using mass spectrometry.
Pofut2 targets (Du et al., 2010)
Domain structures (Hofsteenge et al., 2001; Leonhard-Melief and Haltiwanger, 2010; Ricketts et al., 2007; Wang et al., 2007) (Leonhard-Melief et al., in preparation)
Functions (Cork and Van Meir, 2011; Dubail and Apte, 2015; Holbourn et al., 2008)

Chapter 2

Is the *Pofut2-LoxP* allele identical to the *Pofut2-RST434* allele?

Introduction

In previous work, disruption of the *Pofut2* gene using the *RST434* gene-trap allele eliminated POFUT2 function throughout the embryo, resulting in defects during gastrulation. The gene-trap inserted a lacZ-neomycin fusion sequence at the 3'-end of exon 6 in the mouse *Pofut2* gene (Figure 2). The resulting allele eliminated POFUT2 function through the removal an essential ERE motif required for activity with exon 9 (Chen et al., 2012; Du et al., 2010). Loss of function was confirmed using an enzyme assay that demonstrated that lysates of tissues from heterozygous animals had half of the POFUT2 activity found in tissues from the wild-type animals. Through a combination of approaches, it was demonstrated that mice homozygous for the *Pofut2 RST434* gene-trap expanded the production of mesoderm. Embryos homozygous for the gene-trap allele failed to survive past E 10.5 (Du et al., 2010).

We sought to further evaluate the *Pofut2* allele and understand what tissues require POFUT2 function during gastrulation. Using a conditional allele would allow us to disrupt the *Pofut2* allele in specific tissues; therefore a *Pofut2* conditional mutants was created with *LoxP* sites surrounding exons 2 and 5 (*Pofut2 Floxed*; Figure 2). In these initial experiments, we wanted to determine whether elimination of this region (to generate the *Pofut2 LoxP* allele; Figure 2) had the same phenotype as the *RST434* allele. If the *Pofut2 LoxP* and *RST434* alleles had similar phenotypes, then the alleles could be used in combination to generate tissue specific mutations.

Methods

Mating Strategy

Male and Female mice heterozygous for the *Pofut2 LoxP* allele were crossed and females checked daily for mating plugs indicating pregnancy. The male would then be removed from the cage and the female would be euthanized on the desired day of gestation. Female mice were euthanized according to IACUC protocol (#05401), by exposure to carbon dioxide for one minute before cervical spine dislocation. Embryos were then dissected in cold PBS with EGTA and isolated in 4% PFA.

Preparation of DIG-labeled RNA probe

Plasmid containing the probe of interest was linearized using the specific digestion enzyme. Using the kit (Life Technologies) transcription of the RNA was performed using RNA polymerase and DIG-UTP. The probe was then aliquoted for future use without further purification steps.

In situ hybridization

Mouse embryos were isolated and fixed in PFA before being dehydrated in methanol and stored in freezer for up to a month. The *in situ* procedure started by rehydrating the embryos before adding warm hybridization buffer along with 1:10-1:20 dilution of DIG labeled RNA probe (*Snail* 638ng/µL and *Bmp4* 1005ng/ µL and incubating at 65^{o}C overnight. The next day, embryos were thoroughly rinsed with washing solution and MABT before adding blocking reagent with 1/2000 to 1/5000 dilution of anti-DIG-AP and incubated at 4 degrees overnight. On the following day, the embryos are rinsed in

MABT all day while rotating. On the last day of the procedure, the embryos incubated with 1.5 mL NTMT + 6.75 µL NBT + 5.25 µL BCIP and rocked in the dark. The color developed within the day or was left to develop up to three days in the 4°C fridge. When color development had reached the desired intensity the embryos were fixed again in 4% PFA and transferred to an 80% glycerol plate for photography (Supplemental Protocol 2)

Photography

After *in situ* hybridization, embryos were transferred into 80% glycerol on a 1% agarose background. Embryos are then positioned under dissecting microscope (Zeiss Discovery.V8) with anterior end facing the bottom of the frame and the proximal end toward the left. Depending on embryo size, photographs were taken at 6.3x or 8x magnification using (AxioCam MRc) camera and AxioVisionLE program.

Genotyping

After *in situ*, embryos were rinsed in individual tubes with PBS before adding lysis buffer containing Proteinase K. Approximately 20 µL -60 µL of lysis buffer was used according to the size of the embryos being lysed. The embryos were incubated overnight to one week at 55 °C until completely lysed and no longer visible. The proteinase K was heat inactivated at 95 degrees for 10 minutes and the embryos stored indefinitely at -20 °C.

Genotyping of the *Pofut2 LoxP* allele was performed using polymerase chain reaction (PCR) to amplify the *LoxP* allele. The *Pofut2 LoxP* allele was amplified using the forward primer POFUT2CommonL2 (a) and the Pofut2LoxPL2 reverse (d) primer amplified a region of 689 base pair region of DNA. The *Pofut2* wild-type allele was

amplified using the forward primer POFUT2CommonL2 (a) and the reverse primer Pofut2WTR2 (b) which amplified a region of 823 base pairs (Figure 2, Supplemental Table 1, Supplemental Protocol 1).

Pofut2 RST434 was genotyped using a common forward primer MS45 (e) and the reverse primer MS89 (f) to amplify a 955bp region of wild-type DNA whereas the common forward primer MS45 (e) and the reverse primer RST434down2A (f) amplified a region of 1344 base pairs indicating the presence of the *RST434* allele (Figure 2, Supplemental Table 1, Supplemental Protocol 1).

RT-PCR

An alternative splice form of the *Pofut2 RST434* allele was evaluated using RT-PCR. RNA was isolated from a pool of 8 E 8.5 embryos from a *RST434*/+ and wild-type cross. The RNA isolation was carried out using the RNAquenous micro kit from Life Technologies and RT-PCR was performed using the SuperScript III One-Step RT-PCR System with Platinum Taq DNA Polymerase from Life Technologies. The first reaction used Pofut2Exon4CommonLeft (a') as the forward primer and Pofut2Exon8CommonRight (b') as the reverse primer. The *Pofut2* wild-type allele produces a band of 451 base pairs whereas the presence of an alternative splice, skipping the gene-trap in the mRNA product, would amplify a region of 325 base pairs. Confirming the presence of the gene-trap required the Pofut2Exon4CommonLeft primer and the Genetrapreverse (-) (d') primer which amplified a region of 452 base pairs in the *Pofut2 RST434* cDNA. Two positive controls, reactions 3 and 4, confirmed the RT-PCR protocol was working using *Gapdh* primers. One reaction used Gapdhforward1 and

Gapdhreverse1 which amplified a band of 377 bp while the other reaction used the previously reported Gapdhforward2 and Gapdhreverse2 primers to amplify a band of 452 bp. Lastly the function of the Gentrapreverse (-) primer was tested using the forward primer POFUT2Exon5forward (c') to amplify a band of 231 bp in genomic tail DNA (Figure 6; Supplemental Table 2).

Results

Bmp4 and *Snail* expression in *Pofut2 LoxP* mutants is absent in early gastrulation

Previously, expression of *Bmp4* in *RST434* embryos was significantly expanded at E 7.5. From examination of tissue slides, *RST434* mutants appeared to expand mesoderm production, while in the *LoxP* mutants, mesoderm was not present. The extra-embryonic ectoderm, which appeared disorganized in our mutants (Figure 9), is an important tissue in providing signaling to the epiblast and BMP4 is required to maintain reciprocal signaling of WNT3 and NODAL in the epiblast for the formation of mesoderm. Without this reciprocal signaling, EMT is disrupted during gastrulation (Arnold and Robertson, 2009). We hypothesized that loss of *Bmp4* expression in our *LoxP* mutants would have restricted mesoderm formation. *Snail* was used to indicate new mesoderm formation from the primitive streak in the gastrulating embryos (Lim and Thiery, 2012).

At embryonic day (E) 7.5, gastrulation was underway in *Pofut2* wild-type embryos (Figure 5A). These embryos had organized columnar epithelia in the epiblast and a defined extra-embryonic ectoderm. The visceral endoderm was visible around the outside of the epiblast and extra-embryonic tissues. *Bmp4* expression in wild-type embryos was visibly present in the extra-embryonic ectoderm adjacent to the epiblast. On the other hand, *Pofut2 LoxP* null mutants (Figure 5B) were considerably smaller than their wild-type or heterozygous counterparts. The proximal end of the embryo appeared to be pinched and an organized epiblast and extra-embryonic ectoderm are not visible in any of the *Pofut2 LoxP* null mutants. The *Pofut2 LoxP* homozygous mutant

(Figure 5B) failed to express *Bmp4* at high levels suggesting that tissue constriction resulted in the loss *Bmp4* expression.

The failure of embryos to express *Bmp4* suggested a loss of mesoderm formation. Using the marker, *Snail,* we examined the formation of mesoderm in our *LoxP* mutants. The *Pofut2* wild-type embryos (Figure 7 A) displayed robust *Snail* expression in the mesoderm migrating from the posterior toward the anterior of the embryo as well as expression in the trophoblast. The *LoxP* mutants (Figure 7B) failed to express *Snail* in the epiblast, indicating disrupted mesoderm formation

The phenotype of the *LoxP* mutants differed significantly from previously published data. The discrepancy in *Bmp4* and *Snail* expression between *LoxP* and *RST434* alleles lead us to examine the possibility of an alternative splice form of the *RST434* allele resulting in a partially functional protein.

An alternative splice of the *Pofut2 RST434* gene-trap allele is not formed

Previously published data suggested that the *Pofut2 RST434* gene-trap inactivated the *Pofut2* gene and expanded EMT during gastrulation of the embryo (Du et al., 2010). In contrast, our data (*Bmp4* and *Snail* expression; Figure 5 and 7) demonstrated that EMT was severely depleted in *Pofut2 LoxP* mutants, which was also believed to inactivate the *Pofut2* gene. We hypothesized that a possible alternative splice form of the *RST434* allele, skipping the gene-trap, may be present in the mutants maintaining partial POFUT2 activity.

Using pooled RNA from E 8.5 embryos obtained from an RST434 intercross, RT PCR was used to evaluate the presence of a possible alternative splice (Figure 6).

Reaction 1 amplified a region of embryonic cDNA made from RNA with primers in Exon 4 and Exon 8. These primers would amplify a band of 451 base pairs in the presence of wild-type mRNA, but would amplify a region of 325 base pairs in the case of an in frame alternative splice around the gene-trap from exon 5 to exon 7. The bands showed that no alternative splice was present in the lysate (Figure 6).

The second reaction confirmed the presence of the *RST434* allele amplifying a region of DNA 452 base pairs long using a primer in Exon 4 and within the gene-trap. Both Reaction 1 and Reaction 2 were sequenced to verify that the correct predicted regions were amplified using these primers (data not shown). Reactions 3 and 4 were *Gapdh* controls and Reaction 5 confirmed the ability of the *RST434* reverse primer to work in genomic tail DNA. We concluded that an alternative splice made by skipping the gene-trap and creating a possible functional protein was not present in embryos with the *RST434* allele (Figure 6 and Supplemental Figure 2). The absence of an alternative splice form of *RST434* prompted us to reevaluate the *RST434* allele.

Pofut2 is required for Epithelial to Mesenchymal Transition during gastrulation

The lack of *Bmp4* and *Snail* expression in our *LoxP* mutants differed from previously studied *RST434* mutants where these markers were expanded in the *RST434* mutants. Without supporting evidence of an alternative splice form of the *RST434* allele, we reexamined *Bmp4* and *Snail* expression in these mutants. Whole mount *RST434* mutant embryos (Figure 5D and 7D) resembled *LoxP* mutants with compressed epiblast and extra-embryonic tissues as compared to the wild-types (Figure 5C and 7C) from the same litter. As expected, wild-type embryos (Figure 5C)

maintained *Bmp4* expression in the extra-embryonic ectoderm. In the *RST434* mutants (Figure 5D) *Bmp4* expression was absent or depleted, similar to our *LoxP* mutants. Additionally, wild-type embryos (Figure 7C) had prominent *Snail* expression in the posterior embryo, marking the migrating mesoderm. Most of the *RST434* mutant embryos (Figure 7D) lacked *Snail* expression or *Snail* expression was significantly reduced. These data demonstrated these two mutant alleles resulted in loss of *Pofut2* function and disruption mesoderm formation during gastrulation.

Discussion

We demonstrated that the *Pofut2 LoxP* and *RST434* gene-trap allele both disrupt Pofut2 function within the embryo around the onset of gastrulation. At the point when the wild-type embryos begin to form mesoderm and have a clearly defined anterior-posterior axis, *Pofut2* null mutants were significantly compressed without any defined formation of mesoderm. Upon further evaluation of gene expression, *Bmp4* and *Snail* are either lost or significantly depleted in out *Pofut2* null mutants as compared to their wild-type counterparts.

The discrepancy between previously published data and the data we presented lead us to reevaluate the *Pofut2 RST434* allele. Previous data demonstrated that loss of POFUT2 function expanded *Bmp4* and *Snail* expression during gastrulation, increasing the amount of EMT occurring during gastrulation (Du et al., 2010). To address this discrepancy, we performed RT-PCR to eliminate the possibility of a functional alternative splice form of the protein. The *RST434* gene-trap was inserted within exon 6 and a possible splicing around the exon 6 splice site would produce an in frame shift of the protein. Our results indicated an alternative splice form was not formed. The difference between previously published data is likely caused by genetic background homogeneity with backcrossing the mice with wild-type strain of mice for more than 30 generations, suggesting the possibility that genetic modifiers influence the phenotype of these mutants. Therefore we concluded that the two alleles are likely identical in the elimination of POFUT2 function manifested in similar phenotypes.

Although our results clearly show that POFUT2 is essential for early development, they do not provide a mechanism as to why the enzyme is required. Several of POFUT2's targets include members of the ADAMTS family of metalloproteases which function in the ECM. ADAMTS9 is expressed in early embryogenesis and has been reported to be embryonic lethal around the same time as our *Pofut2 LoxP* mice (Enomoto et al., 2010). With 15 TSRs available for potential modification, ADAMTS9 is a likely POFUT2 target to cause the gastrulation defects in our *Pofut2 LoxP* and *RST434* mutants.

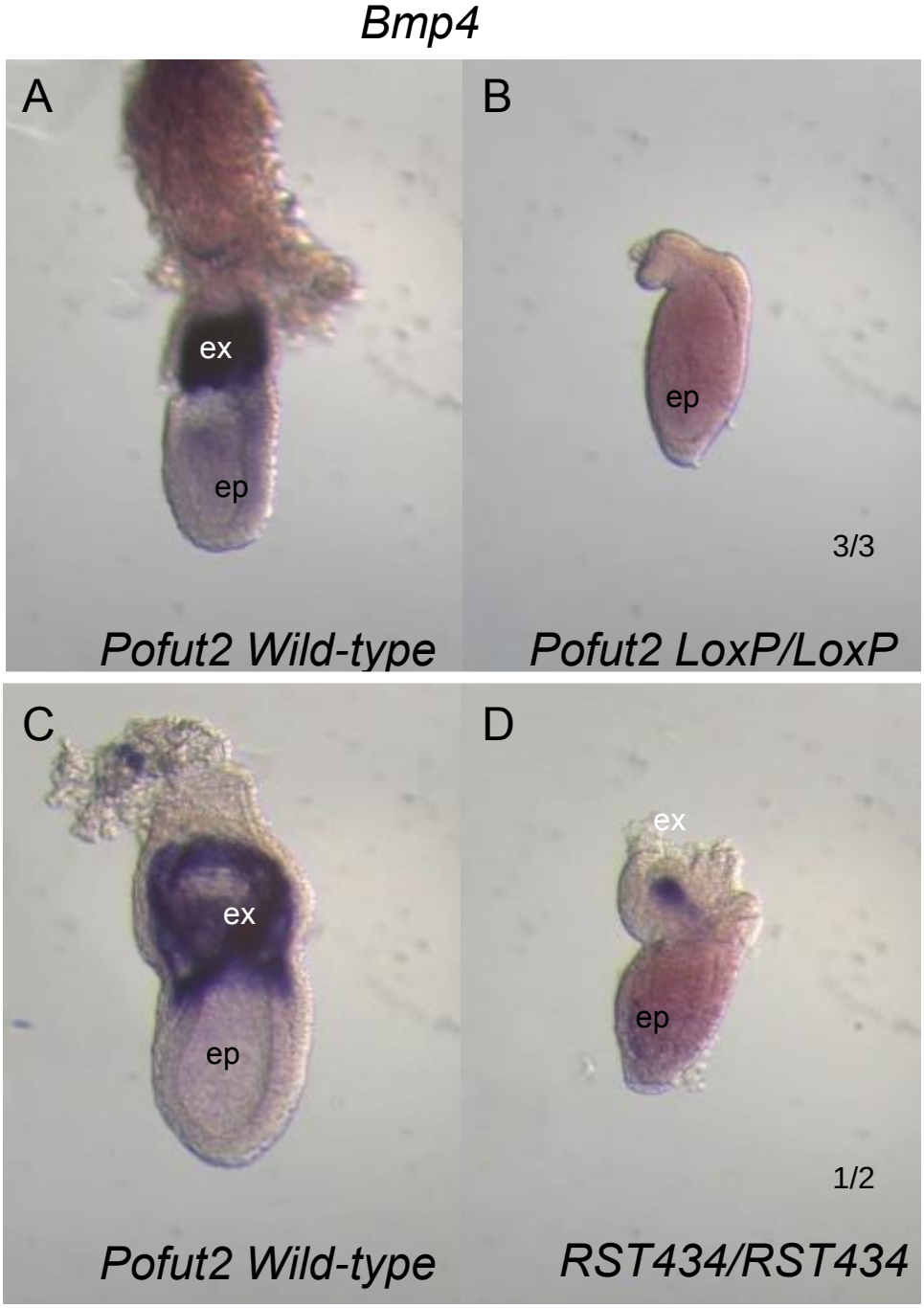

Figure 5: *Bmp4* is not expressed in *Pofut2 LoxP* mutants at E 7.5 during gastrulation. *Bmp4* expression in the extra-embryonic ectoderm is necessary for mesoderm induction from the primitive streak in the epiblast. (A*) Pofut2 LoxP* wild-type embryos have expression of *Bmp4* in the extra-embryonic ectoderm (ex) whereas (B) *Pofut2 LoxP* null embryos appear to lack extra-embryonic ectoderm and do not have expression of *Bmp4* at E 7.5. (C) *Pofut2 RST434* wild-type have similar expression to *LoxP* wild-type but in (D) *RST434* mutants is expressed at low levels in the *RST434* gene-trap mutants.

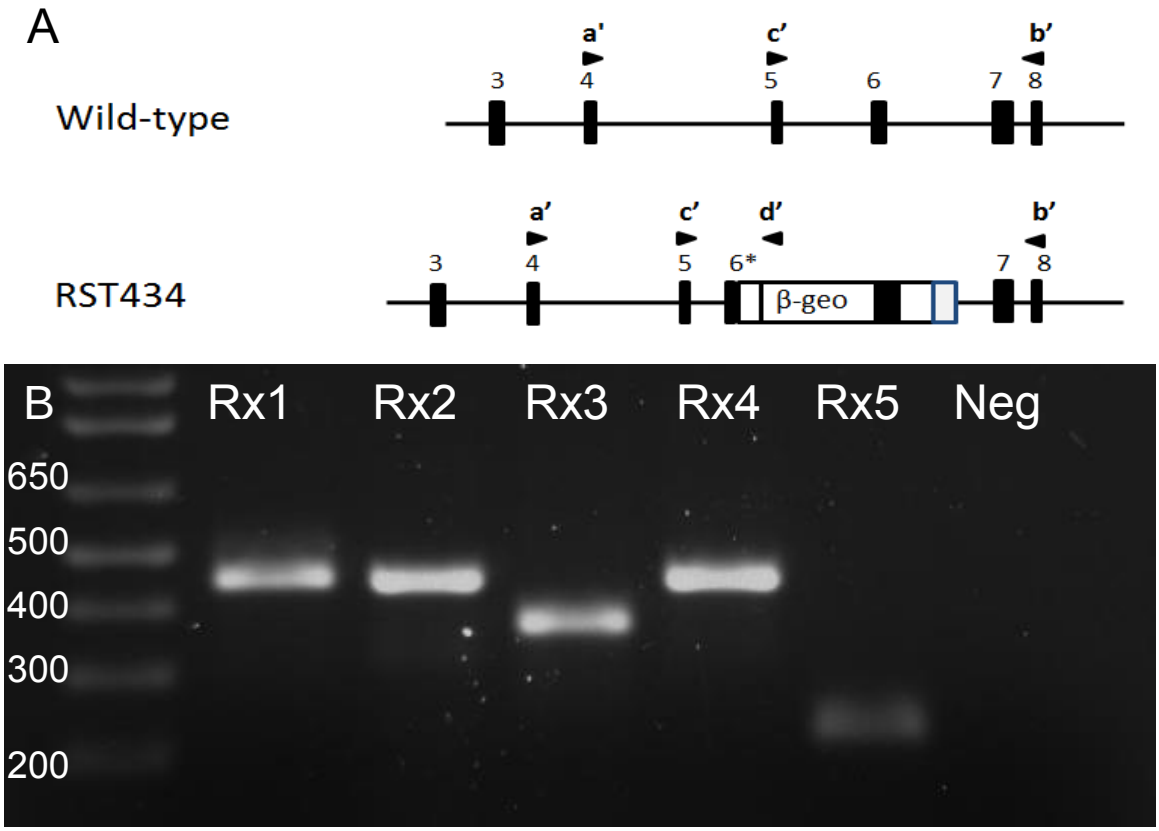

Figure 6: An alternative splice form skipping the gene-trap is not produced by *Pofut2 RST434* gene-trap. Using RT-PCR, we determined an alternative splice form of the *RST434* gene-trap was not present. (A) The first reaction used Pofut2Exon4CommonLeft (a') as the forward primer and Pofut2Exon8CommonRight (b') as the reverse primer. The *Pofut2* wild-type allele produces a band of 451 base pairs whereas the presence of an alternative splice, skipping the gene-trap in the mRNA product, would amplify a region of 325 base pairs. Confirming the presence of the gene-trap required the Pofut2Exon4CommonLeft primer and the Gene-trapreverse(-) (d') primer which amplified a region of 452 base pairs in the *Pofut2 RST434* cDNA. Two positive controls, reactions 3 and 4, confirmed the RT-PCR protocol was working using *Gapdh* primers. One reaction used Gapdhforward1 and Gapdhreverse1 which amplified a band of 377 bp while the other reaction used the previously reported Gapdhforward2 and Gapdhreverse2 primers to amplify a band of 452 bp. Lastly the function of the Gentrapreverse(-) primer was tested using the forward primer POFUT2Exon5forward (c') to amplify a band of 231 bp in genomic tail DNA (Supplementary Table 2) (B) RT-PCR of pooled embryos from Wild-type x *RST434*/+ litter does not identify an alternative splice of the *RST434* gene-trap allele. Reaction 1(Rx1) shows amplification of the spliced wild-type allele with the absence of any alternatively spliced band. Reaction 2 confirms the presence of the spliced *RST434* gene-trap allele. Reaction 3 and 4 are positive controls for GAPDH, while reaction 5 confirms the proper reverse primer used in Reaction 2 in the genomic DNA. The wild-type allele and *RST434* allele are represented with the respective primers.

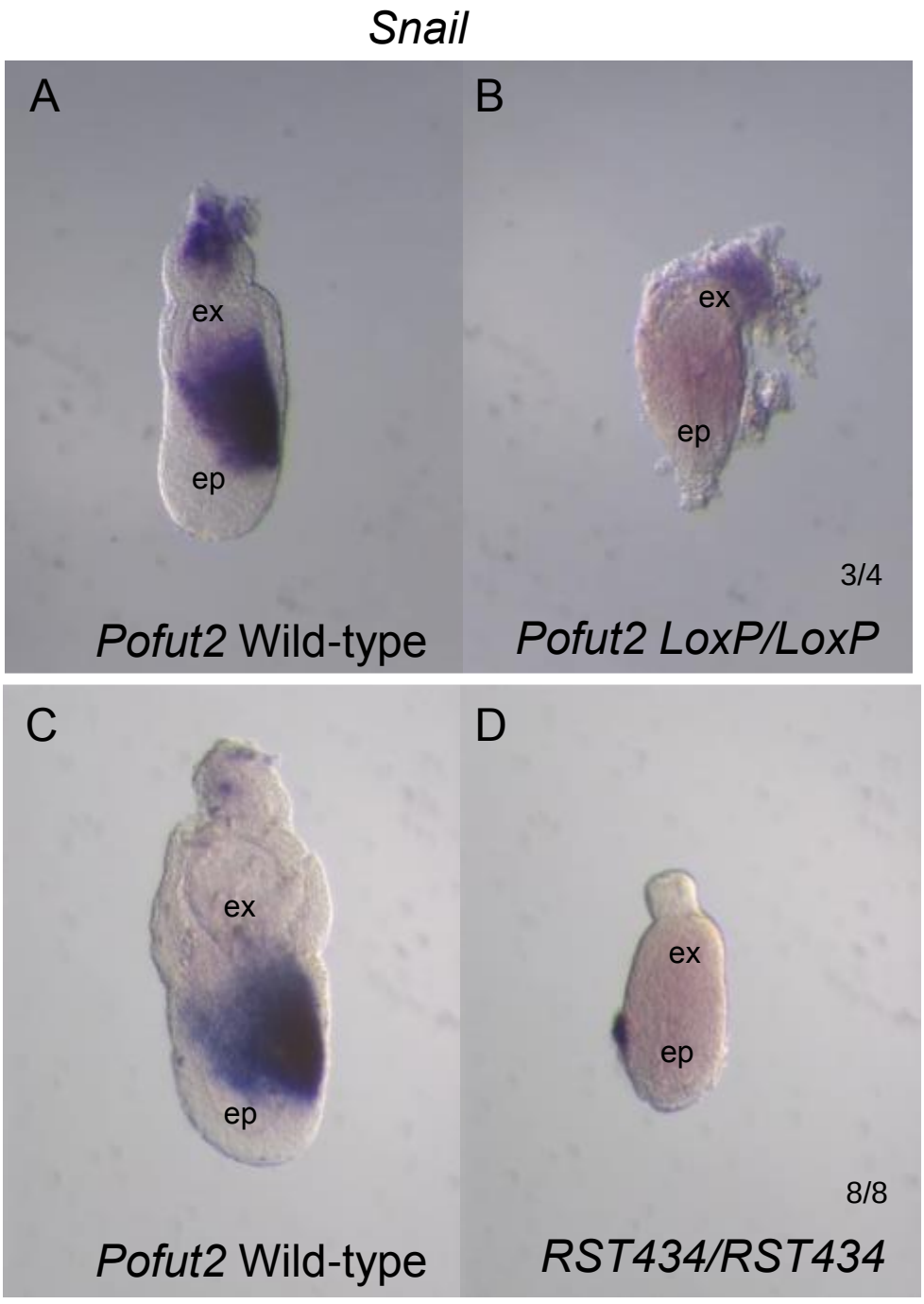

Figure 7: *Snail* expression is absent in *Pofut2 LoxP* mutants at E 7.5. In the *Pofut2 LoxP* wild-type embryo (A), expression of *Snail* marks of the mesoderm migrating from the primitive streak at E 7.5. *Snail* expression is absent in *Pofut2 LoxP* mutants (B) indicating the loss of mesoderm formation (*In situ* by Megumi Takeuchi). Similarly, the expression of *Snail* was present in the *Pofut2 RST434* wild-type (C) and absent in the *RST434* gene-trap mutants (D).

Chapter 3

Do defects in ADAMTS9 contribute to gastrulation defects in *Pofut2-LoxP* mutants?

Introduction

The ADAMTS family members are metalloproteases that function in remodeling of the ECM. One member of this family, ADAMTS9 contains 15 TSR domains in its sequence (Figure 8). In cell culture, ADMATS9 fails to be secreted when *Pofut2* is silenced using siRNA. Loss of *Adamts9* in mice results in embryonic lethality during gastrulation (Enomoto et al., 2010).

Based on the fact that POFUT2 appears to be required for secretion of ADAMTS9 and that *Adamts9* null mice die during gastrulation, we hypothesized that loss of POFUT2 would lead to the loss of ADAMTS9 secretion in early embryos, causing lethality. If impaired ADAMTS9 function is responsible for defects in *Pofut2* mutant embryos, then we predict that *Adamts9* null mutants would resemble our *Pofut2 LoxP* mutants. To test this hypothesis we compared *Adamts9* and *Pofut2* null embryo histology and gene expression.

Methods

Mating Strategy

Male and Female mice heterozygous for the *Adamts9* null allele were crossed and females checked daily for mating plugs indicating pregnancy. *Adamts9* null mouse obtained from Apte Lab at the Cleveland Clinic (Dubail, 2014).

In situ hybridization

In situ hybridization protocol was followed as described in Chapter 2 Methods.

Photography

Photography protocol was followed as described in Chapter 2 Methods.

Genotyping

Genotyping of the *Adamts9* null allele was performed using polymerase chain reaction (PCR) to amplify the *Adamts9* null allele. The *Adamts9* null allele was amplified using the forward primer TS9_I45_FW and reverse primer TS9_I89_Rev which amplifies a band of 650bp (Performed by Megumi Takeuchi).

Results

Adamts9 and *Pofut2* null mutants have similar gastrulation defects

ADAMTS9 is modified by POFUT2, and *Adamts9* null mutants display embryonic lethality at the same point as our *Pofut2 LoxP* and *RST434* mutants. If loss of POFUT2 causes a secretion defect from ADAMTS9, then the phenotypes of the null mutants should be similar. Initially, we examined the tissue morphology of the *Pofut2 LoxP* null and the *Adamts9* null using H&E staining of sectioned embryos.

In the *Pofut2* and *Adamts9* wild-type embryos (Figure 9 A and C), the amnion and chorion were forming proximal to the epiblast. Migrating mesoderm was visible in the posterior epiblast as well. Surrounding the embryo, the parietal and visceral endoderm was visible and the visceral endoderm contained large apical vacuoles. In contrast to wild-type embryos, the *Pofut2 LoxP* null embryo (Figure 9B) was much smaller and constricted at the proximal end. The epiblast was disorganized, lacking the columnar epithelia and the extra-embryonic ectoderm is unrecognizable. The parietal and visceral endoderm surround the embryo were also constricted and the visceral endoderm lacked apical vacuoles. Mesoderm in the posterior was not present in these mutants. The *Adamts9* null (Figure 9D) was similar to our *Pofut2 LoxP* null and was very constricted with a disorganized epiblast and extra-embryonic ectoderm. The visceral and parietal endoderm layers were constricted and the visceral endoderm lacked apical vacuoles. Mesoderm formation was significantly reduced in the posterior epiblast. This initial examination provided preliminary evidence supporting our hypothesis that *Adamts9* is a relevant target of POFUT2 during early mouse embryogenesis.

Bmp4 expression is similar in *Adamts9* and *Pofut2* null mutants at E 7.5

Since *Adamts9* and *Pofut2 LoxP* mutants both showed limited or no formation of mesoderm in the posterior of the embryo at E 7.5, we examined *Bmp4* expression in both *Adamts9* and *Pofut2 LoxP* mutants at E 7.5.

In the previous chapter, we looked at *Bmp4* expression in the *Pofut2 LoxP* mice (Figure 5 A and B). At E 7.5, expression of *Bmp4* was visible in extra-embryonic ectoderm of wild-type embryos, whereas the *Pofut2 LoxP* mutants failed to express *Bmp4* and the tissues surrounding the embryo appeared to be constricted. *Snail in situ* (Figure 7 A and B) confirmed the lack of mesoderm formation in the epiblast of *Pofut2 LoxP* mutants.

As with the *Pofut2* null mutants, the expression of *Bmp4* in the *Adamts9* null mutants was similar to *LoxP* mutants. The *Adamts9* wild-type embryos (Figure 10A) morphology was similar to that described of the *Pofut2* wild-type (Compare Figure 5 and 10), and the expression of *Bmp4* was present in extra-embryonic ectoderm. In the same litter, the *Adamts9* mutants (Figure 10B) had the hallmarks of a *Pofut2 LoxP* mutant and appeared pinched at the proximal end of the embryo and had constricted endoderm surrounding a compressed epiblast. Thus, *Adamts9* mutants failed to express *Bmp4* in the extra-embryonic ectoderm.

ADAMTS9 maintains mesoderm formation at E 6.5

At E 6.5, *Bmp4* is expressed in the extra-embryonic ectoderm before the onset of gastrulation. We wanted to evaluate *Bmp4* expression at E 6.5 to see if expression is present or absent. *Pofut2* and *Adamts9* wild-type embryos (Figure 11 A and C) were

very small before epiblast and extra-embryonic ectoderm were visible. Wild-type embryos expressed *Bmp4* in the ectoderm adjacent to the epiblast. In *Pofut2 LoxP* null mutants (Figure 11B) from the same litter appeared very similar but failed to express *Bmp4* in the extra-embryonic ectoderm. *Adamts9* null mutants (Figure 11D) looked almost identical to wild-type embryos of the same litter and *Bmp4* expression was visible around the same intensity in the extra-embryonic ectoderm. Although similarities in the phenotypes and BMP4 expression at E 7.5 argue that ADAMTS9 is a major target for POFUT2 during early embryogenesis, the loss of BMP4 expression in *Pofut2* null embryos at E 6.5 suggests that additional targets other than ADAMTS9 may be affected.

Adamts9 **is dynamically expressed throughout gastrulation**

The similarities between *Pofut2 LoxP* and *Adamts9* null embryos suggested that *O*-fucosylation of ADAMTS9 by POFUT2 is required for the embryo to progress through gastrulation. Prior studies have shown that POFUT2 is widely expressed through the embryo during this time (Du et al., 2010). To better understand the role of ADAMTS9, we examined *Adamts9* expression during gastrulation of E 7.5 Wild-type embryos (Figure 12 A-D). The expression of *Adamts9* in wild-type embryos was quite dynamic. Some embryos exhibited *Adamts9* expression in the trophoblast giant cells, the parietal endoderm (Figure 12A) and in the proximal visceral endoderm in a ring adjacent to the ectoplacental cone (Figure 12A and B). At the same stage of development, *Adamts9* was also expressed in the anterior primitive streak (Figure 12B and C). However, after the extra-embryonic membranes have completely formed, expression in the anterior primitive streak is absent and there is expression in the extra-embryonic membranes

(Figure12D). This data suggests that early expression of *Adamts9* in the extra-embryonic tissues, the trophoblast giant cells, the parietal endoderm, and ring of visceral endoderm, are responsible for the defects in gastrulation observed in *Pofut2* mutants.

Discussion

Since ADAMTS9 is a target of POFUT2, loss of POFUT2 likely causes a loss of ADAMTS9 secretion in tissue culture systems (Dubail et al., submitted), and *Adamts9* null mice display an early embryonic phenotype (Enomoto et al., 2010). We proposed that Adamts9 null mutants would display many of the defects seen in the *Pofut2 LoxP* null mutants. We demonstrated that the two mutants have very similar morphology at E 7.5 when gastrulation is underway. With this observation, we then examined *in situ* hybridization of *Bmp4* at E 7.5 and E 6.5. This genetic evaluation also demonstrated the similarity in the two mutations since *Bmp4* expression at E 7.5 was clearly absent at this stage. However, *Bmp4* expression at E 6.5 differed in that *Adamts9* mutants maintained expression at this early stage where the *Pofut2 LoxP* mutants lacked *Bmp4* expression. The similarities of these two mutant alleles lead to the conclusion that *Adamts9* contributes to gastrulation defects in the Pofut2 mutants, but the difference at E 6.5 suggests that there may be addition relevant POFUT2 targets during early embryogenesis.

To better understand the role of ADAMTS9 during early embryogenesis, we examined its expression pattern at E 7.5. Prior studies have shown that POFUT2 is expressed throughout the embryo (Du et al., 2010). *Adamts9* was expressed in a much more dynamic pattern, with expression in the proximal visceral endoderm near the ectoplacental cone, the parietal endoderm and the trophoblast giant cells around gastrulation. ADAMTS9 is known to cleave proteoglycans aggrecan, brevican, and versican found in the extracellular matrix. Proteoglycans, such as versican, can complex with hyaluronic acids and link to other components of the ECM such as

fibronectin, and signaling molecules (Apte, 2004; Nandadasa et al., 2014). Loss of cleavage of these ADAMTS9 targets due to loss of secretion to the ECM is likely to be responsible for the gastrulation defects in *Pofut2 LoxP* mutants.

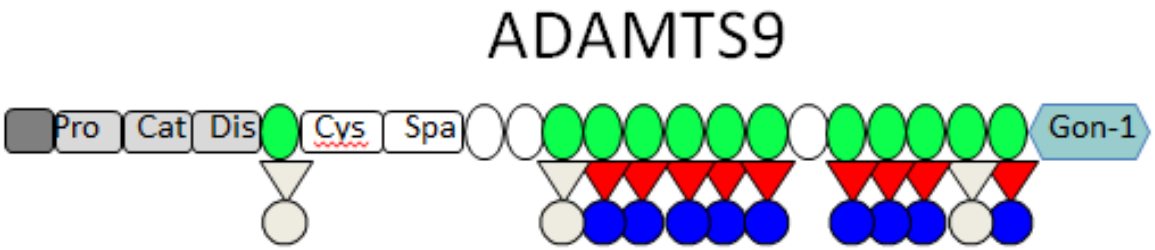

Figure 8: ADAMTS9 domain map
The ADAMTS9 protein contains a Catalytic domain in the N-terminus and the Gon-1 domain at the C-terminus. 15 TSRs are represented by ovals and green ovals represent TSRs with the consensus sequence modified by POFUT2. TSR7 is not completely glycosylated. Triangles represent fucose and circles represent glucose. Colored sugars were confirmed modifications through mass spectrometry (Dubail et al., submitted)

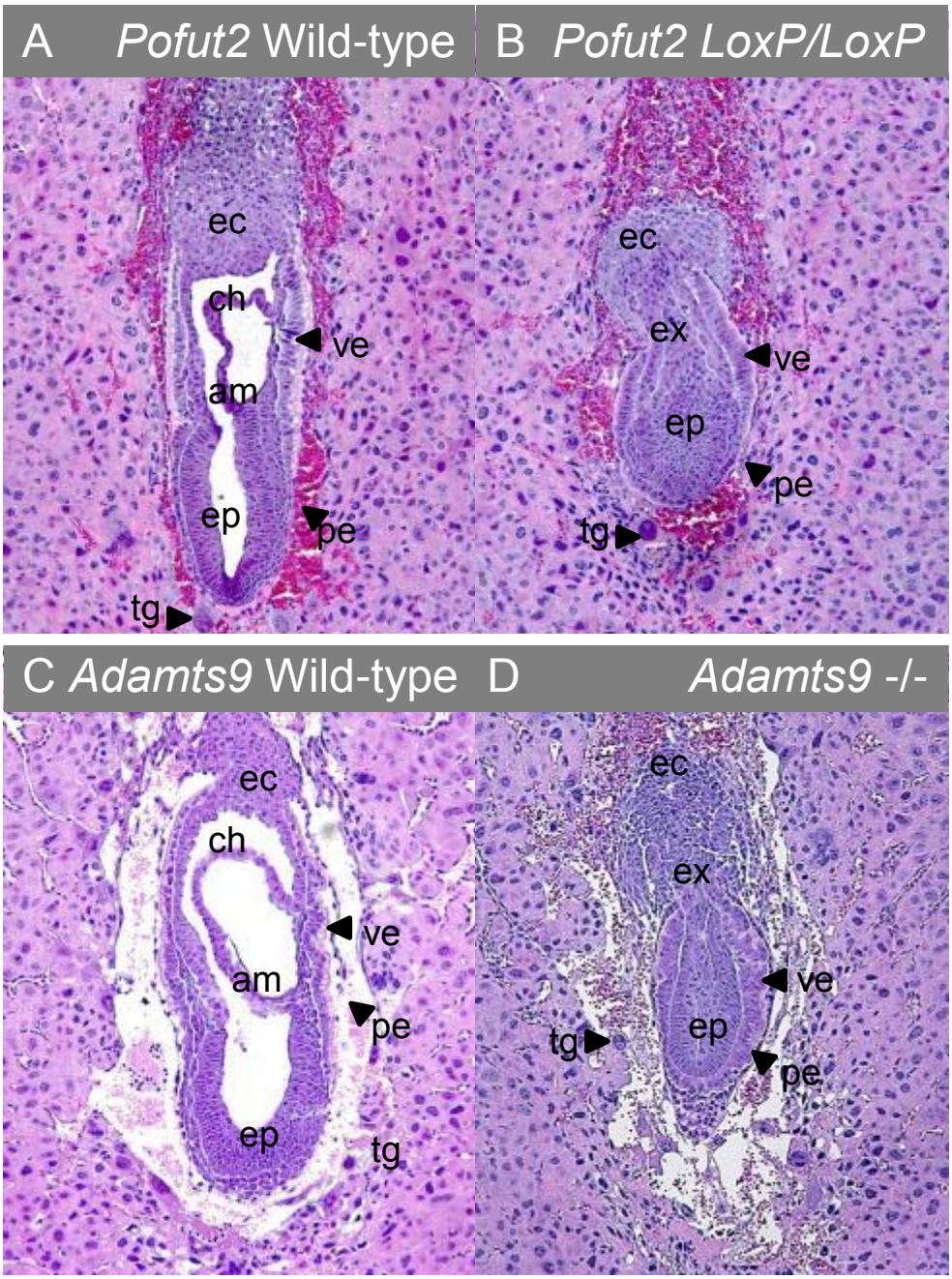

Figure 9: ***Pofut2* and *Adamts9* are required for mesoderm formation**
(A-D) Comparison of H and E staining of E 7.5 embryos. In the *Pofut2* and *Adamts9* wild-type embryos (A and B), the epiblast has formed an organized columnar epithelia. The visceral endoderm around the embryo is organized with large apical vacuoles and the parietal endoderm is spaced apart. Mesoderm is forming from the primitive streak in the anterior of the embryo. The extra-embryonic ectoderm is being displaced by the amnion and chorion forming proximal to the epiblast. In the *Pofut2 LoxP* mutant (B) the epiblast is compressed and lacks the formation of mesoderm. The extra-embryonic ectoderm appears to be pinched in the proximal end. The visceral endoderm lacks

large apical vacuoles and the visceral and parietal endoderm appears disorganized and compressed. Similarly, in *Adamts9* null mutants (D), the epiblast is compressed and lacks mesoderm. The extra-embryonic ectoderm is pinched and the visceral and parietal endoderms are compressed.

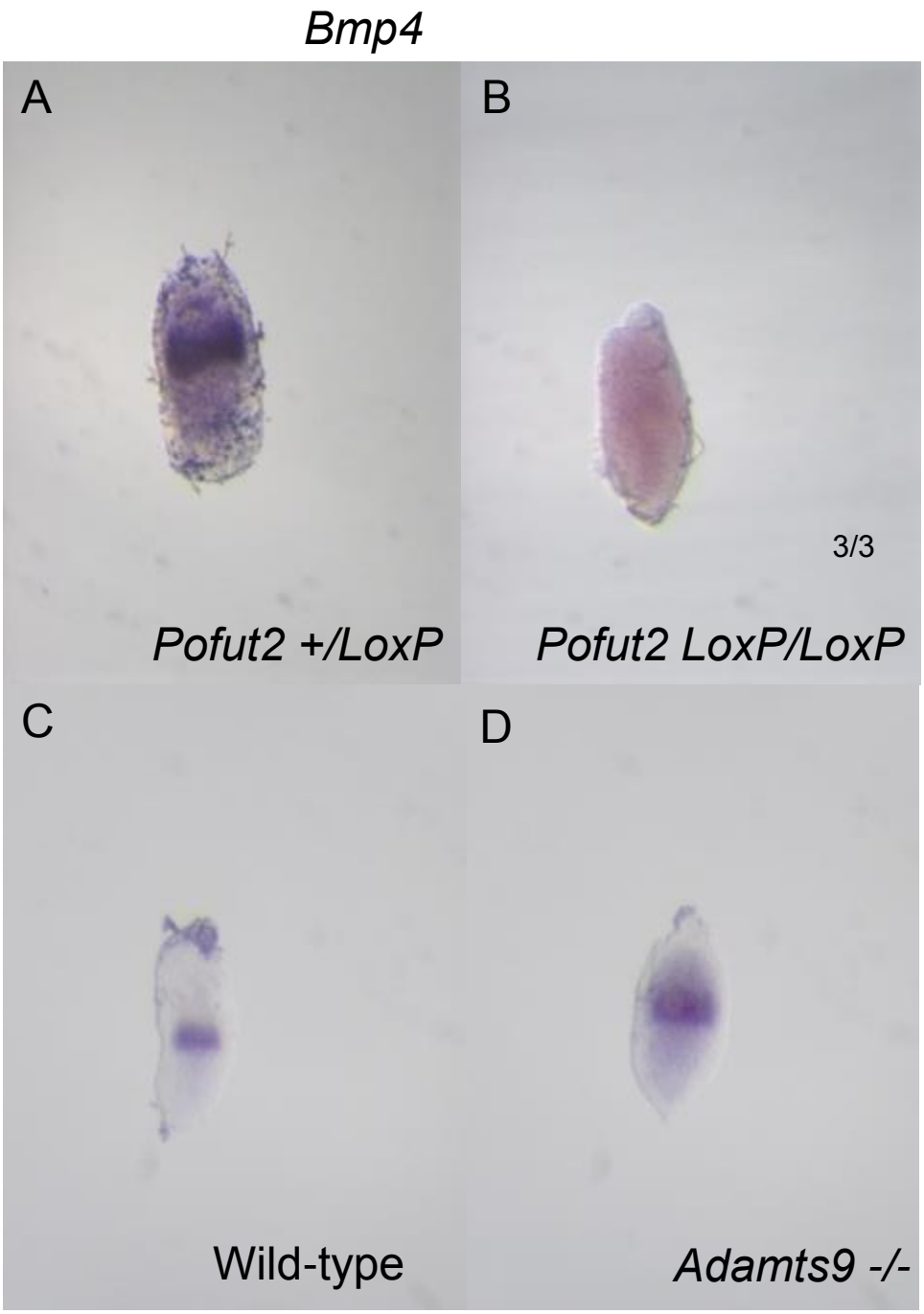

Figure 10: *Pofut2 LoxP* mutants lack *Bmp4* expression at E 6.5 and *Adamts9* null mutants express *Bmp4* at E 6.5. (A-D) Comparison of *Bmp4* expression of E 6.5 embryos. In *Pofut2* wild-type embryos, (A), *Bmp4* expression is restricted to the extra-embryonic ectoderm. In contrast, *Bmp4* is not present in the *Pofut2 LoxP* mutant. Similar to the *Pofut2* wild-type, *Bmp4* expression was observed in extra-embryonic ectoderm of the *Adamts9* wild-type embryos (C). The expression in *Adamts9* mutants was present, in contrast with the *Pofut2 LoxP* null (*Adamts9 in situ* by Megumi Takeuchi).

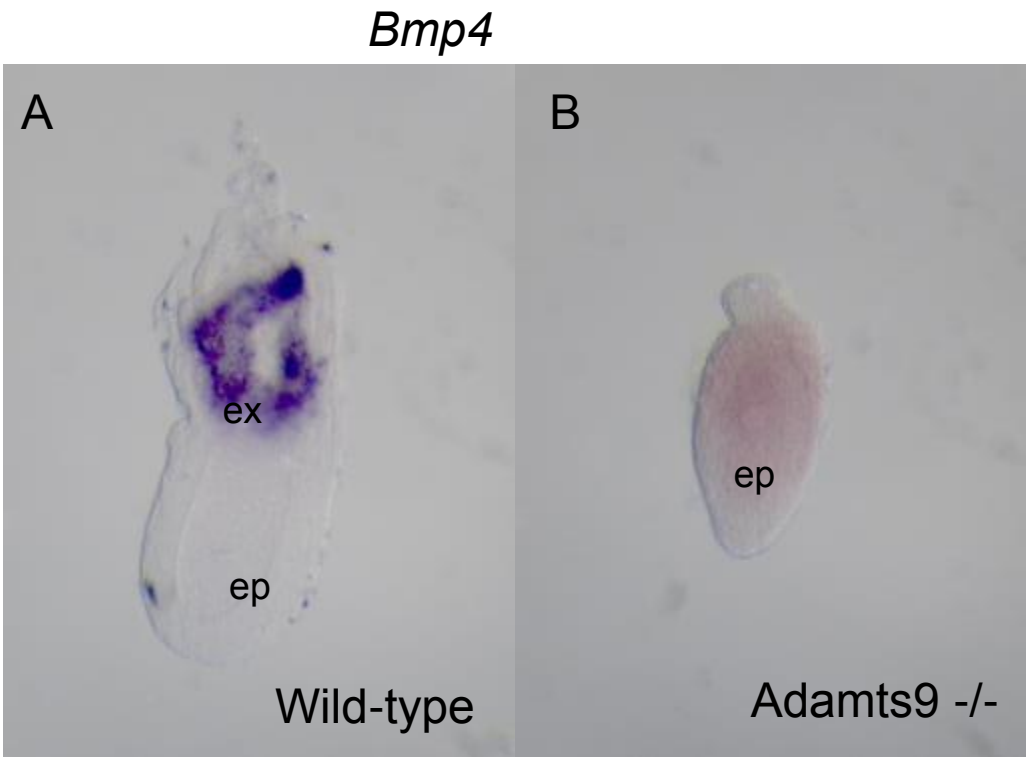

Figure 11: *Bmp4* expression is lost in E 7.5 *Adamts9* null embryos
(A and B) Comparison of *Bmp4* expression at E 7.5. In the *Adamts9* wild-type embryo (A), the expression of *Bmp4* is present in the extra-embryonic ectoderm. In the *Adamts9* null embryo, the expression of *Bmp4* has been lost. (*Adamts9 in situ* by Megumi Takeuchi).

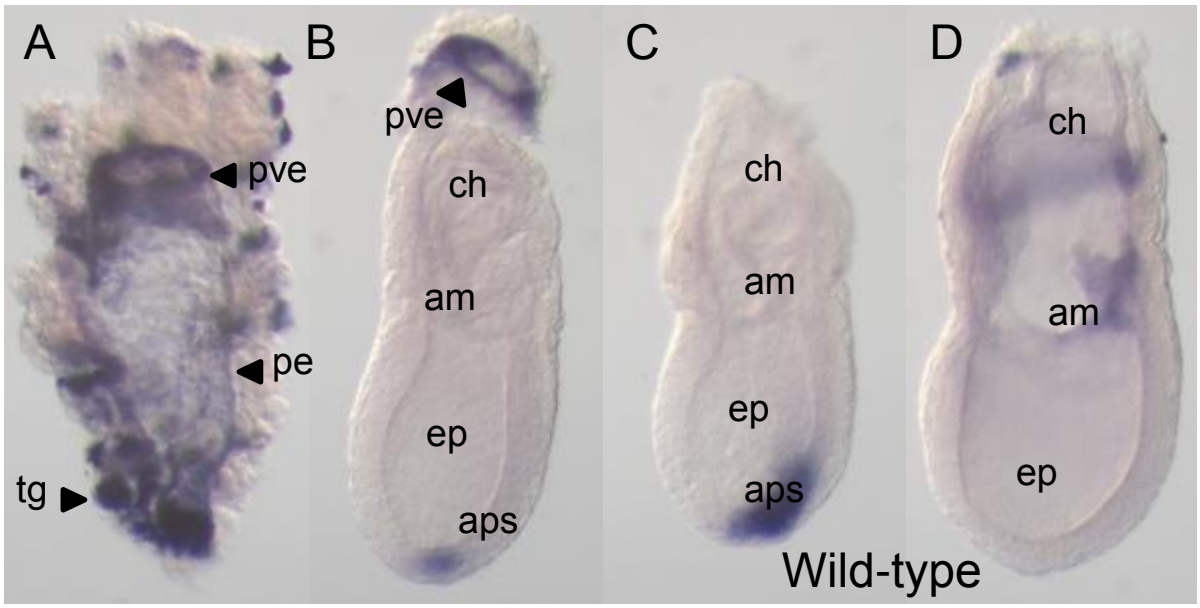

Figure 12: Dynamic expression of *Adamts9* during gastrulation.
(A and D) Expression of *Adamts9* during gastrulation in wild-type embryos. The expression of *Adamts9* is seen in a ring of proximal visceral endoderm (A and B), the parietal endoderm and trophoblast giant cells (A). There is also expression in the anterior primitive streak (B and C) as well as the extra-embryonic membranes (D). (*in situ* by Megumi Takeuchi).

Chapter 4

Which tissues require POFUT2 activity?

Introduction

Loss of *Pofut2* in the developing mouse embryo disrupts gastrulation by embryonic day (E) 7.5 (Chapter 2, (Du et al., 2010)). The epiblast and extra-embryonic ectoderm in *Pofut2* mutants were compressed and lacked distinct columnar epithelia. The overlying visceral endoderm also appeared compressed and lacked large apical vacuoles. The defects in vacuoles could result from altered transfer of lipids across Reichert's membrane, suggesting an alteration in the composition or structure of Reichert's membrane. This alteration, could also account for the compression of epiblast and extra-embryonic ectoderm.

The similarities between the *Pofut2* and *Adamts9* knockout (Chapter 3) suggest that loss of ADAMTS9 function is a major contributor to the *Pofut2* mutant phenotype. *Adamts9* was expressed in trophoblast giant cells, parietal endoderm, a ring of proximal visceral endoderm adjacent the ectoplacental cone, the anterior primitive streak, and extra-embryonic mesoderm. We hypothesized that loss of ADAMTS9 function in the extra-embryonic tissues was responsible for the compressed extra-embryonic ectoderm and epiblast, and as a result block mesoderm formation of the *Pofut2* mutants.

We used a conditional mutant of the *Pofut2* knockout, to determine whether wild-type *Pofut2* in extra-embryonic tissues could rescue the gastrulation defects in epiblast mutant *Pofut2* embryos. Expression of *Brachyury* and *Foxa2* in *Pofut2* epiblast mutants provides evidence that the wild-type extra-embryonic tissues rescued the defects in gastrulation. However, abnormalities in elongation of the anterior/posterior axis suggest

that *Pofut2* was required in the epiblast for progression of gastrulation. Given the localization of *Adamts9* expression, we hypothesize that loss of ADAMTS9 function in either the anterior primitive streak and/or extra-embryonic mesoderm is essential for the progression of gastrulation.

Methods

Mating Strategy

Floxed/Floxed females were placed in a cage with a RST/+; Sox2::Cre/+ or Sox2::Cre/Sox2::Cre males at the beginning of the week (Figure 13). Female mice were checked daily for mating plugs indicating mating and pregnancy. The males were then removed from the cage and females removed at the desired gestational day. Female mice were euthanized according to IACUC protocol (#05401), Carbon dioxide for one minute before cervical spine dislocation. Embryos were then dissected in cold PBS with EGTA and isolated in 4% PFA.

In situ hybridization

In situ hybridization protocol was followed as described in Chapter 2,

The *in situ* procedure started by rehydrating the embryos before adding hybridization buffer along with 1:10-1:20 dilution of DIG labeled RNA probe overnight (*Foxa2* 60.3ng/ µL and *Brachyury* 118.2ng/ µL). The next day, embryos are thoroughly rinsed before adding blocking reagent and 1/2000 to 1/5000 dilution of anti-DIG-AP and incubated at 4ºC overnight. On the last day of the procedure, the embryos incubated with 1.5 mL NTMT + 6.75 µL NBT + 5.25 µL BCIP and rocked in the dark. The color can develop within a day or can be left to develop up to three days in the 4ºC fridge (Supplemental Protocol 2).

Photography

Photography of embryos followed the same protocol as in Chapter 2.

Genotyping

As described in Chapter 2, *LoxP* and *RST* primers were evaluated using the same primers to amplify the same alleles. For every reaction, approximately 2 µL - 3 µL of embryo lysis was used depending on the size of the embryos. This procedure also required the amplification of two additional alleles, *Floxed* and *Sox2::Cre*. The *Floxed* allele was amplified in the same reaction with the *LoxP* and wild-type control alleles. Using the primers Pofut2CommonL2 and Pofut2FloxedR1, a 479 base pair *Floxed* band was amplified. To confirm the presence of the *LoxP* allele, the *Sox2::Cre* allele was amplified using generic primers described by Jackson Labs. Using the oIMR7338 forward primer and the oIMR7339 reverse primer, a 324 base pair sequence was amplified as an internal positive control present in all embryos. The *Sox2::Cre* band of 100 base pairs was amplified using the oIMR1084 forward primer and the oIMR1085 reverse primer (Supplemental Table 1 and Supplemental Protocol 1).

Results

POFUT2 in the extra-embryonic tissues restored gastrulation defects

The purpose of this study was to understand how *Pofut2* in the extra-embryonic tissues affected gastrulation and formation of mesoderm. We used a *Sox2::Cre* conditional mutation of *Pofut2* to eliminate *Pofut2* in the epiblast. In these mutants, *Pofut2* expression was maintained in the extra-embryonic tissues including the parietal endoderm, proximal visceral endoderm, and trophoblast giant cells where *Adamts9* was expressed. We mated *Pofut2 Floxed* homozygous females with *Pofut2 RST/+; Sox2::Cre/+* or *Sox2::Cre/Sox2::Cre* males and isolated embryos during mid-gastrulation. One quarter to one half of the embryos were expected to inherit both mutant alleles and be useful to our study (Figure 13). We examined markers of mesoderm in these embryos using *in situ* hybridization, and then genotyped the embryos as described in Chapter 2 and Chapter 4 methods.

At embryonic day (E) 7.5, wild-type embryos (Figure 14A) completed gastrulation and reached the early head fold stage (Downs and Davies, 1993). Extra-embryonic mesoderm displaced the extra-embryonic ectoderm and a distinct amnion and chorion were visible. The allantois was visible in the posterior of the amniotic cavity. An indentation at the distal end of the epiblast identified the formed node structure. *Brachyury* was expressed throughout the primitive streak and axial mesoderm. In littermates lacking POFUT2 activity in the epiblast (Figure 14D), embryos appear to have undergone gastrulation. Head folds appear to be present and extra-embryonic membranes appear disorganized. An indentation at the distal end of the primitive streak

might have indicated the presence of a node structure. *Brachyury* expression confirmed the formation of the primitive streak and axial mesoderm.

In a second E 7.5 litter, wild-type embryos reached the late head fold stage (Figure 14B). The head folds at the anterior epiblast were more pronounced and the foregut pocket was visible. The amnion and chorion had completely formed and generated the amniotic and exocoelom cavities. The node structure was visible as a prominent indentation at the anterior end of the primitive streak. *Brachyury* was expressed in the primitive streak and the notochord extending along the anterior/posterior axis. In the epiblast mutants (Figure 14E) clear head folds were not visible in the anterior embryo, and mutants lacked distinct extra-embryonic membranes. In this mutant, *Brachyury* expression identified a shortened primitive streak and split axial mesoderm.

Combined, these morphological observations and *Brachyury* expression patterns demonstrated that *Pofut2* in the extra-embryonic tissues rescued the gastrulation defects of the *Pofut2* null mutants. However, the shortened primitive streak, disorganized extra-embryonic membranes, and limited axial mesoderm suggested that *Pofut2* expression in the epiblast was needed for axial elongation and extra-embryonic membrane formation.

Loss of *Pofut2* in the epiblast resulted in disorganized extra-embryonic membranes and abnormal node structure

To further examine the structure of the extra-embryonic membranes and midline axis in epiblast mutants, we examined H&E stained sections of mutants during late

gastrulation. In wild-type embryos, the epiblast cells formed an organized epithelia layer and head folds are visible in the anterior (Figure 15A). Extra-embryonic mesoderm displaced the extra-embryonic ectoderm and the chorion and amnion was formed. In the regions of mesoderm connecting the amnion and chorion, blood islands were observed. An organized visceral endoderm surrounded the embryonic tissues and the allantois was visible in the anterior embryo. In the distal end of the embryo a node structure was visible (Figure 15 A and A').

Epiblast mutant littermates appeared to form an organized epiblast and head folds were prominent (Figure 15 B and C). Extra-embryonic mesoderm migrated to form the amnion and chorion; however, a point of these two membranes remained attached toward the anterior of the embryo. In the extra-embryonic membranes, blood islands were visible and the visceral endoderm surrounding the embryo appeared similar to the wild-type littermate. The allantois was also visible in the posterior and the node was visible at the distal tip. In the anterior of the mutant embryo, the head folds were tilted back toward the posterior end obscuring the curve of the epiblast. Anterior to the head folds, a mass of mesodermal cells was present that may have resulted from convergent extension defects. These observations confirmed the presence of the disorganized extra-embryonic membranes and a tilted axis.

POFUT2 was required in epiblast tissue for axis elongation

Loss of *Pofut2* in the epiblast caused defects in the elongation of the axial mesoderm and organized extra-embryonic membranes. To determine how loss of POFUT2 function in the epiblast affected the elongation of the notochord, we looked at

Brachyury expression in epiblast mutant embryos during early somite formation. At E 8.5, Wild-type embryos (Figure 14C) formed head folds and heart in the anterior. The amnion extended from the anterior to posterior end of the embryo, forming the amniotic cavity. *Brachyury* expression was visible in the primitive streak and notochord. Somites were visible along the notochord extending along the anterior/posterior axis. In the mutant littermate (Figure 14F), the embryo was delayed in stage. The head folds and heart were visible but compressed in the anterior. The allantois extended from the epiblast and appears toward the chorion within the exocoelom cavity. The amnion and chorion were disorganized with a region of connection between the two membranes. *Brachyury* expression indicated a thickened anterior streak and extended notochord. The mutant epiblast appeared square in shape due to a kink in the anterior axis.

The combined data demonstrated that *Pofut2* was needed in the epiblast for the proper formation of the extra-embryonic mesoderm and the elongation of the notochord. Knowing *Adamts9 wa*s expressed in the anterior primitive streak, we next examined the formation of definitive endoderm in epiblast mutants.

POFUT2 in the epiblast is not required for specification of definitive endoderm

Loss of *Pofut2* in the epiblast caused defects in the elongation of the primitive streak and axial mesoderm as well as abnormal formation of extra-embryonic membranes. Definitive endoderm is derived from the anterior primitive streak, a region where *Adamts9* was expressed. To determine if definitive endoderm was specified, we examined the expression of *Foxa2. Foxa2* is dynamically expressed during mouse

gastrulation and marks definitive endoderm, notochord and floorplate. (Dufort et al., 1998)

Wild-type E 7.5 embryos (Figure 16A) developed organized columnar epithelia in the epiblast at the early streak stage. The extra-embryonic membranes had begun to form although they were not completely extended. *Foxa2* at the distal tip identified the definitive endoderm precursors. Epiblast mutant embryos (Figure 16F) also developed into the early streak stage and defined columnar epithelia was apparent in epiblast tissue. Mutant embryos expressed *Foxa2* similar to that of the wild-type embryos.

By late streak stages, wild-type embryos (Figure 16B) had begun forming the extra-embryonic membranes and displacing the extra-embryonic ectoderm. A distinct amnion and chorion were still hard to distinguish at this stage. *Foxa2* expression was identified in the early notochord in the anterior of the embryo. In the mutant embryos at the late streak stage (Figure 16G), the extra-embryonic membranes had begun to form although the displacement of the extra-embryonic ectoderm was unusual in these mutants. As in wild-type, *Foxa2* expression identified the notochord in these mutants.

At E 8.5 early, wild-type embryos (Figure 16C) reached the late bud stage and head folds were visible in the anterior embryo. The node was present at the distal tip and the extra-embryonic membranes formed two distinct layers separating the amniotic cavity and exocoelom cavity. At the point of the node, *Foxa2* expression extended to the anterior indicating the presence of the anterior notochord. In the mutant littermates (Figure 16H), head folds had formed in the anterior. Extra-embryonic membranes formed, but an area of connection was visible within the exocoelom cavity. An

indentation indicated the node was present, and *Foxa2* was expressed through the anterior notochord. At this point, the square phenotype of the epiblast was noticeable.

Mid-day dissection at E 8.5, wild-type embryos (Figure 16D) reached the early head fold stage. The head folds were noticeable in the anterior but had not yet fused together. A distinct amnion and chorion were visible in these embryos as well. The allantois had formed at the posterior extending toward the proximal end. The expression of *Foxa2* indicated the notochord and floorplate, extended from the indentation of the node and through the anterior. In the epiblast mutant embryo (Figure 16I), head folds were present, but the epiblast was disorganized. In the extra-embryonic membranes, there was a point of attachment between the amnion and chorion, similar to the late bud stage mutants. The allantois was visible and extended much larger than that of the wild-type. *Foxa2* expression marked the notochord and floorplate of the embryo, however the expression did not appear continuous in the notochord. Mutant embryos at this stage had a kinked axis which resulted in a very distinct square phenotype in the epiblast tissue.

Turned Wild-type embryos (Image 16E) dissected at E 8.5 late, had visible optical vesicles and heart. Along the axis of the embryo, somites had formed. *Foxa2* expression extended the length of the notochord as well as the floorplate in the embryo and some areas of the gut. The mutant embryos from the same litter (Figure 16J) are much less advanced than wild-types. Head folds were present; however at this point the embryo failed to turn and appeared constricted. *Foxa2* expression marked the notochord and floorplate of the embryo. These combined data demonstrated that the loss of *Pofut2* in the epiblast did not affect the specification of the definitive endoderm or

formation of the notochord. However, because of the kinked axis in these mutants, we asked if the definitive endoderm was able to displace the visceral endoderm.

Definitive endoderm displaces visceral endoderm in *Pofut2* epiblast mutants

The definitive endoderm, formed from the anterior primitive streak, intercalates into the surrounding visceral endoderm displacing it toward the proximal end of the embryo. Since the expression of *Foxa2* is dynamic, marking primitive streak, axial mesoderm, and notochord; our analysis of *Foxa2* could not determine if the definitive endoderm was able to displace the visceral endoderm.

We removed the tissue proximal to the embryonic tissue and used PCR to analyze this tissue separate from the distal tissue. We would expect that in the epiblast mutants, the distal tissue would contain a majority of cells that were derived from the epiblast and not the extra-embryonic tissues (Lewis and Tam, 2006). In these mutants, the only alleles present in epiblast derived tissue would be the recombined *Pofut2 LoxP* allele and the *Pofut2 RST434* allele, with little presence of the *Pofut2 Floxed* allele. In Figure 17, litter 70 mutant embryos contained the *LoxP* allele and significantly less *Floxed* allele indicating the visceral endoderm has begun to be displaced. Litter 71, a slightly more advanced litter, Embryos 5 and 6 were confirmed to be mutant embryos. They lacked any *Pofut2 Floxed* allele from the distal portion of the embryo which indicated the absence of visceral endoderm from the reaction. This result confirmed that the visceral endoderm is displaced, most likely by the newly formed definitive endoderm.

Discussion:

In our *Pofut2 LoxP* null mutants, we demonstrated that *Pofut2* is needed for gastrulation (Chapter 2). Loss of POFUT2 activity resulted in reduced formation of mesoderm and disorganized extra-embryonic tissues. Using conditional deletion analysis we demonstrated that embryos without POFUT2 in the epiblast could still gastrulate, suggesting that loss of *Pofut2* in the extra-embryonic tissues was responsible for the gastrulation defects. The epiblast conditional mutant presented a new set of phenotypes not observed in the knockout, including: shortened axis, irregular node structure, and defects in formation of the amnion and chorion. These results suggest additional roles for POFUT2 in the epiblast post-gastrulation

POFUT2 *O*-fucosylates TSRs on target proteins such as ADAMTS9, a metalloprotease that functions to remodel the extracellular matrix. Prior results also suggest that POFUT2 is required for secretion of ADAMTS9 into the extracellular matrix. The similarities between our *Pofut2 LoxP mutants* and *Adamts9* mutants suggested that loss of ADAMTS9 function contributes to the gastrulation defects seen in our *LoxP* mutants. *Adamts9* was expressed in distinct areas of the embryo during gastrulation, including the parietal endoderm, proximal visceral endoderm adjacent the ectoplacental cone, trophoblast giant cells, the anterior primitive streak, and the extra-embryonic mesoderm. Combined, these results suggest that loss of ADAMTS9 function in one or more extra-embryonic tissues is responsible for the gastrulation defects observed in *Pofut2* and *Adamts9* mutants. Additionally, expression of *Adamts9* in the anterior primitive streak and extra-embryonic mesoderm suggests that loss of

ADAMTS9 function in *Pofut2* epiblast mutants may also contribute to axis elongation defects.

Partial or complete loss of function of the ADAMTS9 protein has been examined in different developmental contexts in the mouse. The function of ADAMTS9 in these tissues may provide insight into ADAMTS9 function in our *Pofut2* mutants. ADAMTS9 is known to cleave large proteoglycans such as aggrecan and versican in the ECM. In cardiac development, ADAMTS9 haploinsufficiency is associated with the reduction of cleaved versican in the ECM of the developing heart. Reduced veriscan cleavage in *Adamts9* haploinsufficient embryos led to cartilaginous nodes in the valvular sinuses and thickened leaflets as well as malformations of the adult heart (Kern et al., 2010). Also, haploinsufficiency of *Adamts9* also leads to increased neovascularization—the new formation of vasculature, and opacity of the cornea of the mouse, suggesting that ADMATS9 function plays a role in suppressing angiogenic mechanisms by way of proteolytic cleavage (Koo et al., 2010). Conditional deletion of *Adamts9* in limb bud mesenchyme leads to reduced web regression, which is further exacerbated by loss of *Adamts5.* In addition, defects in *Adamts20 (Bt)* are exacerbated by *Adamts9* haploinsufficiency causing as failure in mouse palate closure and interdigit web regression due to restricted versican cleavage (Dubail et al., 2014; McCulloch et al., 2009; Silver et al., 2008). In our *LoxP* mutants, we showed a compressed primitive endoderm. It is possible that this phenotype is the result of proteolytic cleavage in our mutants that fails to allow the primitive endoderm to maintain connections with the extra-embryonic ectoderm.

Unlike the null *Adamts9* mutants, when ADAMTS9 protein is constitutively anchored to the cell membrane, mutant embryos are able to undergo gastrulation and develop beyond E 11.5. The allele is hypomorphic, rescuing defects of the eye, but failed to rescue cleft palate defects when combined with *Adamts20 (Bt)* mutant. During the formation of umbilical vessels, the gene-trap mutants had less cleaved versican in the umbilical vascular wall as well as the enhancement of fibronectin and fibrillin-2. The gene-trap mutants also had disorganized cilia orientation compared to wild-type. Cilia are important in signaling and gene-trap mutants also demonstrated a reduction in PDGFβ signaling resulting in impaired rotation of vascular smooth muscle cells suggesting cytoskeletal defects as a result of signaling loss (Nandadasa et al., 2015). The function of ADAMTS9 in organizing the basement membrane for proper orientation of ciliated cells may relate to our epiblast mutants, playing a role in tissues such as the node, properly orienting the ciliated cells responsible for signaling.

GON-1, the *Adamts9* orthologue in *C. elegans*, provides a possible mechanism for function of the ADAMTS9 protein in mice. GON-1 is an important protein in regulation during gonad formation through contributions to the migration of the distal tip cell (DTC) (Blelloch et al., 1999a). Defects that lead to the reduction of fibulin rescued the defects in the gon-1 mutants. Fibulin is a structural protein associated with the basement membrane, binding to laminin, as well as aggrecan and versican (de Vega et al., 2009). *Emb-9* mutations, mutations in collagen IV, in *C. elegans* rescued the defects of fibulin mutants as well (Kubota et al., 2012). Hemicentin is an ECM protein that is related to fibulin, linking the double basement membrane between the anchor cell and vulva precursor cell during formation of the gonad (Morrissey et al., 2014). It is

suggested that GON-1 functions in the ECM to allow for the migration of the DTC and release the inhibitory effects of fibulin on cell migration. Human ADAMTS9 was able to recue some of the defects of the *gon-1* mutants (Hesselson et al., 2004). *Gon-1* mutations suggest that *Adamts9* will play a role in the restructuring of the basement membrane in mouse embryos.

Role of POFUT2 in the extra-embryonic tissues and influence on gastrulation

We hypothesize that the loss *Pofut2*, resulting in loss of ADAMTS9 secretion, may disrupt the connections of the basement membrane separating the visceral endoderm and ectoplacental cone. In our *Pofut2 LoxP* and *Adamts9* null mutants, the visceral endoderm appears ruffled and the extra-embryonic ectoderm is displaced. These observations suggest that the visceral endoderm has detached from the ectoplacental cone and slipped down the embryo, causing a constriction of the epiblast and the extra-embryonic ectoderm to be pinched off. In *C. elegans*, the gonadal and ventral basement membranes separating the anchor cell and the vulva precursor cells, are connected through the interactions of hemicentin with integrins and plakin of the hemidesmosomes. Absence of hemicentin causes the basement membrane layers to shift against each other disrupting anchor cell invasion during formation of the gonad (Morrissey et al., 2014). Hemicentin in mice is found in basement membranes associated with lens fibers, vasculature of the lung and arteriole vessels near the optic disk, and skin epithelia. It has also been linked to cytokinesis in early embryogenesis of the mouse (Xu et al., 2007; Xu et al., 2013). Without ADAMTS9 function, basement

membrane associations may be disrupted causing the visceral endoderm to slip away from the extra-embryonic ectoderm. This slipping would displace the extra-embryonic ectoderm resulting in the loss of *Bmp4* signaling that we observed in our mutants which is required for mesoderm formation.

Alternatively, we suggest that POFUT2-mediated *O*-fucosylation of ADAMTS9 in the parietal endoderm is required for PDGF signaling to promote proliferation of the parietal endoderm and alter the structure of the Reichert's membrane. Our *Pofut2 LoxP* and *Adamts9* mutants have a compressed parietal and visceral endoderm surrounding the epiblast. ADAMTS9 function has been implicated in PDGF signaling of the mouse embryo. ADAMTS9 gene-trap mutants, where ADAMTS9 is anchored to the cell membrane, have reduced PDGFβ signaling because of reduced versican cleavage in the ECM (Nandadasa et al., 2015). *Pdgfrα* is expressed in the extra-embryonic endoderm lineages, including the parietal and visceral endoderm. Inhibition of the PDGF receptor in XEN cells demonstrated a need for PDGF signaling for cell proliferation. In diapause embryos, the absence of *Pdgfrα* leads to an expansion of epiblast cells. This suggests that *Pdgfrα* or the primitive endoderm may affect epiblast size and proliferation (Artus et al., 2010). Although knockouts of *Pdgfrα* in vivo are not embryonic lethal before gastrulation (Soriano, 1997), it is possible that without expansion of the parietal endoderm lineage, the tissues become compressed around a growing epiblast. This compression may force the extra-embryonic ectoderm away from the epiblast, cutting off signaling needed for gastrulation.

Lastly, we hypothesized that the requirement of POFUT2 activity in the parietal endoderm for maintaining the integrity of the primitive endoderm's ability to uptake

nutrients from the maternal environment. If you altered the Reichert's membrane structure, you might decrease permeability which could lead to decreased uptake in the visceral endoderm. The compressed endoderm and lack of apical vacuoles in the visceral endoderm suggested that defects in *Pofut2 LoxP* and *Adamts9* mutants could result from defects in signaling and nutrient uptake. Defects in vesicular trafficking across the visceral endoderm, such as in *Rap7* mutants, resulted in embryonic lethality during gastrulation, lack of apical vacuoles in the visceral endoderm, and disorganized mesoderm formation (Kawamura et al., 2012). MESD is a protein required to localize the LRP receptors to the apical visceral endoderm. LRP receptors mediate endocytosis of nutrients and signals, such as involved in *Wnt* signaling, and fail to localize to the visceral endoderm membrane in *Mesd* mutants (Lighthouse et al., 2011). Taken together these studies demonstrate the importance of the integrity of the visceral endoderm for nutrient uptake. Without POFUT2 in the primitive endoderm, the tissues become compressed and block the uptake of nutrients, including signaling molecules, such as Wnt, that are necessary for mesoderm formation.

Role of POFUT2 in Epiblast derived tissues

Disruption of node structure and formation, ciliary function, planar cell polarity, and convergent extension all contribute to axial elongation defects in the mouse embryo. Defects in the structure and function of the node may result in the defects in axis elongation. In our epiblast mutants, hematoxylin and eosin stained sections revealed an irregular node structure. The transcription factor, *FoxH1,* maintains *Nodal*

signaling during gastrulation through an autoregulatory loop and is required for the formation of the node structure and anterior-posterior patterning. Mutations in *FoxH1* lead to multiple phenotypes—including loss of anterior structures, fused headfolds, and the anterior primitive streak fails to form (Yamamoto et al., 2001). Similarly, loss of *Foxa2* function in the mouse embryo results in loss of the node structure and failure of the primitive streak to elongate. It is also needed to induce definitive endoderm formation and displace the visceral endoderm (Ang and Rossant, 1994). Therefore, it is unlikely that the the axial defects we observe are due to node formation but the structural and functional defect. Foxa2 marks the specified definitive endoderm, as well as the node, notochord and floorplate in more developed embryos (Dufort et al., 1998). Combined, examination of the expression of *Foxa2* in our epiblast mutants and PCR of epiblast mutants with extra-embryonic tissues removed, suggest that the node structure is formed and retains some function.

The axial elongation defects of our mutant embryos may contribute to defects in node structure and formation that require primary cilia formation—an important structural feature present on each cell of the ventral layer of the node. It is this structure that allows for the left-right patterning of the embryo and axis elongation. Without motile cilia providing a leftward flow of the fluid across the node, left right asymmetry of the embryo is disrupted (Lee and Anderson, 2008). Our mutants developed a node and partial function of the node remains. *Foxj1* is an important transcription factor for forming motile cilia. When *Foxj1* expression is eliminated, the cilia of the node are still able to form but lack motility. However, in these mutants the left-right patterning is disrupted (Zhang et al., 2004). *Rfx3* is also present in the node at E 7.5, cilia are

present, but they develop later in gestation and remained shorter, disrupting the left right polarity as well (Bonnafe et al., 2004). These transcription factors both develop a node, but the elongation of the axis and left/right patterning is disrupted by ciliary defects. *Adamts9* gene-trap mutants also demonstrated ciliary defects caused by the disorientation of the epithelial layer (Nandadasa et al., 2015). In our *Pofut2* epiblast mutants, remodeling of the ECM near the node may be required to properly orient the ventral surface of the node. Failure to properly orient the cells would lead to disoriented primary cilia and cause a disruption in the signaling coming from the node.

Defects in planar cell polarity may also result in the axial elongation defects of the epiblast mutants. Our epiblast mutants appeared to have a shorted axis and a kink in the anterior and posterior of the embryo. Genetic contributions to convergent extension include the *Looptail* mutants and *Dishevelled* 1 and 2 double mutants. In *Looptail* (*Vangl2)* homozyogous mutants, the axis, comprised of the axial mesoderm and neural plate, appeared to be thicker and shorter due to a failure of convergent extension. Markers of the notochord and axial mesoderm of these mutants appeared broader in the region near the node (Ybot-Gonzalez et al., 2007). Similar to the *Looptail* mutants, *Dvl1 and Dvl2* double mutants have a similar effect on convergent extension with a shorter, wider axis (Wang et al., 2006). *Lulu* mutants also display defects during gastrulation and neural plate formation through anchoring of with the cytoskeleton to the cell membrane. *Lulu* mutants have a shortened axis and the neural plate was folded and failed to close (Lee et al., 2007). This is similar to our epiblast mutants where the axis is shorter than wild-type and some markers of axial mesoderm are broadened near

the node structure. These similarities, along with the observation of a formed node, suggest that *Pofut2* may play a role in convergent extension.

Lastly, we hypothesized that formation of the extra-embryonic membranes can result in axis elongation defects. Analysis of whole mount and sectioned epiblast mutant embryos also revealed disorganization of the extra-embryonic membranes—the amnion and chorion appeared to remain connected. Important in the formation of the amnion and chorion, *Bmp2* is expressed in the extra-embryonic mesoderm and allantois during head fold stages. Loss of BMP2 activity in the mouse embryo results in a failure of some embryos to close the proamniotic canal and have a kinked shape similar to our epiblast mutants (Madabhushi and Lacy, 2011). Heart formation of these mutants also appears to develop in abnormal positions and the allantois failed to extend to the full length as compared to wild-type (Zhang and Bradley, 1996).

Another mutant, *Pagr1a (*PAXIP1 associated glutamate rich protein 1A which is associated with epigenetic regulation) null embryos, also showed similarities to our mutant. During the formation of the extra-embryonic membranes, the extra-embryonic ectodermal layer of the membranes appears to become incorporated into the junction between the amnion and chorion. This extra-embryonic ectoderm then becomes localized in the amnion, instead of the normal embryonic ectoderm contribution. This defects also results in incomplete separation of the two membranes as well (Kumar et al., 2014). Fibronectin is an important ECM protein which is present in the early embryo. One particular area of interest is the region between the mesoderm and ectoderm of the amnion and surrounding the somites. When the gene encoding the fibronectin proteins is absent, mutants demonstrate a shortened anterior-posterior axis

and demonstrate a kink in the neural tube. These mutants also had defects in the amnion formation, being that the mutants were smaller in size (George et al., 1993). These mutants demonstrate a defect in the formation of the extra-embryonic membranes that results in a kinking of the axis, with the headfolds being pulled back by the amnion toward the posterior. The similarities in these mutants suggests that POFUT2 may influence the structure and formation of the amniotic cavity. Attachment of the extra-embryonic membranes creates tension on the underlying tissues pulling back the headfolds and creating the characteristic kink in the axis.

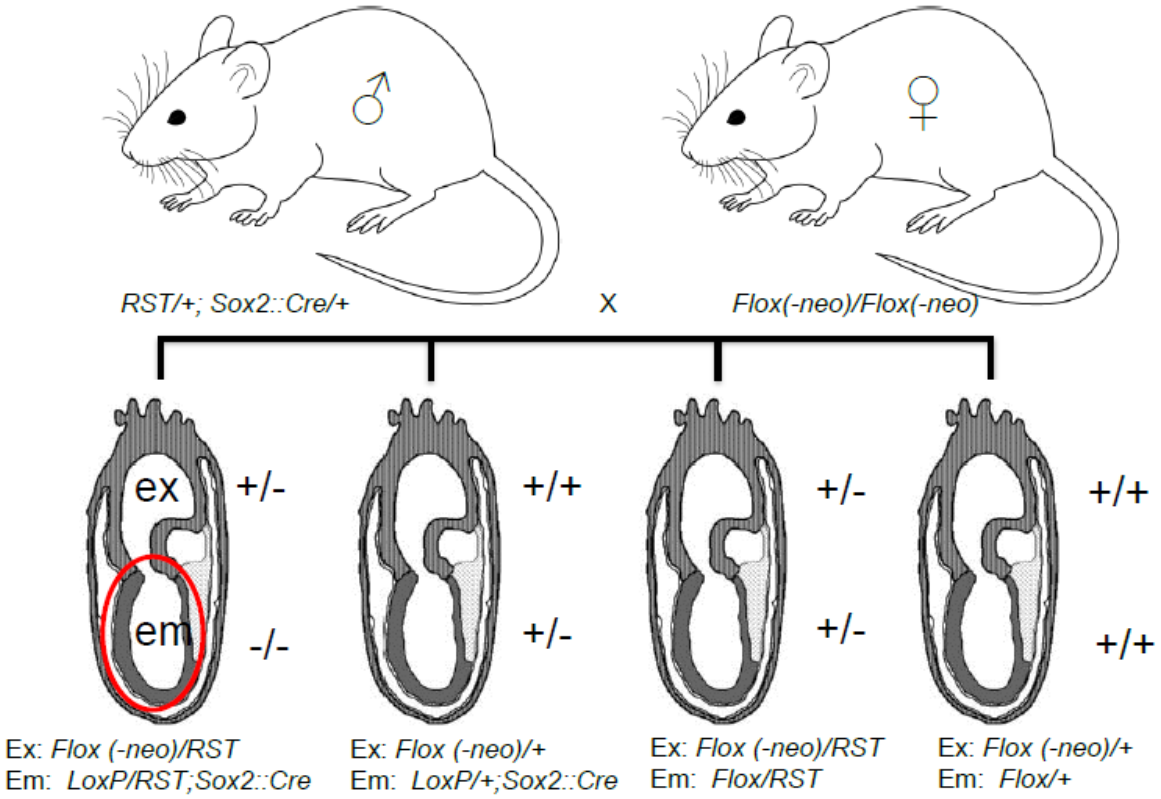

Figure 13: *Pofut2* epiblast mutant mating strategy
Floxed/Floxed females were mated with a *RST/+; Sox2::Cre/+* males. A quarter of the resulting embryos were expected to have inherited the *Pofut2 LoxP* and *RST434* allele in the epiblast. Embryo image: (Baldock et al., 1992)

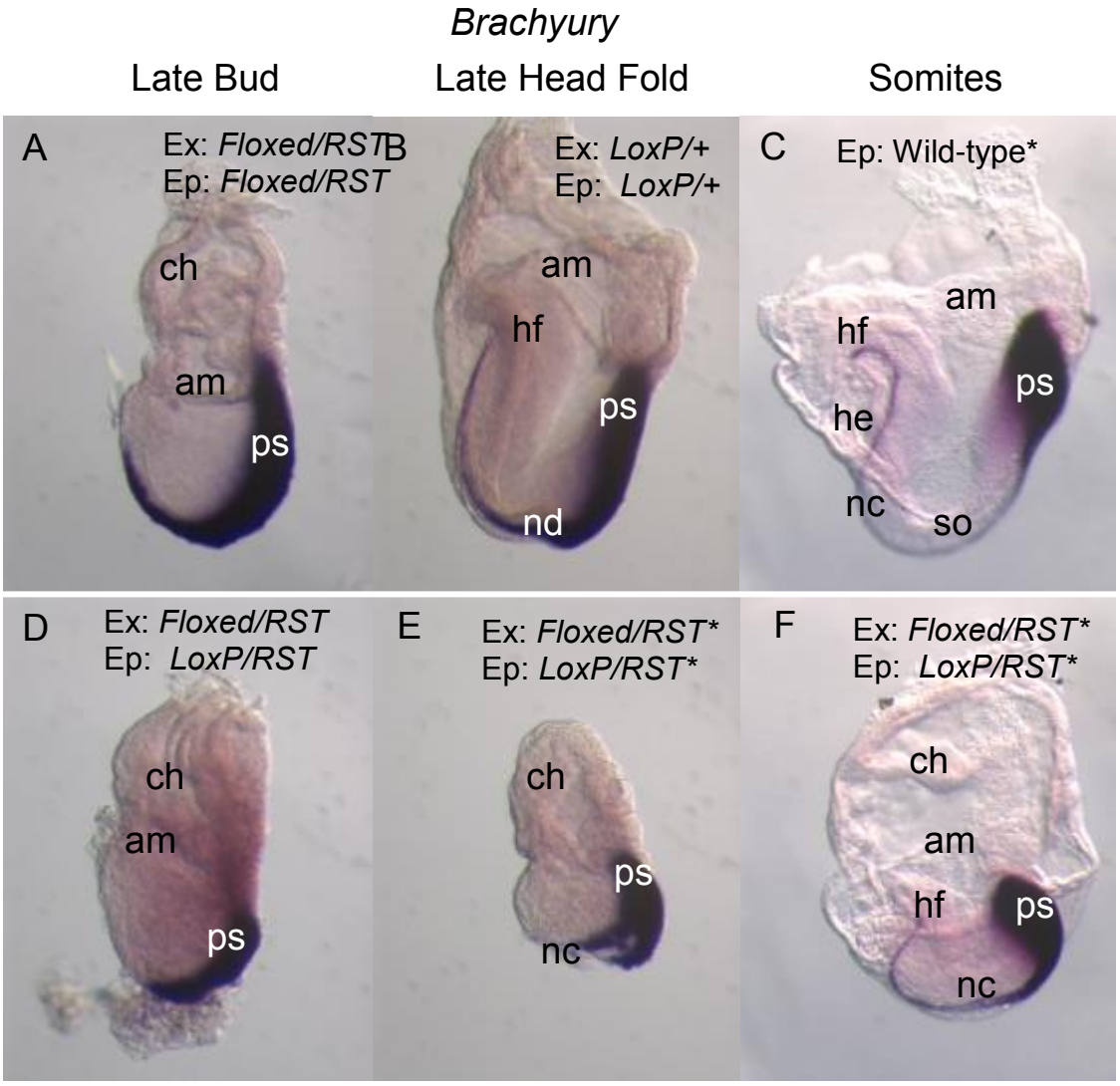

Figure 14: **Pofut2 is required for axial elongation**
(A-F) Comparison of *Brachyury (T),* marker of primitive streak and axial mesoderm, in *Sox2::Cre* conditional mutants. (A) At late bud stage in wild-type embryos, the axis has formed, as well as a defined amnion and chorion. (B) Wild-type in the late head fold stage have extended their axis and a node is present in the distal tip. Head folds are prominent and the amnion has extended. (C) By the somite stage, *Brachyury* is expressed from the regressed primitive streak and the notochord is formed. The head and heart are clearly visible and somites have begun to form along the axis. Overall (D-F) mutant embryos appear to have shortened axis in the posterior compared to their littermates. (D and E) Mutants at the late bud and late head fold stage have very disorganized extra-embryonic membranes. (E) Staining of *Brachyury* appears to be split in the late head fold mutant embryo. (F) By the somite stage, the axis is severely kinked in both the anterior and posterior of the embryo. The head and heart appear disorganized. In the extra-embryonic membranes, the chorion and amnion appear to remain joined. Anterior is left, Proximal is up. Chorion (ch) amnion (am) node (nd) notochord (nc) head folds (hf) heart (he) primitive streak (ps) somites(so) allantois (al)

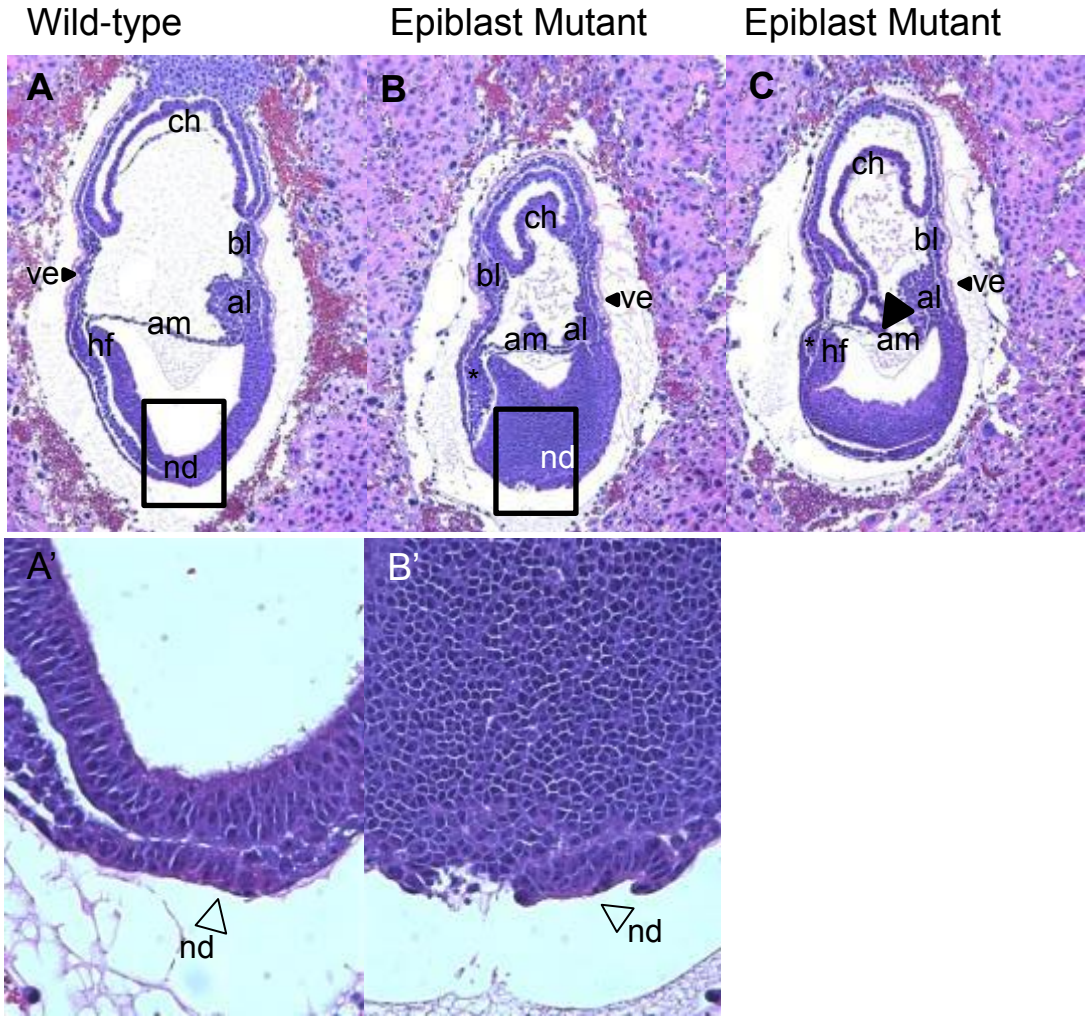

Figure 15: *Pofut2* epiblast mutants disrupt extra-embryonic membrane and node formation.
(A-C, A' and B') Comparison of H and E staining on E late 7.5 embryos. In the wild-type embryo (A) the node has formed at the distal end (A and A', open arrowhead). Head folds have formed in the anterior and the amnion and chorion have formed and displaced the extra-embryonic ectoderm. In the posterior, the allantois has begun to form and blood islands are present in the extra-embryonic mesoderm connecting the amnion and chorion. Epiblast mutants (B and C) have also formed a node (B and B'), but it appears disorganized. Adjacent to the node the tissue appears to be ruptured.(B'). Head folds have formed bit they appear to be bent back toward the posterior. To the anterior of the head folds, a mass of tissue has formed (C, asterisk) The amnion and chorion have formed, however they have remained connected in the anterior (C, arrowhead). Blood islands have also begun to form in the extra-embryonic mesoderm. The allantois has formed in the posterior. Anterior is left, Proximal is up. Chorion (ch) amnion (am) node (nd) head folds (hf) primitive streak (ps) allantois (al) blood islands (bi) visceral endoderm (ve)

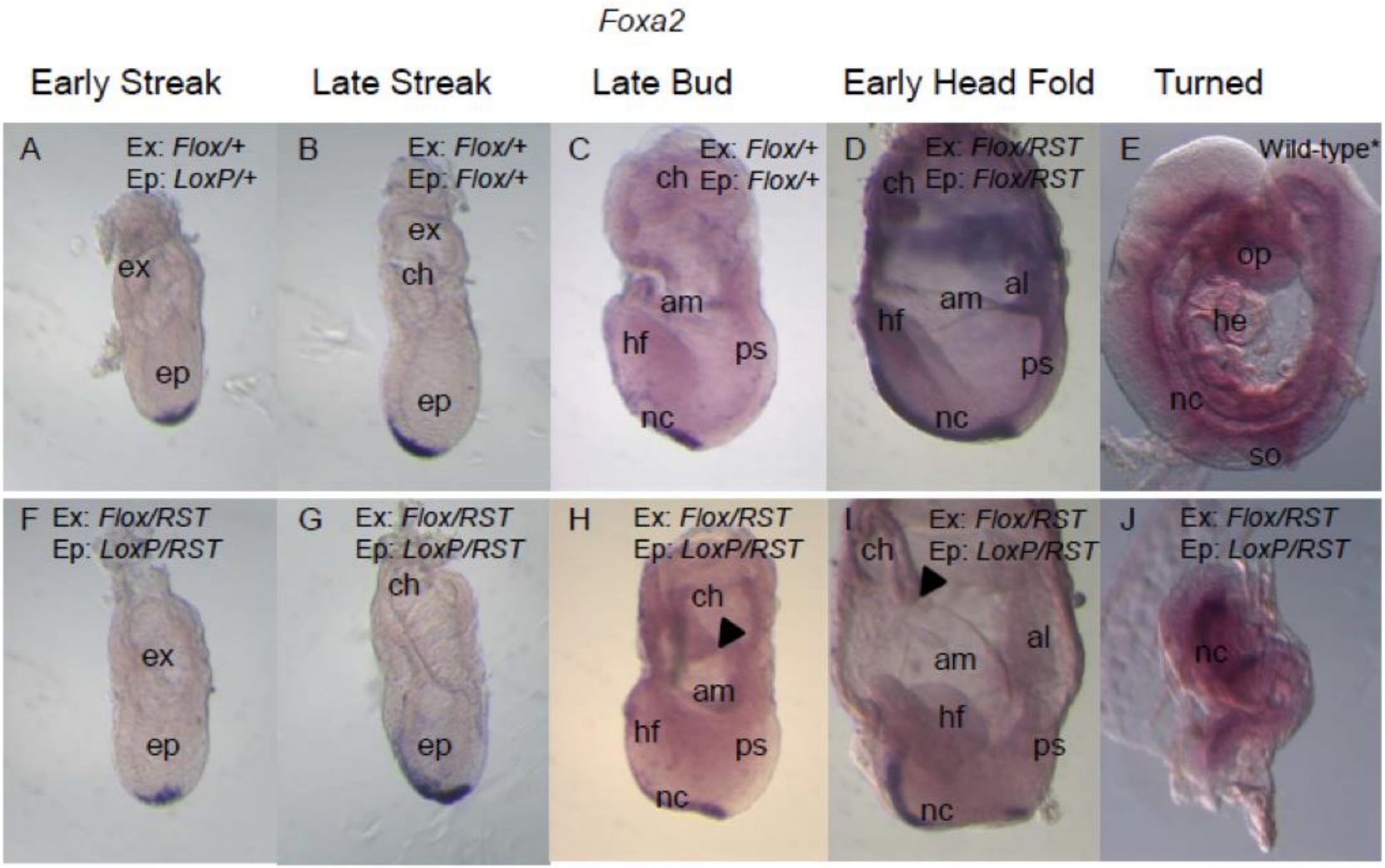
Foxa2
Early Streak
Late Streak
Late Bud
Early Head Fold
Turned
A
Ex: Flox/+
Ep: LoxP/+
ex
ep
B
Ex: Flox/+
Ep: Flox/+
ex
ch
ep
C
Ex: Flox/+
Ep: Flox/+
ch
am
hf
ps
nc
D
Ex: Flox/RST
Ep: Flox/RST
ch
am
al
hf
ps
nc
E
Wild-type*
op
he
nc
so
F
Ex: Flox/RST
Ep: LoxP/RST
ex
ep
G
Ex: Flox/RST
Ep: LoxP/RST
ch
ep
H
Ex: Flox/RST
Ep: LoxP/RST
ch
am
hf
ps
nc
I
Ex: Flox/RST
Ep: LoxP/RST
ch
am
al
hf
ps
nc
J
Ex: Flox/RST
Ep: LoxP/RST
nc

Figure 16: Definitive endoderm and notochord are formed in *Pofut2* epiblast mutants. (A-J) Comparison of dynamic *Foxa2* expression using whole mount *in situ* hybridization of embryos. (A and B) Wild-type embryos at early streak and late streak stages are able to specify definitive endoderm. Amnion and chorion in these embryos has not completely formed at this stage. At the late bud stage (C), *Foxa2* expression is observed within the notochord. Headfolds are present in the anterior and the amnion and chorion have formed, displacing the extra-embryonic ectoderm. As compared to late bud embryos, early head fold stage embryos (D) have extending *Foxa2* expression further up the notochord into the floorplate. The amnion and chorion are visible and the allantois has formed in the posterior. After the embryo has turned (E) expression of *Foxa2* is apparent in the notochord, floorplate, and foregut. An optic vessel and heart are visible in the anterior and somites have formed along the axis. (F and G) Epiblast mutant embryos at early streak and late streak stages express *Foxa2* in definitive endoderm, similar to wild-type littermates. The amnion and chorion in these mutants appear to be disorganized. At the late bud stage, epiblast mutants (H) express *Foxa2* in the notochord, and headfolds are visible. The axis takes on the distinct kinked shape and μL the amnion and chorion of the extra-embryonic membranes appear to be fused. In the early head fold stage epiblast mutants (J), *Foxa2* expression is discontinuous in the notochord and floorplate. The kinked appearance appears exasperated and the linkage between the amnion and chorion is visible. Head folds are present and the allantois is formed in the posterior. The turned epiblast mutant embryo (J) is significantly smaller than the wild-type littermate. *Foxa2* appears to be expressed in the notochord and floorplate, but is discontinuous. The embryo has failed to turn and distinct features are difficult to observe.
Anterior is left, Proximal is up. Chorion (ch) amnion (am) node (nd) head folds (hf) primitive streak (ps) allantois (al) blood islands (bl) visceral endoderm (ve)

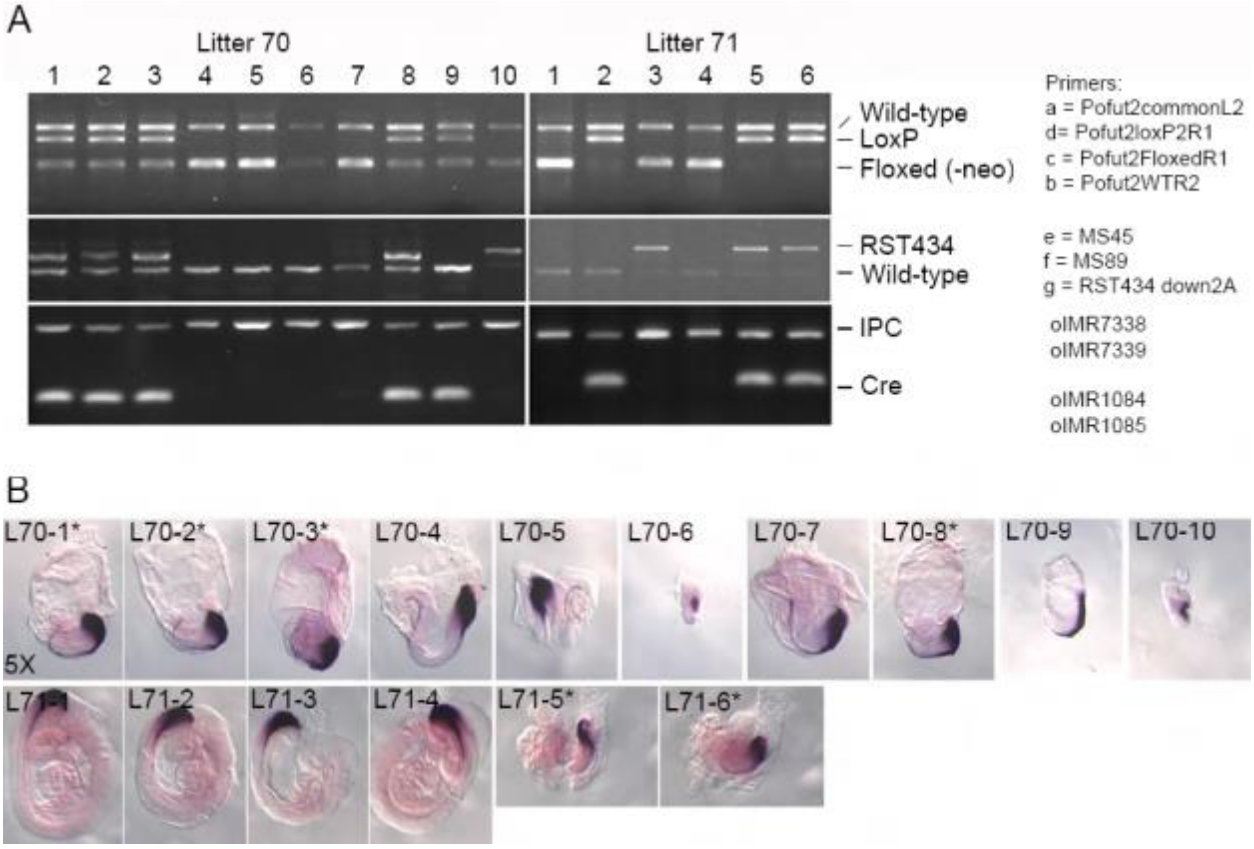

Figure 17: The definitive endoderm displaces the visceral endoderm
Embryos were genotyped after removal of the extra-embryonic tissues from the embryos (B). The resulting genotypes (A) demonstrated that the definitive endoderm had displaced the visceral endoderm indicated by loss of *Floxed* band in epiblast mutant embryos in Litter 71.

References

Aliferis, K., Marsal, C., Pelletier, V., Doray, B., Weiss, M.M., Tops, C.M., Speeg-Schatz, C., Lesnik, S.A., Dollfus, H., 2010. A novel nonsense B3GALTL mutation confirms Peters plus syndrome in a patient with multiple malformations and Peters anomaly. Ophthalmic genetics 31, 205-208.

Ang, S.L., Rossant, J., 1994. HNF-3 beta is essential for node and notochord formation in mouse development. Cell 78, 561-574.

Apte, S.S., 2004. A disintegrin-like and metalloprotease (reprolysin type) with thrombospondin type 1 motifs: the ADAMTS family. The international journal of biochemistry & cell biology 36, 981-985.

Arnold, S.J., Robertson, E.J., 2009. Making a commitment: cell lineage allocation and axis patterning in the early mouse embryo. Nat Rev Mol Cell Biol 10, 91-103.

Artus, J., Panthier, J.J., Hadjantonakis, A.K., 2010. A role for PDGF signaling in expansion of the extra-embryonic endoderm lineage of the mouse blastocyst. Development 137, 3361-3372.

Baldock, R., Bard, J., Kaufman, M., Davidson, D., 1992. A real mouse for your computer. BioEssays : news and reviews in molecular, cellular and developmental biology 14, 501-502.

Beck, S., Le Good, J.A., Guzman, M., Ben Haim, N., Roy, K., Beermann, F., Constam, D.B., 2002. Extraembryonic proteases regulate Nodal signalling during gastrulation. Nat Cell Biol 4, 981-985.

Beddington, R.S., Robertson, E.J., 1999. Axis development and early asymmetry in mammals. Cell 96, 195-209.

Blelloch, R., Anna-Arriola, S.S., Gao, D., Li, Y., Hodgkin, J., Kimble, J., 1999a. The gon-1 gene is required for gonadal morphogenesis in Caenorhabditis elegans. Developmental biology 216, 382-393.

Blelloch, R., Newman, C., Kimble, J., 1999b. Control of cell migration during Caenorhabditis elegans development. Current opinion in cell biology 11, 608-613.

Bonnafe, E., Touka, M., AitLounis, A., Baas, D., Barras, E., Ucla, C., Moreau, A., Flamant, F., Dubruille, R., Couble, P., Collignon, J., Durand, B., Reith, W., 2004. The transcription factor RFX3 directs nodal cilium development and left-right asymmetry specification. Molecular and cellular biology 24, 4417-4427.

Chen, C.I., Keusch, J.J., Klein, D., Hess, D., Hofsteenge, J., Gut, H., 2012. Structure of human POFUT2: insights into thrombospondin type 1 repeat fold and O-fucosylation. The EMBO journal 31, 3183-3197.

Cork, S.M., Van Meir, E.G., 2011. Emerging roles for the BAI1 protein family in the regulation of phagocytosis, synaptogenesis, neurovasculature, and tumor development. Journal of molecular medicine 89, 743-752.

de Vega, S., Iwamoto, T., Yamada, Y., 2009. Fibulins: multiple roles in matrix structures and tissue functions. Cellular and molecular life sciences : CMLS 66, 1890-1902.

Downs, K.M., Davies, T., 1993. Staging of gastrulating mouse embryos by morphological landmarks in the dissecting microscope. Development 118, 1255-1266.

Du, J., Takeuchi, H., Leonhard-Melief, C., Shroyer, K.R., Dlugosz, M., Haltiwanger, R.S., Holdener, B.C., 2010. O-fucosylation of thrombospondin type 1 repeats restricts epithelial to mesenchymal transition (EMT) and maintains epiblast pluripotency during mouse gastrulation. Developmental biology 346, 25-38.

Dubail, J., Apte, S.S., 2015. Insights on ADAMTS proteases and ADAMTS-like proteins from mammalian genetics. Matrix biology : journal of the International Society for Matrix Biology 44-46, 24-37.

Dubail, J., Aramaki-Hattori, N., Bader, H.L., Nelson, C.M., Katebi, N., Matuska, B., Olsen, B.R., Apte, S.S., 2014. A new Adamts9 conditional mouse allele identifies its non-redundant role in interdigital web regression. Genesis 52, 702-712.

Dufort, D., Schwartz, L., Harpal, K., Rossant, J., 1998. The transcription factor HNF3beta is required in visceral endoderm for normal primitive streak morphogenesis. Development 125, 3015-3025.

Enomoto, H., Nelson, C.M., Somerville, R.P., Mielke, K., Dixon, L.J., Powell, K., Apte, S.S., 2010. Cooperation of two ADAMTS metalloproteases in closure of the mouse palate identifies a requirement for versican proteolysis in regulating palatal mesenchyme proliferation. Development 137, 4029-4038.

George, E.L., Georges-Labouesse, E.N., Patel-King, R.S., Rayburn, H., Hynes, R.O., 1993. Defects in mesoderm, neural tube and vascular development in mouse embryos lacking fibronectin. Development 119, 1079-1091.

Hesselson, D., Newman, C., Kim, K.W., Kimble, J., 2004. GON-1 and fibulin have antagonistic roles in control of organ shape. Current biology : CB 14, 2005-2010.

Hofsteenge, J., Huwiler, K.G., Macek, B., Hess, D., Lawler, J., Mosher, D.F., Peter-Katalinic, J., 2001. C-mannosylation and O-fucosylation of the thrombospondin type 1 module. The Journal of biological chemistry 276, 6485-6498.

Holbourn, K.P., Acharya, K.R., Perbal, B., 2008. The CCN family of proteins: structure-function relationships. Trends in biochemical sciences 33, 461-473.

Kawamura, N., Sun-Wada, G.H., Aoyama, M., Harada, A., Takasuga, S., Sasaki, T., Wada, Y., 2012. Delivery of endosomes to lysosomes via microautophagy in the visceral endoderm of mouse embryos. Nature communications 3, 1071.

Kern, C.B., Wessels, A., McGarity, J., Dixon, L.J., Alston, E., Argraves, W.S., Geeting, D., Nelson, C.M., Menick, D.R., Apte, S.S., 2010. Reduced versican cleavage due to Adamts9 haploinsufficiency is associated with cardiac and aortic anomalies. Matrix biology : journal of the International Society for Matrix Biology 29, 304-316.

Kinder, S.J., Tsang, T.E., Quinlan, G.A., Hadjantonakis, A.K., Nagy, A., Tam, P.P., 1999. The orderly allocation of mesodermal cells to the extraembryonic structures and the anteroposterior axis during gastrulation of the mouse embryo. Development 126, 4691-4701.

Koo, B.H., Coe, D.M., Dixon, L.J., Somerville, R.P., Nelson, C.M., Wang, L.W., Young, M.E., Lindner, D.J., Apte, S.S., 2010. ADAMTS9 is a cell-autonomously acting, anti-angiogenic metalloprotease expressed by microvascular endothelial cells. The American journal of pathology 176, 1494-1504.

Kozma, K., Keusch, J.J., Hegemann, B., Luther, K.B., Klein, D., Hess, D., Haltiwanger, R.S., Hofsteenge, J., 2006. Identification and characterization of abeta1,3-glucosyltransferase that synthesizes the Glc-beta1,3-Fuc disaccharide on thrombospondin type 1 repeats. The Journal of biological chemistry 281, 36742-36751.

Kubota, Y., Nagata, K., Sugimoto, A., Nishiwaki, K., 2012. Tissue architecture in the Caenorhabditis elegans gonad depends on interactions among fibulin-1, type IV collagen and the ADAMTS extracellular protease. Genetics 190, 1379-1388.

Kumar, A., Lualdi, M., Loncarek, J., Cho, Y.W., Lee, J.E., Ge, K., Kuehn, M.R., 2014. Loss of function of mouse Pax-Interacting Protein 1-associated glutamate rich protein 1a (Pagr1a) leads to reduced Bmp2 expression and defects in chorion and amnion development. Developmental dynamics : an official publication of the American Association of Anatomists 243, 937-947.

Lee, J.D., Anderson, K.V., 2008. Morphogenesis of the node and notochord: the cellular basis for the establishment and maintenance of left-right asymmetry in the mouse.

Developmental dynamics : an official publication of the American Association of Anatomists 237, 3464-3476.

Lee, J.D., Silva-Gagliardi, N.F., Tepass, U., McGlade, C.J., Anderson, K.V., 2007. The FERM protein Epb4.1l5 is required for organization of the neural plate and for the epithelial-mesenchymal transition at the primitive streak of the mouse embryo. Development 134, 2007-2016.

Leonhard-Melief, C., Haltiwanger, R.S., 2010. O-fucosylation of thrombospondin type 1 repeats. Methods in enzymology 480, 401-416.

Lesnik Oberstein, S.A., Kriek, M., White, S.J., Kalf, M.E., Szuhai, K., den Dunnen, J.T., Breuning, M.H., Hennekam, R.C., 2006. Peters Plus syndrome is caused by mutations in B3GALTL, a putative glycosyltransferase. American journal of human genetics 79, 562-566.

Lewis, S.L., Tam, P.P., 2006. Definitive endoderm of the mouse embryo: formation, cell fates, and morphogenetic function. Developmental dynamics : an official publication of the American Association of Anatomists 235, 2315-2329.

Lighthouse, J.K., Zhang, L., Hsieh, J.C., Rosenquist, T., Holdener, B.C., 2011. MESD is essential for apical localization of megalin/LRP2 in the visceral endoderm. Developmental dynamics : an official publication of the American Association of Anatomists 240, 577-588.

Lim, J., Thiery, J.P., 2012. Epithelial-mesenchymal transitions: insights from development. Development 139, 3471-3486.

Lu, C.C., Brennan, J., Robertson, E.J., 2001. From fertilization to gastrulation: axis formation in the mouse embryo. Current opinion in genetics & development 11, 384-392.

Luo, Y., Koles, K., Vorndam, W., Haltiwanger, R.S., Panin, V.M., 2006. Protein O-fucosyltransferase 2 adds O-fucose to thrombospondin type 1 repeats. The Journal of biological chemistry 281, 9393-9399.

Luther, K.B., Haltiwanger, R.S., 2009. Role of unusual O-glycans in intercellular signaling. The international journal of biochemistry & cell biology 41, 1011-1024.

Madabhushi, M., Lacy, E., 2011. Anterior visceral endoderm directs ventral morphogenesis and placement of head and heart via BMP2 expression. Developmental cell 21, 907-919.

Maillette de Buy Wenniger-Prick, L.J., Hennekam, R.C., 2002. The Peters' plus syndrome: a review. Annales de genetique 45, 97-103.

McCulloch, D.R., Nelson, C.M., Dixon, L.J., Silver, D.L., Wylie, J.D., Lindner, V., Sasaki, T., Cooley, M.A., Argraves, W.S., Apte, S.S., 2009. ADAMTS metalloproteases generate active versican fragments that regulate interdigital web regression. Developmental cell 17, 687-698.

Morrissey, M.A., Keeley, D.P., Hagedorn, E.J., McClatchey, S.T., Chi, Q., Hall, D.H., Sherwood, D.R., 2014. B-LINK: a hemicentin, plakin, and integrin-dependent adhesion system that links tissues by connecting adjacent basement membranes. Developmental cell 31, 319-331.

Nandadasa, S., Foulcer, S., Apte, S.S., 2014. The multiple, complex roles of versican and its proteolytic turnover by ADAMTS proteases during embryogenesis. Matrix biology : journal of the International Society for Matrix Biology 35, 34-41.

Nandadasa, S., Nelson, C.M., Apte, S.S., 2015. ADAMTS9-Mediated Extracellular Matrix Dynamics Regulates Umbilical Cord Vascular Smooth Muscle Differentiation and Rotation. Cell reports 11, 1519-1528.

Pereira, P.N., Dobreva, M.P., Graham, L., Huylebroeck, D., Lawson, K.A., Zwijsen, A.N., 2011. Amnion formation in the mouse embryo: the single amniochorionic fold model. BMC developmental biology 11, 48.

Ricketts, L.M., Dlugosz, M., Luther, K.B., Haltiwanger, R.S., Majerus, E.M., 2007. O-fucosylation is required for ADAMTS13 secretion. The Journal of biological chemistry 282, 17014-17023.

Robertson, E.J., Norris, D.P., Brennan, J., Bikoff, E.K., 2003. Control of early anterior-posterior patterning in the mouse embryo by TGF-beta signalling. Philos Trans R Soc Lond B Biol Sci 358, 1351-1357; discussion 1357.

Silver, D.L., Hou, L., Somerville, R., Young, M.E., Apte, S.S., Pavan, W.J., 2008. The secreted metalloprotease ADAMTS20 is required for melanoblast survival. PLoS Genet 4, e1000003.

Soriano, P., 1997. The PDGF alpha receptor is required for neural crest cell development and for normal patterning of the somites. Development 124, 2691-2700.

Sulik, K., Dehart, D.B., Iangaki, T., Carson, J.L., Vrablic, T., Gesteland, K., Schoenwolf, G.C., 1994. Morphogenesis of the murine node and notochordal plate. Developmental dynamics : an official publication of the American Association of Anatomists 201, 260-278.

Tan, K., Duquette, M., Liu, J.H., Dong, Y., Zhang, R., Joachimiak, A., Lawler, J., Wang, J.H., 2002. Crystal structure of the TSP-1 type 1 repeats: a novel layered fold and its biological implication. The Journal of cell biology 159, 373-382.

Vasudevan, D., Haltiwanger, R.S., 2014. Novel roles for O-linked glycans in protein folding. Glycoconj J 31, 417-426.

Vasudevan, D., Takeuchi, H., Johar, S.S., Majerus, E., Haltiwanger, R.S., 2015. Peters Plus Syndrome Mutations Disrupt a Noncanonical ER Quality-Control Mechanism. Current biology : CB 25, 286-295.

Wang, J., Hamblet, N.S., Mark, S., Dickinson, M.E., Brinkman, B.C., Segil, N., Fraser, S.E., Chen, P., Wallingford, J.B., Wynshaw-Boris, A., 2006. Dishevelled genes mediate a conserved mammalian PCP pathway to regulate convergent extension during neurulation. Development 133, 1767-1778.

Wang, L.W., Dlugosz, M., Somerville, R.P., Raed, M., Haltiwanger, R.S., Apte, S.S., 2007. O-fucosylation of thrombospondin type 1 repeats in ADAMTS-like-1/punctin-1 regulates secretion: implications for the ADAMTS superfamily. The Journal of biological chemistry 282, 17024-17031.

Xu, X., Dong, C., Vogel, B.E., 2007. Hemicentins assemble on diverse epithelia in the mouse. The journal of histochemistry and cytochemistry : official journal of the Histochemistry Society 55, 119-126.

Xu, X., Xu, M., Zhou, X., Jones, O.B., Moharomd, E., Pan, Y., Yan, G., Anthony, D.D., Isaacs, W.B., 2013. Specific structure and unique function define the hemicentin. Cell & bioscience 3, 27.

Ybot-Gonzalez, P., Savery, D., Gerrelli, D., Signore, M., Mitchell, C.E., Faux, C.H., Greene, N.D., Copp, A.J., 2007. Convergent extension, planar-cell-polarity signalling and initiation of mouse neural tube closure. Development 134, 789-799.

Zhang, M., Bolfing, M.F., Knowles, H.J., Karnes, H., Hackett, B.P., 2004. Foxj1 regulates asymmetric gene expression during left-right axis patterning in mice. Biochemical and biophysical research communications 324, 1413-1420.

Supplemental Material

Supplementary Table 1: Primers for amplification of *Pofut2* alleles

Allele	Primer Name	Sequence 5' → 3'	Amplification
Conditional PCR			
LoxP	Pofut2CommonL2 (a)	TTTACCCACTTGCCGAGCAG	689 bp
	Pofut2LoxP2R1 (d)	GGAGAGGGGTCTAGACTCTGAAA	
Floxed	Pofut2CommonL2 (a)	TTTACCCACTTGCCGAGCAG	479 bp
	Pofut2FloxedR1 (c)	TTCGGATCGTTGAAGAAGGAGGT	
Wild-type	Pofut2CommonL2 (a)	TTTACCCACTTGCCGAGCAG	823 bp
	Pofut2WTR2 (b)	CTCAGGGGTAGCTGGTCTCT	
RST PCR			
Wild-type	MS45 (e)	GAGGCCGGGAGTACTGGGAT	955 bp
	MS89 (f)	ATCTTCGTCCAGTCTTCCTCC	
RST434	MS45 (e)	GAGGCCGGGAGTACTGGGAT	1344bp
	RST434 down 2A (g)	GGTTGCCAGAACCAGCAAACTGAA	
Sox2::Cre PCR			
IPC	oIMR7338 (forward)	CTAGGCCACAGAATTGAAAGATCT	324 bp
	oIMR7339	GTAGGTGGAAATTCTAGCATCATCC	
Sox2:Cre	oIMR1084	GCGGTCTGGCAGTAAAAACTATC	~100 bp
	oIMR1085	GTGAAACAGCATTGCTCTCACTT	

Supplementary Table 2: *Pofut2* allele RT-PCR Primer Chart

Rx #	Name	POFUT2 Allele	5' → 3' Sequence	Size
1	Pofut2 Exon 4 Common Left (a')	Wild-type	GAATGTCTCCTGCCTGTCCG	451
	Pofut2 Exon 8 Common Right (b')	Possible Alternative Splice	CTCCTTCCTGATGGCGTCTG	325
2	Pofut2 Exon 4 Common Left (a')	RST	GAATGTCTCCTGCCTGTCCG	452
	Gene-trap reverse (-) (d')		CCTCTGTCCAGAGTCAGGGT	
3	GAPDH forward1	GAPDH	GGAGAGTGTTTCCTCGTCCC	377
	GAPDH Reverse 1		CCTTTTGGCTCCACCCTTCA	
4	GAPDH forward 2	GAPDH	TCCACCACCCTGTTGCTGTA	452
	GAPDH reverse 2		ACCACAGTCCATGCCATCAC	
5	POFUT exon 5 forward (c')	Check RST reverse primer in genome—genomic tail DNA	AACTTCTCAGATCTGCGGGC	231
	Gene-trap reverse (-) (d')		CCTCTGTCCAGAGTCAGGGT	

* Refer to Chapter 2 Methods for specifics on isolation of mRNA from E 8.5 embryos.

Supplementary Protocol 1: Embryo Genotyping Protocol

Embryo lysis

1. After *in situ*, remove embryos from 80% glycerol and placed into individual tubes using a Pasteur pipette.
2. Using a pulled Pasteur pipettes (pull using Bunsen burner), remove all glycerol and add 50 µL of 1x PBS and rinse for 1 hour.
3. Remove PBS with pulled pipette avoiding removing the embryo and replace with 20-50 µL(dependent on size- E 6.5 to E 8.5) of embryo lysis buffer and incubate overnight to one week in 55 ºC incubator.
4. Confirm the embryos are dissolved, if not dissolved add 20 µL lysis buffer and incubate overnight
5. heat inactivate for 10 min at 95 ºC and store at -20 ºC

Embryo Lysis Buffer (makes 1.5 mL—aliquot without Proteinase K and freeze
150 µL 10x Invitrogen PCR buffer
45 µL 50mM $MgCl_2$
15 µL DTT
1260 µL HPLC water
10 µL Proteinase K
1.5 mL Total

PCR

1. Add 10 µL of 1X PCR Reaction (below) to each labeled tube (keep on ice)
2. Add 2.0µL of embryo lysate sample
3. Flick tube with finger and centrifuge down
4. Place in thermocycler and choose correct program
5. Once complete, remove from thermocycler and add 2 µL of 10X loading dye and centrifuge
6. Load samples in 2% 50 mL agarose gel (made with 1X TBE) and run for 1 hr at 100 mV

1x PCR Reaction
8.95µL 1x Platinum Taq High Fidelity PCR Buffer (below)
1.00µL Primer mix
0.05µL Platinum Taq Hifi DNA Polymerase (5u/ µL)
Total= 10.0µL

1x Platinum Taq High Fidelity PCR Premix

1.25µL 10x Platinum Taq Hifi Buffer
0.5 µL 50mM $MgSO_4$
0.025µL 100mM dATP
0.025µL 100mM dTTP
0.025µL 100mM dGTP
0.025µL 100mM dCTP
7.1 µL milliQ water
Total= 8.95µL

PCR Programs		
POFUT2CN 94ºC—2 min 94ºC—30 s 61ºC—30 s 72ºC—30 s (x30 cycles) 72ºC—5 min 15ºC—hold Program used in genotyping the *Pofut2* wild-type, *Floxed* and *LoxP* alleles.	**RSTWT30** 94ºC—2 min 94ºC—30s 63ºC—30 s 72ºC—2 min (x30 cycles) 72ºC—10 min 15ºC—hold Program used in genotyping the *Pofut2* wild-type and *RST434* alleles.	**CREEMB** 94ºC—3 min 94ºC—30 s 63ºC—30 s 72ºC—30 s (x35 cycles) 72ºC—10 min 15ºC--hold Program used in genotyping the *Sox2::Cre* and Internal Positive Control.

Supplemental Protocol 2: *In situ* Hybridiztion Protocol
All manipulations using transwells use 1mL volumes for solutions unless otherwise stated

Preparation of embryos for *In situ* Hybridization

1. Transfer the (E 6.5 to E 8.5) embryos into the transwells with 1mL PTW
   PTW→ Add 500uL 10% Tween-20 with 50mL depc PBS
2. Wash twice (10minutes each) with 1mL PTW.
3. Bleach in 5:1 Methanol:30% H_2O_2 for 10 minutes in dark with shaker.4.
4. Rinse 3 times (5 minutes) in 100% Methanol
5. Transfer to another well of 100% methanol and store in -20ºC freezer
   -Can be stored for up to a month in freezer.

Day 1

<u>Pretreatment and hybridization</u>

1. Rehydrate embryos with 75%, 50%, 25% methanol:PTW for 10 minutes each.
   -1mL of fresh methanol:PTW in each well
2. Wash twice with PTW 10 minutes each (up to 30 min. each)
3. Wash once with PTW for 5 minutes
4. Rinse with 1:1 PTW:hybrid buffer and let embryos settle
   <**CAUTION**: embryos turn to REALLY transparent >
5. Rinse with 1 mL hybrid buffer and let embryos settle.
6. Wash with 1 mL hybrid buffer at 65ºC (rotate for 30 min, stationary for 30 min)
7. Replace with **1.5** mL pre-warmed hybrid buffer containing 1 µg/ml DIG labeled RNA probe (5-25 µL of purified probe in 1.5 ml hybridization mix)
   At 65C, rotate for1-2 hrs and stationary overnight

Hybrid buffer

Stock Solution	Preparation	Final Conc.	25mL	50mL
Ultrapure formamide	Aliq. And freeze	50%	12.5	25
SSC (20x pH 5)	DEPC autoclave	1.3x SSC	1.6	3.25
EDTA (0.5M, pH 8)	DEPC autoclave	5mM	0.25	0.5
Yeast RNA (20 mg/mL)	DEPC H_2O	50 µg/mL	62.5uL	125uL
10% Tween-20	DEPC H_2O	0.2%	0.5	1mL
10% CHAPS	DEPC H_2O	0.5%	1.25mL	2.5mL
Heparin (50 mg/mL)	DEPC H_2O	100ug/mL	50 uL	100uL
DEPC H_2O	DEPC autoclave		8.75 mL	17.5 mL

Day 2

Post-hybridization washes

1. Rinse twice (5 min) with pre-warmed (65ºC) hybrid buffer
2. Wash for 10 min at 65C with pre-warmed hybridization mix
3. Wash twice for 30 min. at 65ºC with pre-warmed (65C) washing solution
4. Wash for 10 min. at 65C with pre-warmed 1:1 washing solution:MABT
5. Rinse 3 times (5 min) with MABT.
6. Wash twice (30 min) with MABT.
7. Wash (1 hour) at room temperature with MABT (600µL) and 10% BBR (150µL)
8. Wash and rock (1 hour) at room temperature with MABT (600µL) and 10% BBR (150µL)
9. Replace with 750 µL with MABT (600µL) and 10% BBR (150µL) and1/2000 to 1/5000 dilution of anti-DIG-AP antibody
   Incubate o/n at 4ºC.

Wash Solution

Stock Solution	Final Conc.	25mL	50mL
Ultrapure formamide	50%	12.5mL	25mL
20x SCC (pH 5.0)	1x SCC	1.25mL	2.5mL
10% Tween-20	0.1%	0.25mL	0.5mL
DEPC H_2O		11mL	22mL

MABT (Malic Acid Buffer with Tween)

Stock Solution	Final Conc.	1L
Maleic Acid	100mM	11.6 g
NaCl	150mM	8.7g
10% Tween-20	0.1%	10mL

Adjust the pH with NaOH.

Boehringer Blocking Reagent (BBR)

Make 10% stock in MAB (MABT without Tween-20) by heating to dissolve, autoclave, aliquot and store at -20C Make up to 6ml per hybridization tube. Heat at 65C to dissolve.

Day 3

Post Antibody Washes

1. Rinse 3 times (5 min) with MABT
2. Wash and rock 5 times (1hr) in1 ml MABT
3. Wash and rock overnight in1 ml MABT

Day 4

Histochemistry

1. Wash and rock twice for 10 min and once for 1hr with NTMT
2. Incubate with 1.5 ml NTMT + 6.75 µL NBT + 5.25 µL BCIP
   -Rock for first 20 min in dark
   -Continue to let color develop stationary up to 3 days.
3. When color has developed to desire extent (30 min to 3 days), wash 3 times (5 min) with PTW.

NTMT (make fresh from stocks on the day of use)

Stock Solution	Final conc.	50mL	10mL
5 M NaCl	100mM	1mL	0.2 mL
1 M Tris-HCl (pH 9.5)	100mM	5mL	1mL
1 M $MgCl_2$	50mM	2.5mL	0.5mL
10% Tween-20	1%	5mL	1mL
H_2O		36.5mL	7.3mL

Post-*in situ*

1. Re-fix in 4% paraformaldehyde 2 hr or at room temperature or overnight at 4ºC.
2. Wash 3 times with PTW.
3. Transfer embryos into 50% glycerol (filtered) in small Petri dish
4. Transfer embryos into 80% glycerol (filtered) in small Petri dish
5. Transfer embryos into 1% agarose gel plate filled with 80% glycerol (filtered).

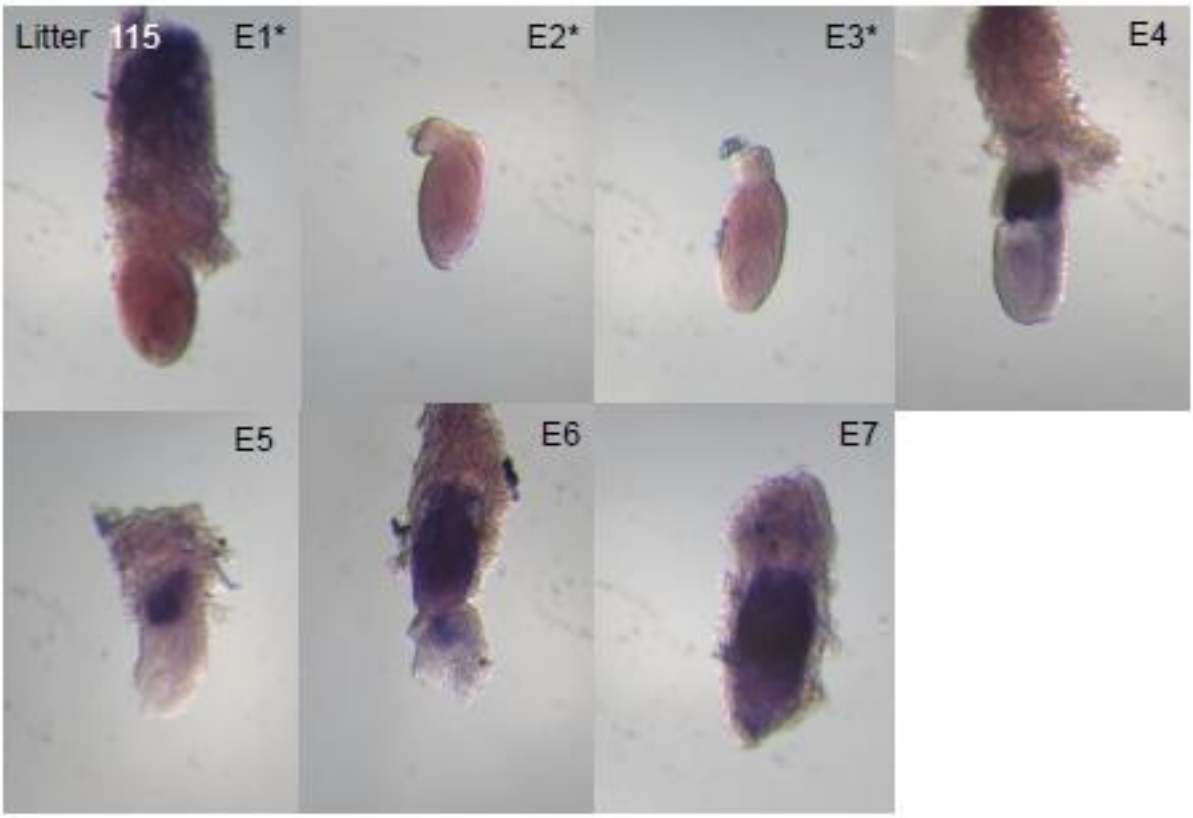

Supplementary Figure 1: *Pofut2 LoxP* intercross Litter 115 *Bmp4 in situ* at E 7.5.
The asterisks represent *Pofut2* mutants as determined by embryo morphology.

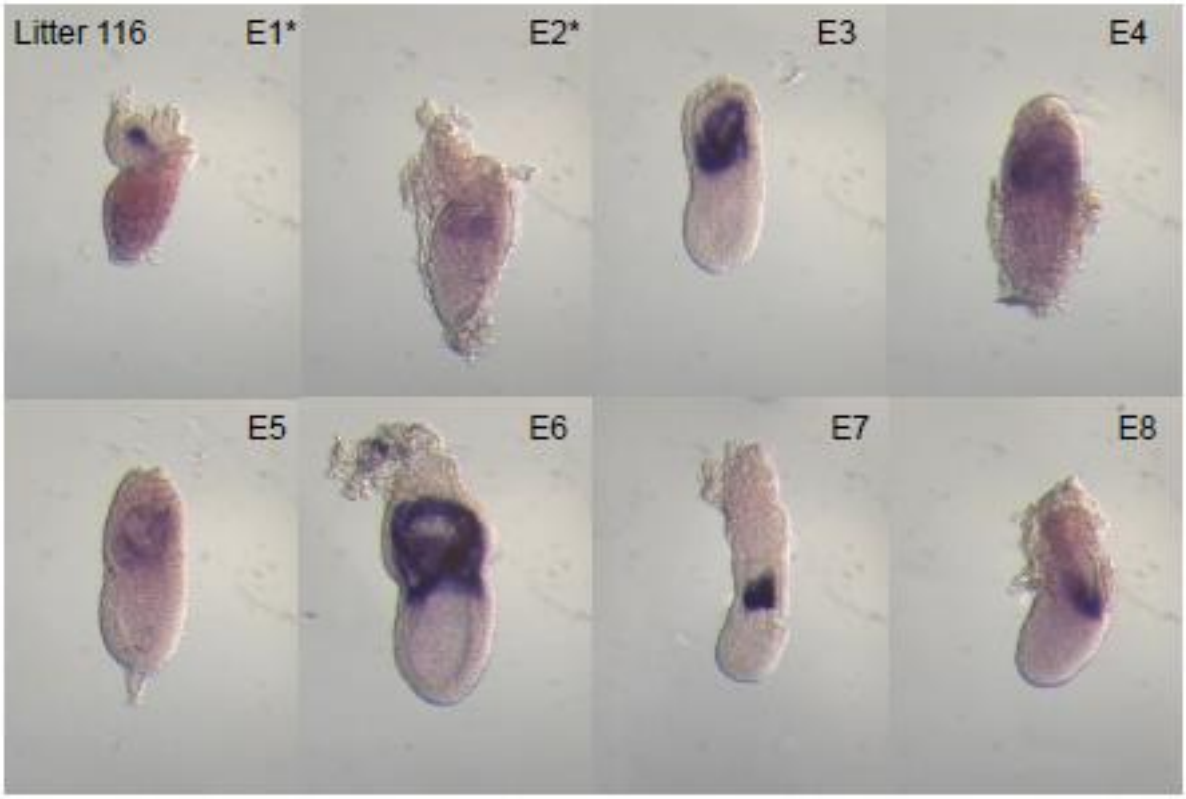

Supplementary Figure 2: *Bmp4* expression of Litter 116 *RST434* gene-trap intercross at E 7.5.
The asterisks represent *Pofut2* mutants as determined by embryo morphology.

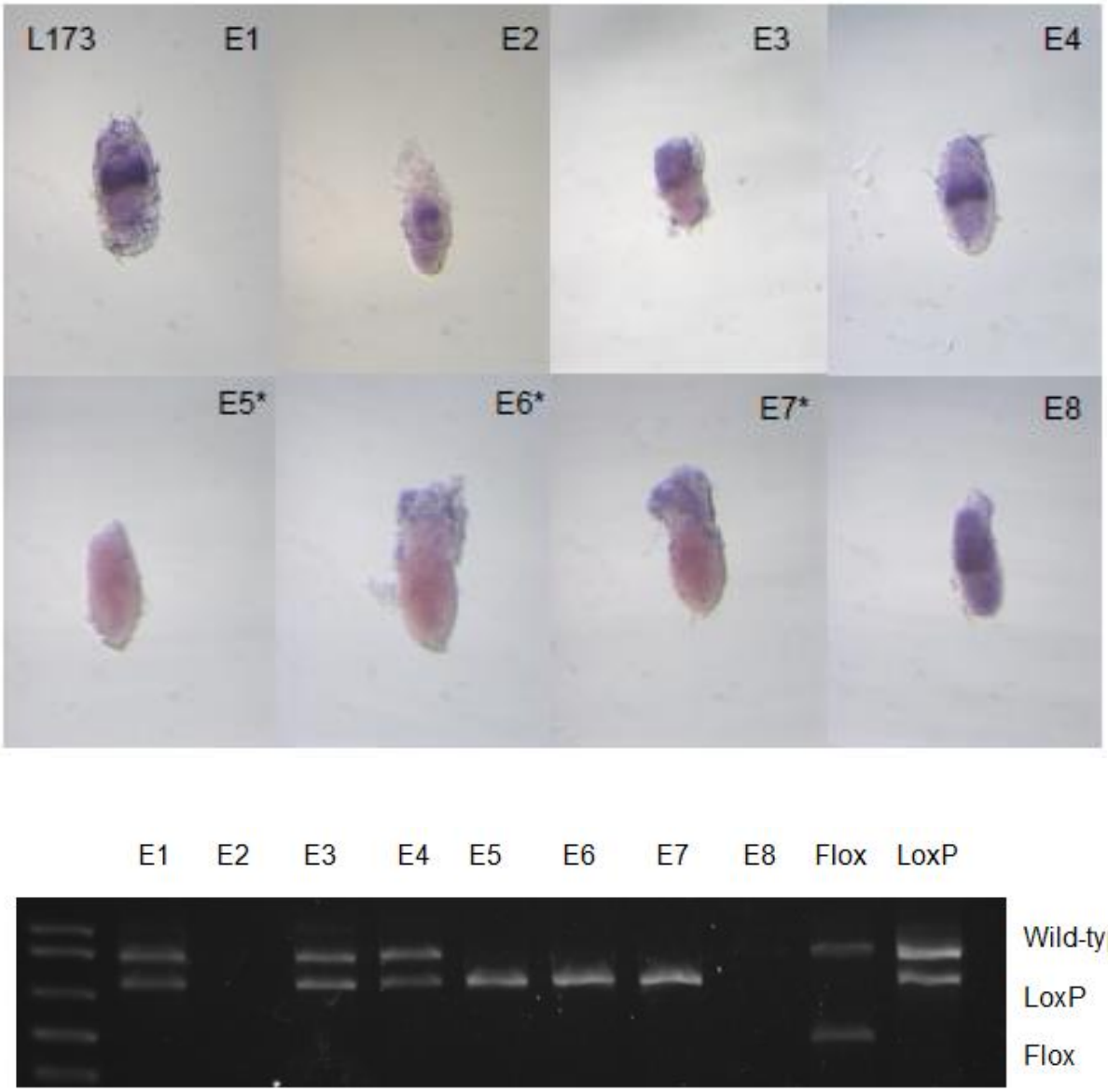

Supplementary Figure 3: *Bmp4 in situ* of *Pofut2 LoxP* intercross L175 at E 6.5. Genotypes of E2 and E8 were not determined, as the PCR reaction did not work. Based on PCR there were three LoxP/LoxP homozygotes in this litter indicated by asterisks.

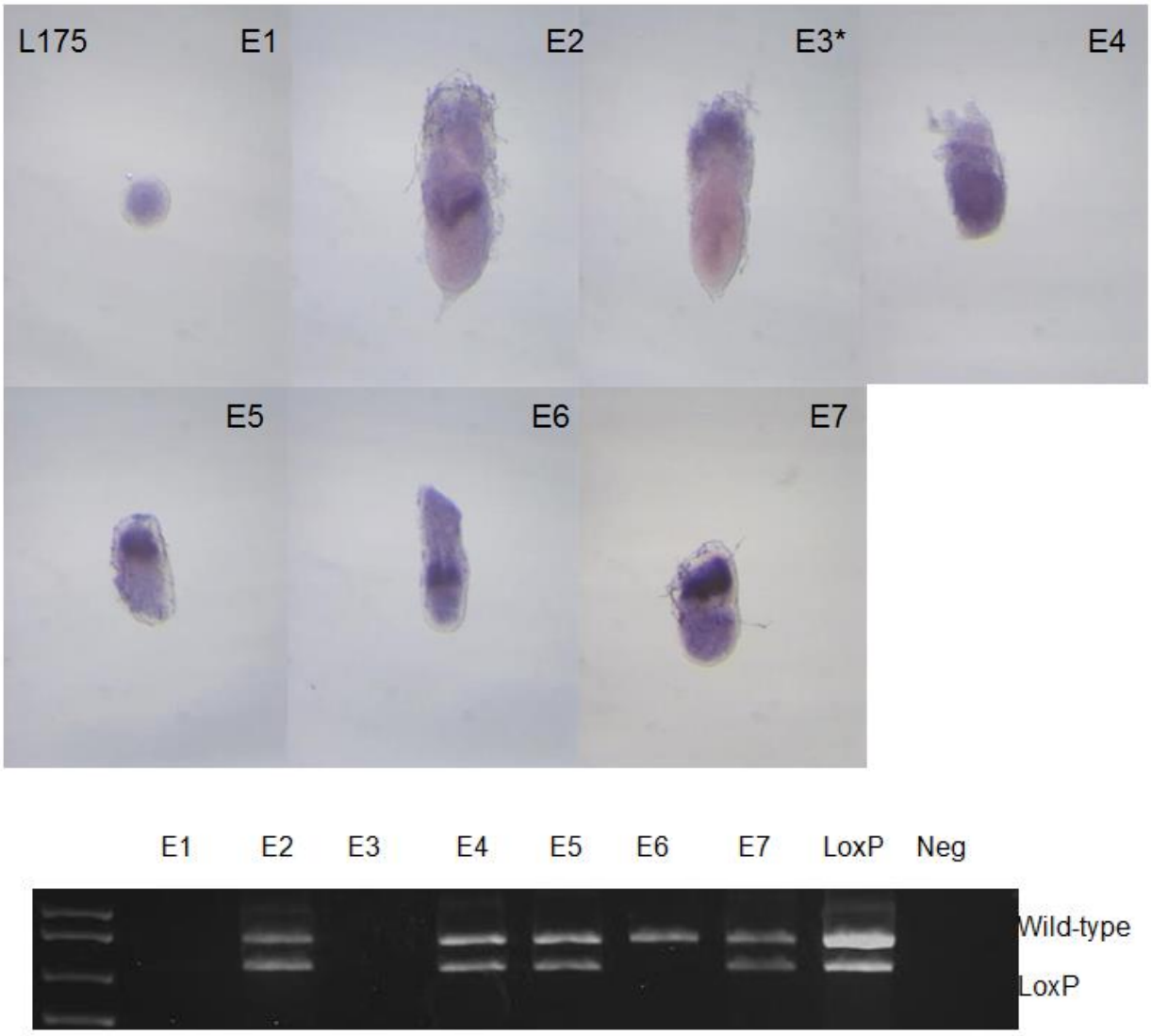

Supplementary Figure 4: *Bmp4 in situ* of *Pofut2 LoxP* intercross L175 at E 6.5. Genotypes of E1 and E3 were not determined, as the PCR reaction did not work. E3 appears mutant by morphology. Based on PCR there were no other no other LoxP/LoxP homozygotes in this litter.

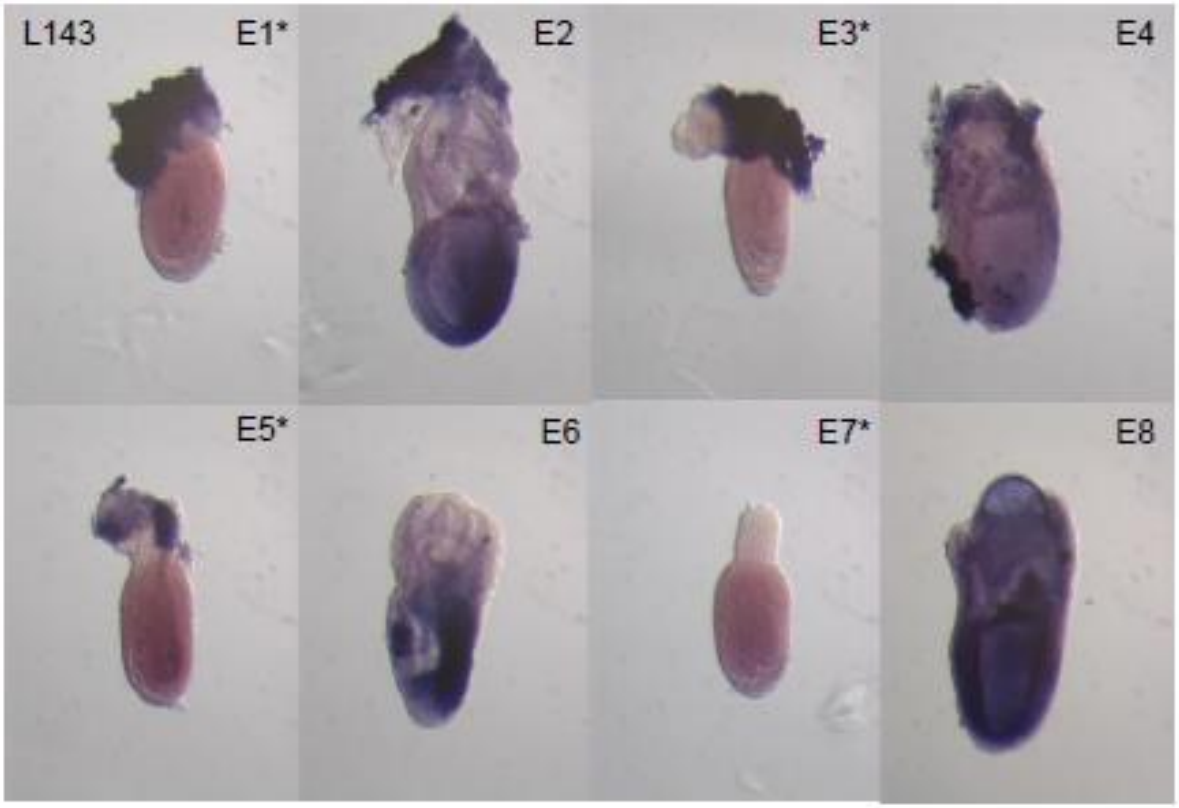

Supplementary Figure 5: *Snail in situ* of *Pofut2 RST434* intercross L143 at E 7.5.
The asterisks represent *Pofut2* mutants as determined by embryo morphology.

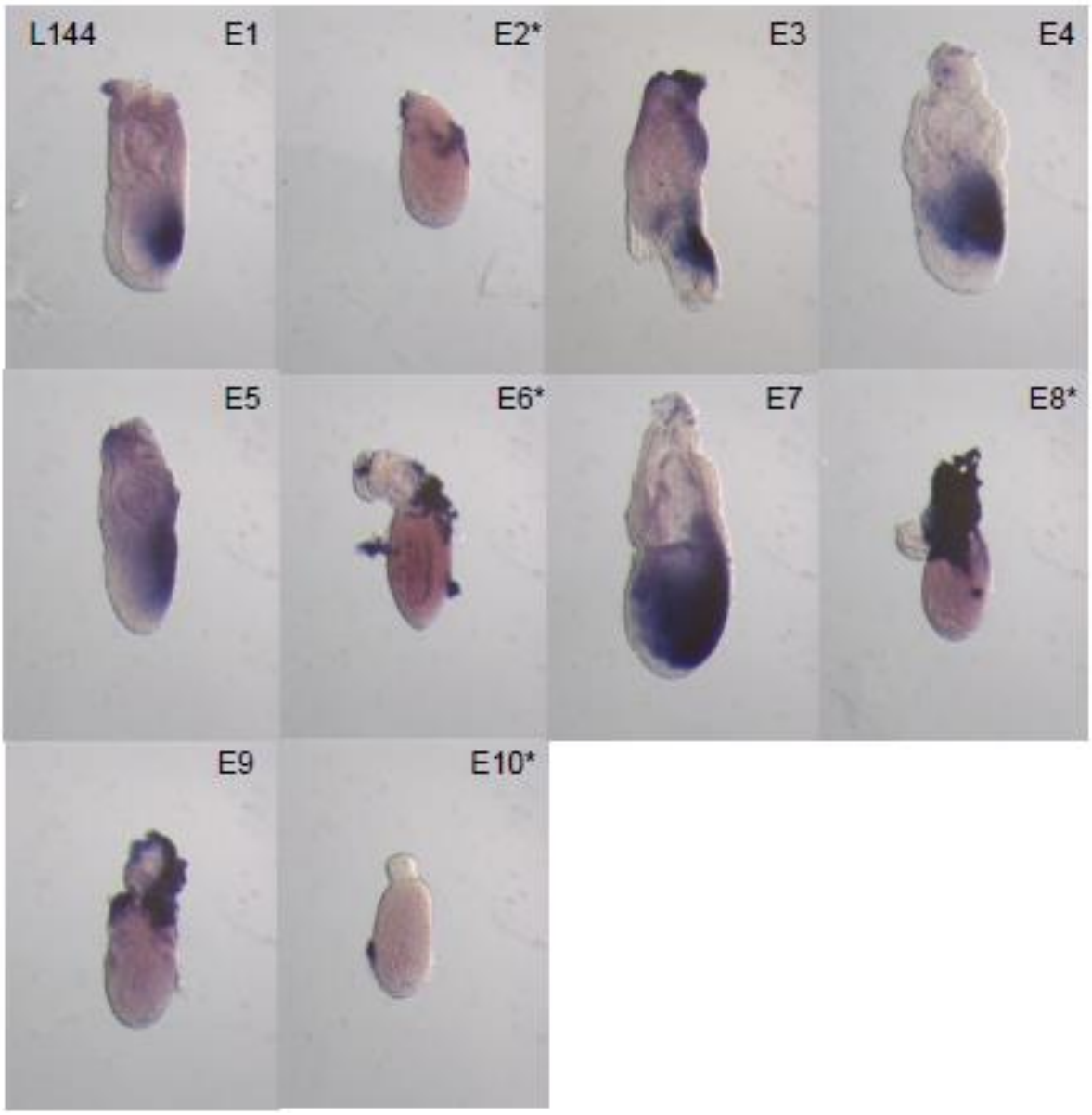

Supplementary Figure 6: *Snail in situ* of *Pofut2 RST434* intercross L144 at E 7.5.
The asterisks represent *Pofut2* mutants as determined by embryo morphology.

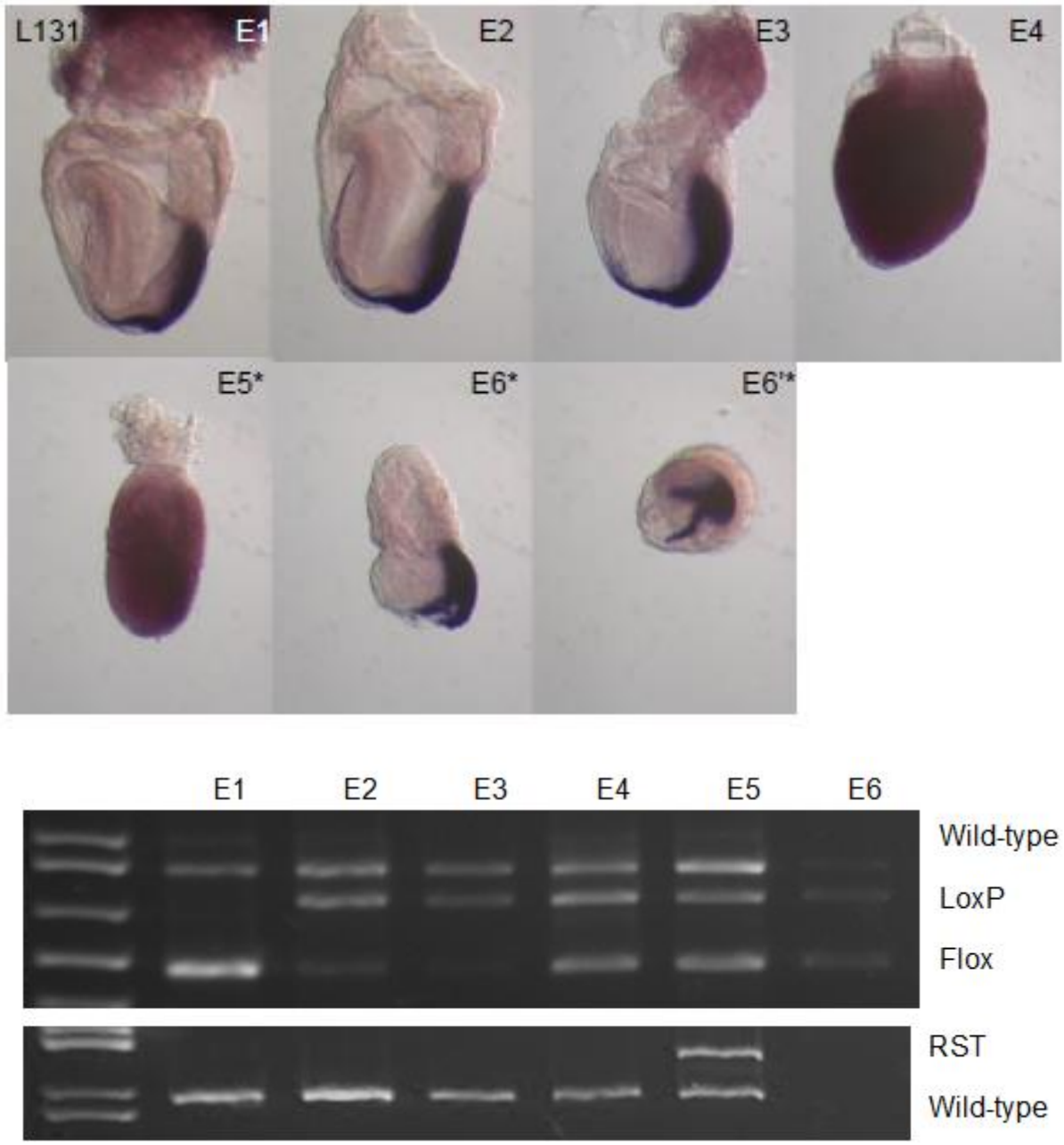

Supplementary Figure 7: *Brachyury in situ* of *Pofut2 Sox2::Cre* Cross L131 at late E 7.5.

E5 genotyped as a *Pofut2* epiblast mutant. E6 appeared abnormal, but was not confirmed by PCR since the RST434 allele did not work for this embryo. No Cre.

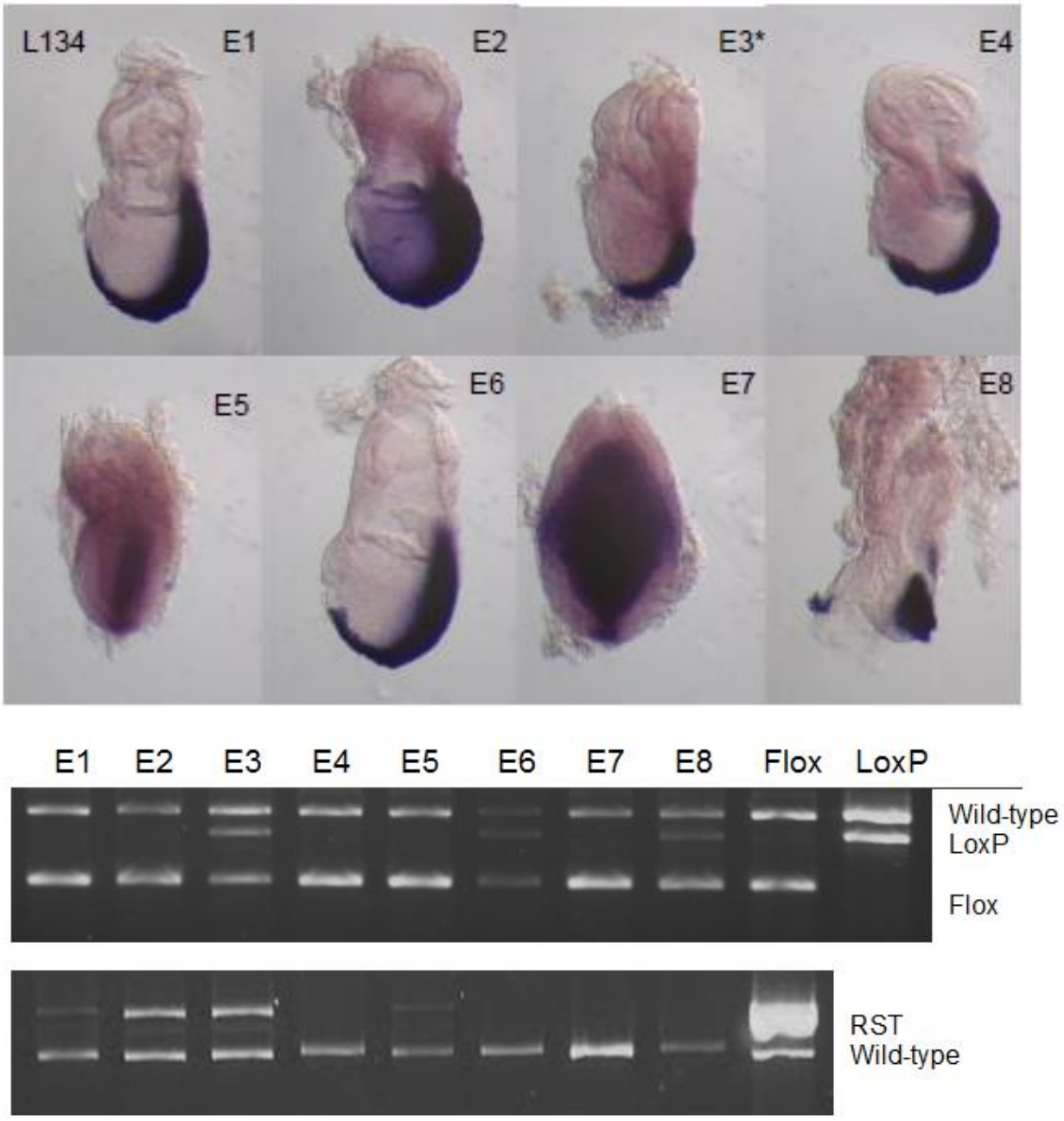

Supplementary Figure 8: *Brachyury in situ* of *Pofut2 Sox2::Cre* Cross L134 at late E 7.5

The asterisks represent *Pofut2* mutants as determined by PCR genotyping.

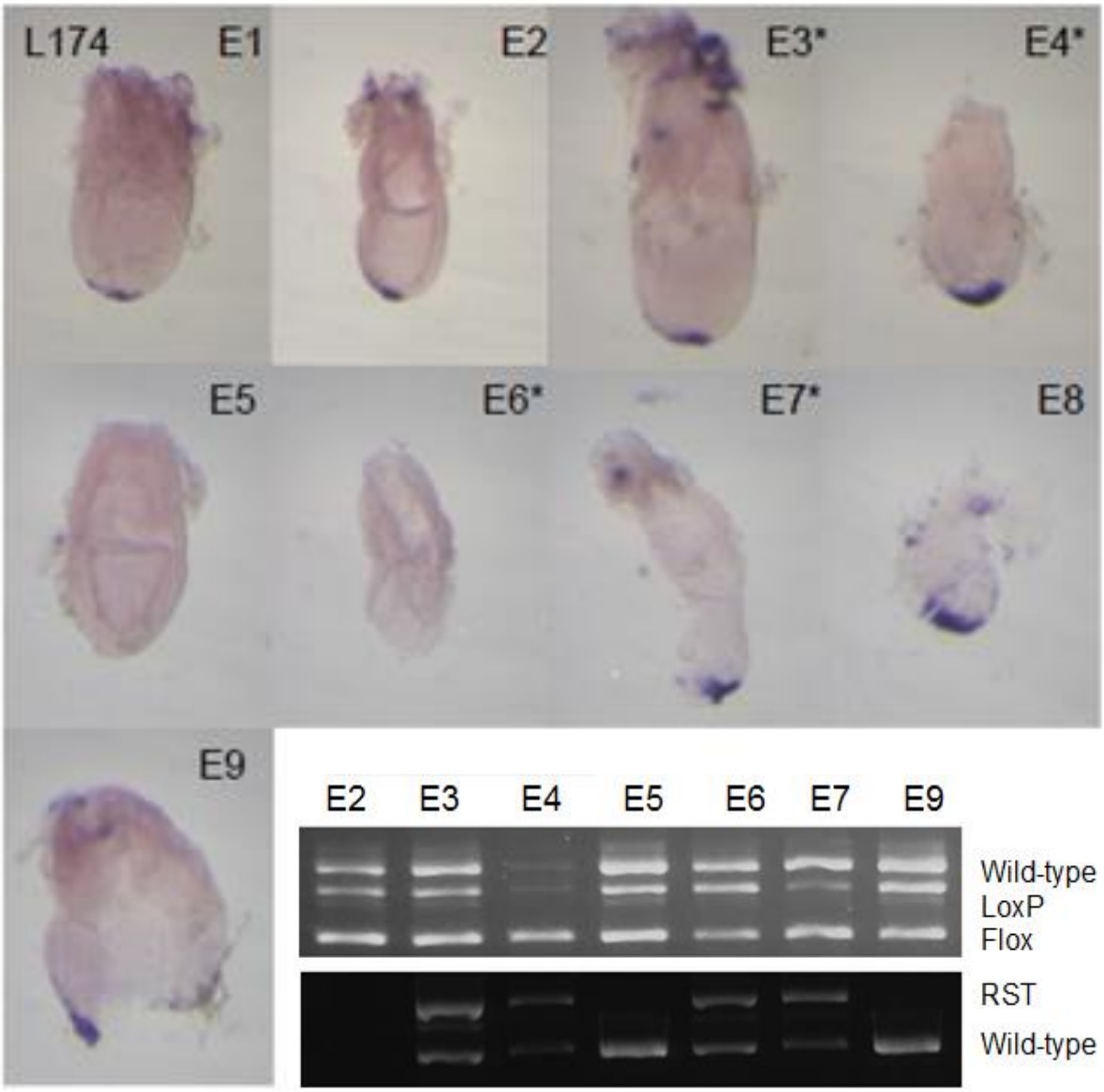

Supplementary Figure 9: *Foxa2 in situ* of *Pofut2 Sox2::Cre* Cross L174 at late E 7.5.
The asterisks represent *Pofut2* mutants as determined by PCR genotyping. E1 and E8 were lost and not confirmed by PCR. No Cre.

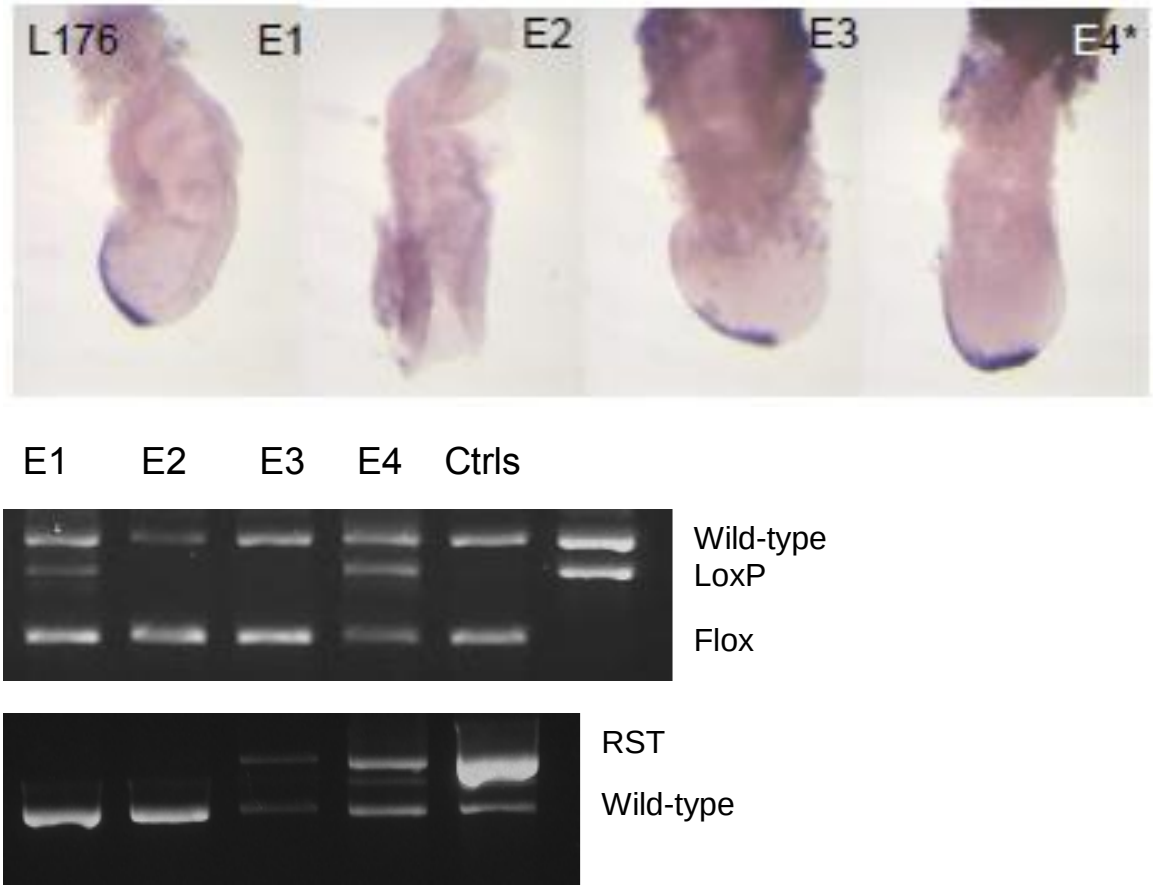

Supplementary Figure 10: *Foxa2 in situ* of *Pofut2 Sox2::Cre* Cross L176 at late E 7.5.
The asterisks represent *Pofut2* mutants as determined by PCR genotyping.

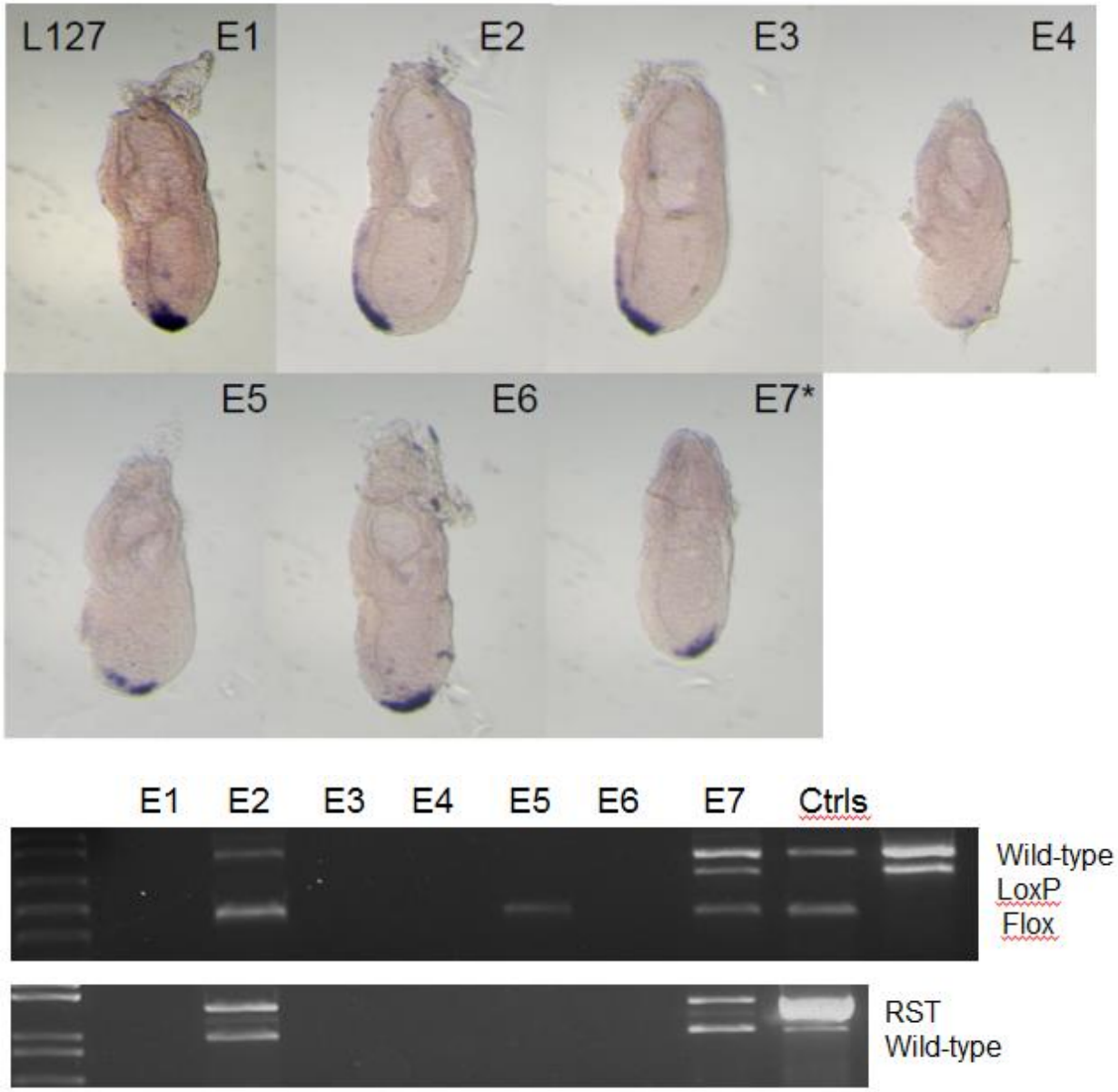

Supplementary Figure 11: *Foxa2 in situ* of *Pofut2 Sox2::Cre* Cross L127 at E 7.5. The asterisks represent *Pofut2* mutants as determined by PCR genotyping. Only E2 and E3 were informative and the remaining embryos were not confirmed by PCR since the *LoxP, Floxed,* and *RST434* alleles did not work for these embryo. Embryos were not evaluated for Cre.

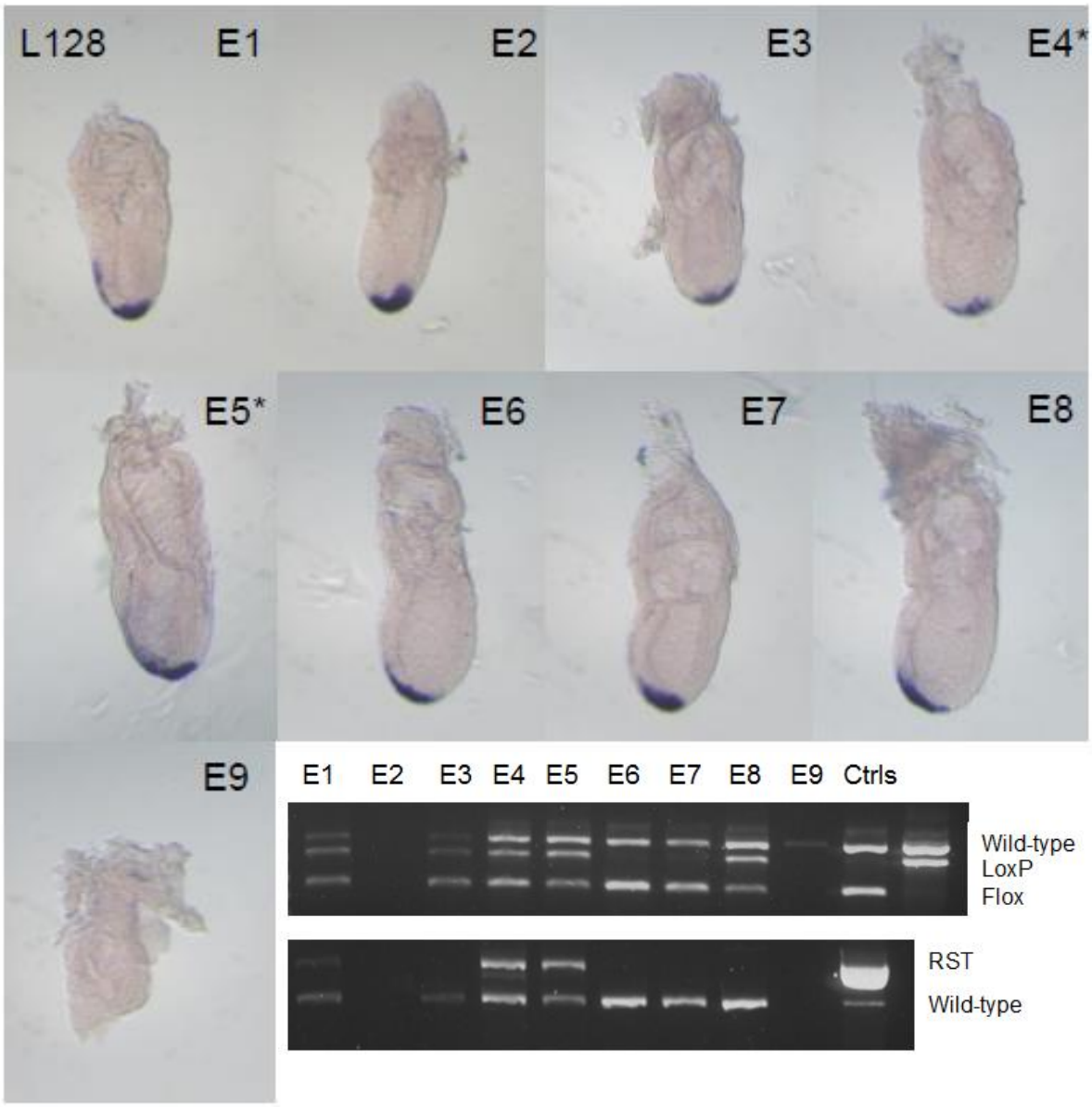

Supplementary Figure 12: *Foxa2 in situ* of *Pofut2 Sox2::Cre* Cross L128 at E 7.5. The asterisks represent *Pofut2* mutants as determined by PCR genotyping. E2 and E9 appeared normal, but were not confirmed by PCR since the *LoxP, Floxed,* and *RST434* alleles did not work for these embryo. Embryos were not evaluated for Cre.

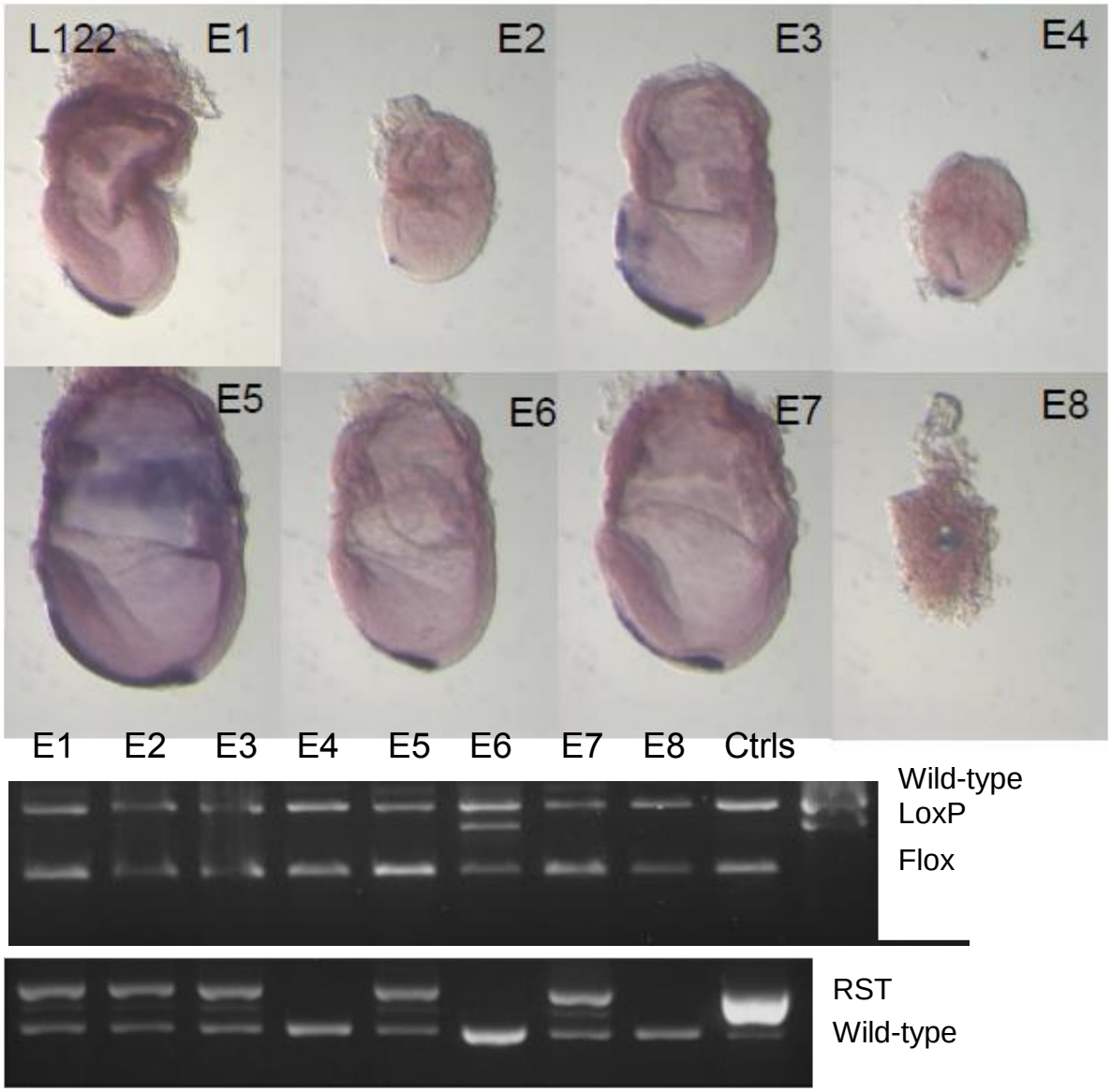

Supplementary Figure 13: *Foxa2 in situ* of *Pofut2 Sox2::Cre* Cross L128 at late E 7.5.
The asterisks represent *Pofut2* mutants as determined by PCR genotyping. Embryos were not evaluated for Cre.

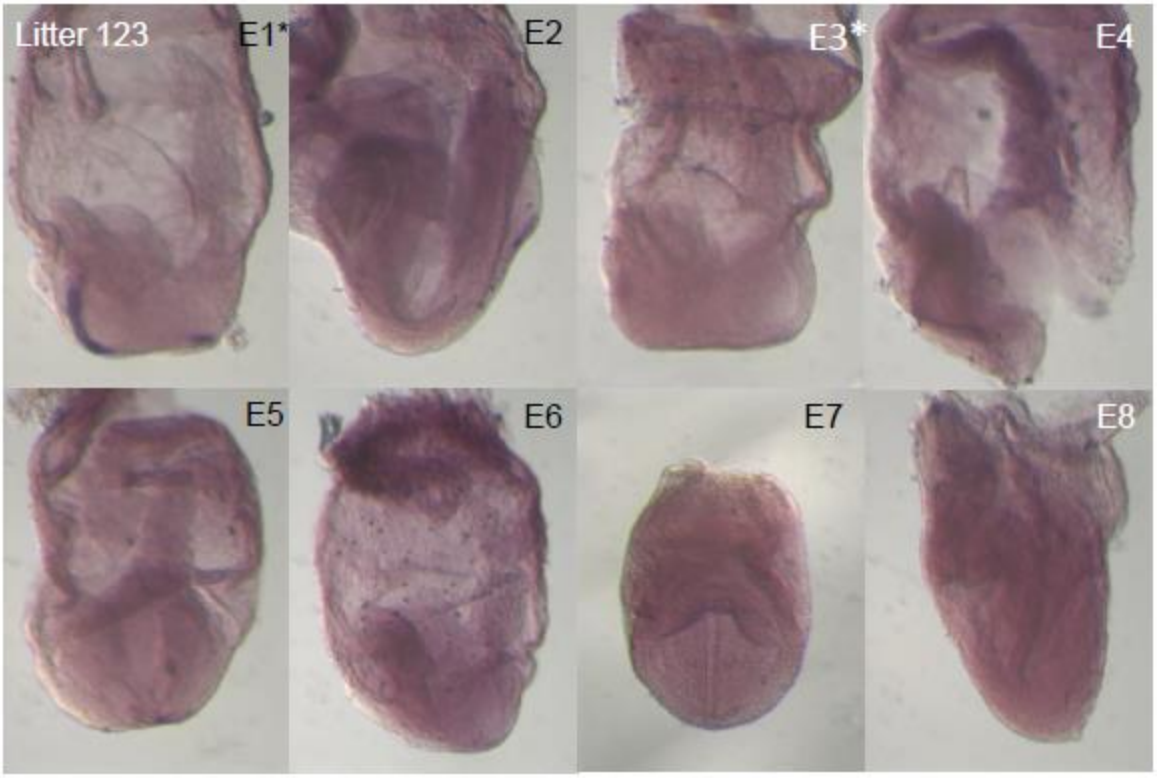

Supplementary Figure 14: *Foxa2 in situ* of *Pofut2 Sox2::Cre* Cross L123 at late E 7.5.
The asterisks represent *Pofut2* mutants as determined by morphology.

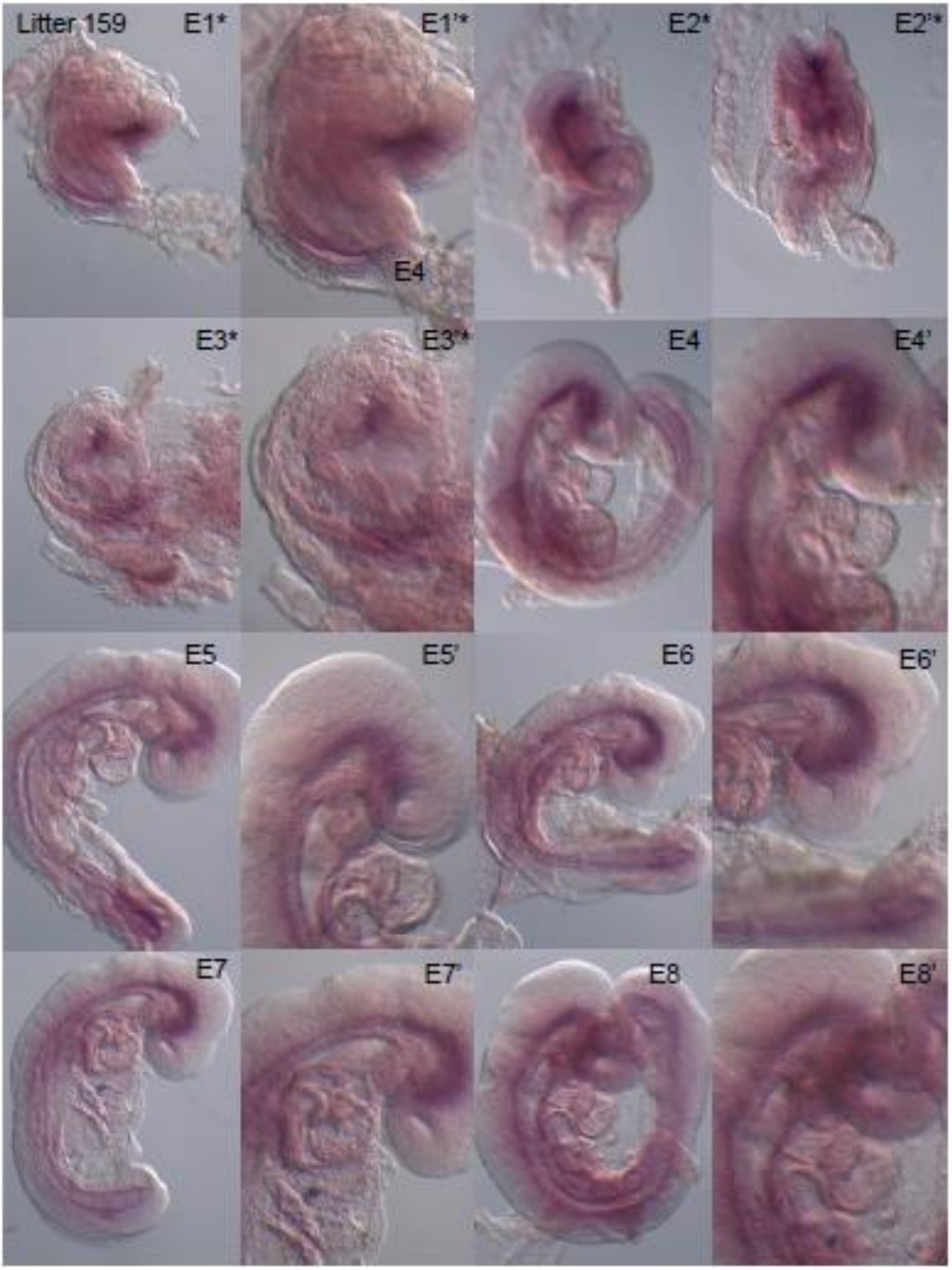

Supplementary Figure 15: *Foxa2 in situ* of *Pofut2 Sox2::Cre* Cross L159 at E 8.5.
The asterisks represent *Pofut2* mutants as determined by morphology.

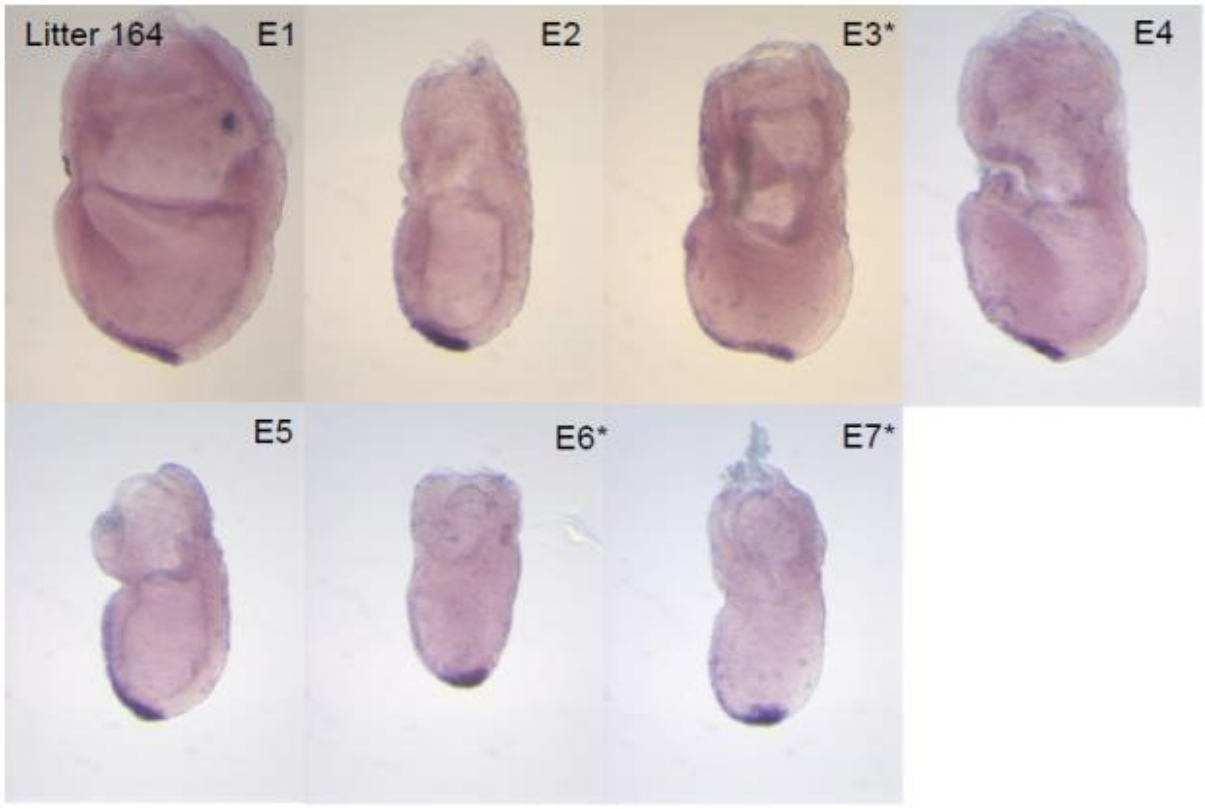

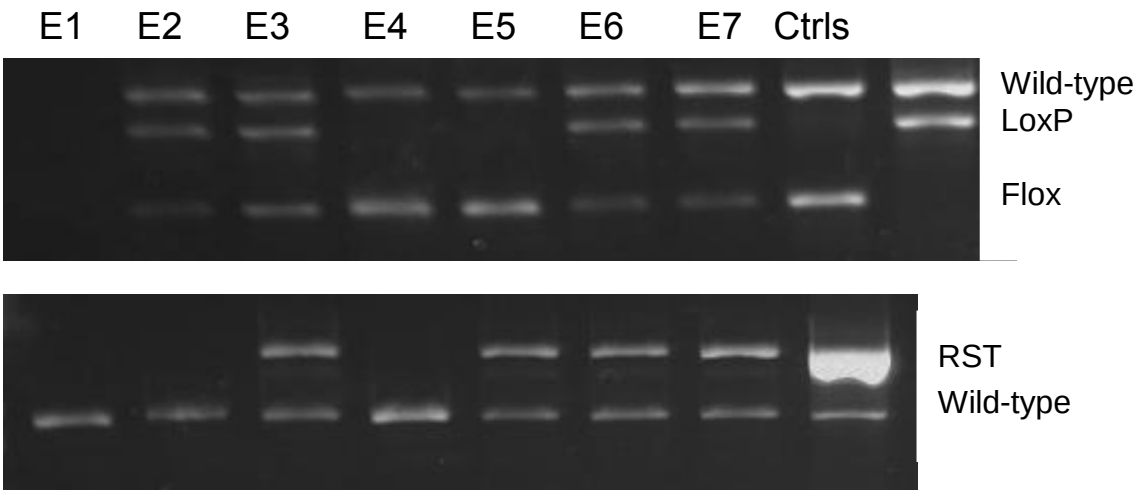

Supplementary Figure 16 *Foxa2 in situ* of *Pofut2 Sox2::Cre* Cross L164 at late E 7.5.
The asterisks represent *Pofut2* mutants as determined by PCR genotyping. No Cre genotyping was performed.

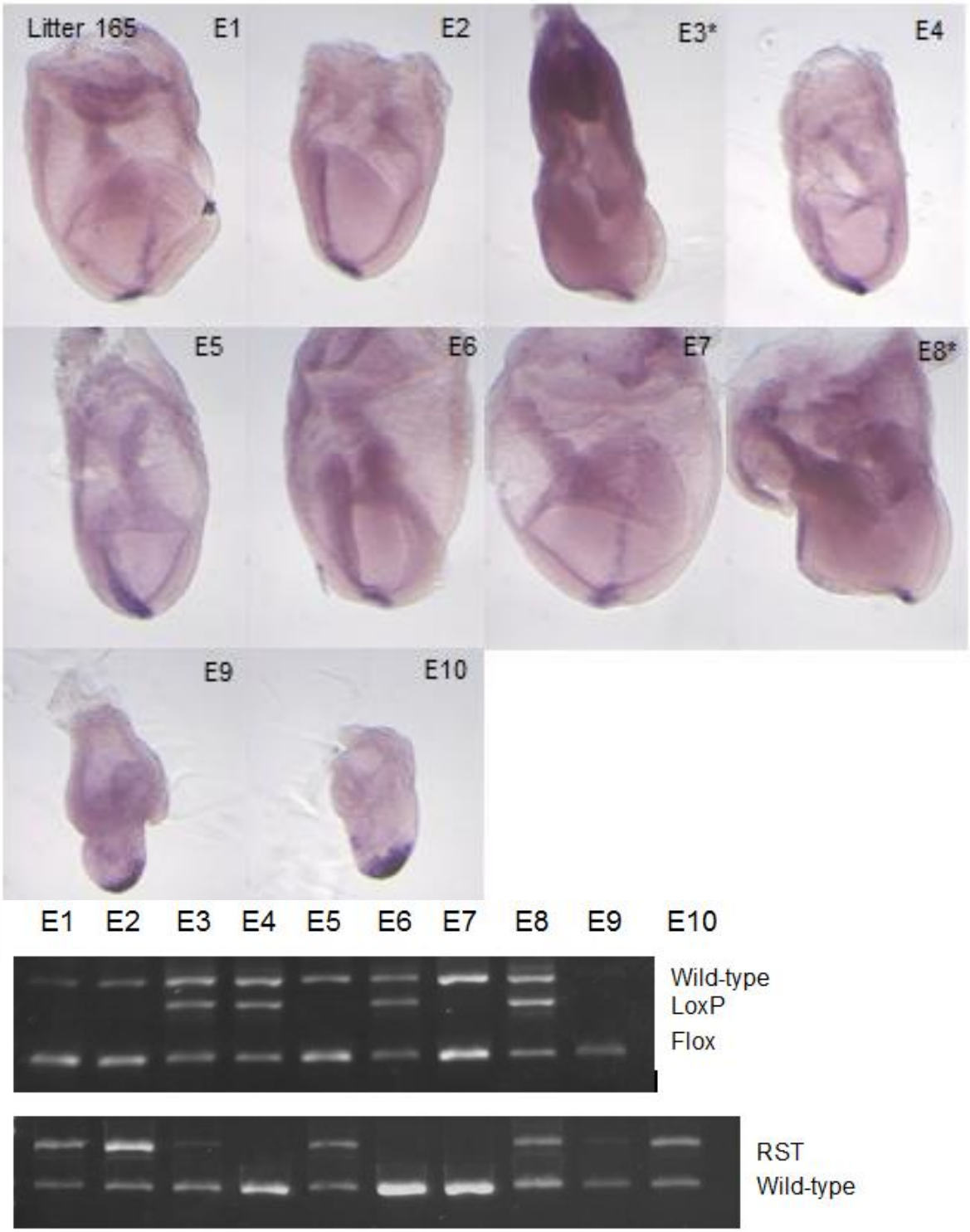

Supplementary Figure 17: *Foxa2 in situ* of *Pofut2 Sox2::Cre* Cross L165 at late E 7.5.
The asterisks represent *Pofut2* mutants as determined by PCR genotyping. E9 and E10 appeared normal, but was not confirmed by PCR since the wild-type, *LoxP,* and *Floxed* alleles did not work for these embryos. No Cre genotyping was performed.

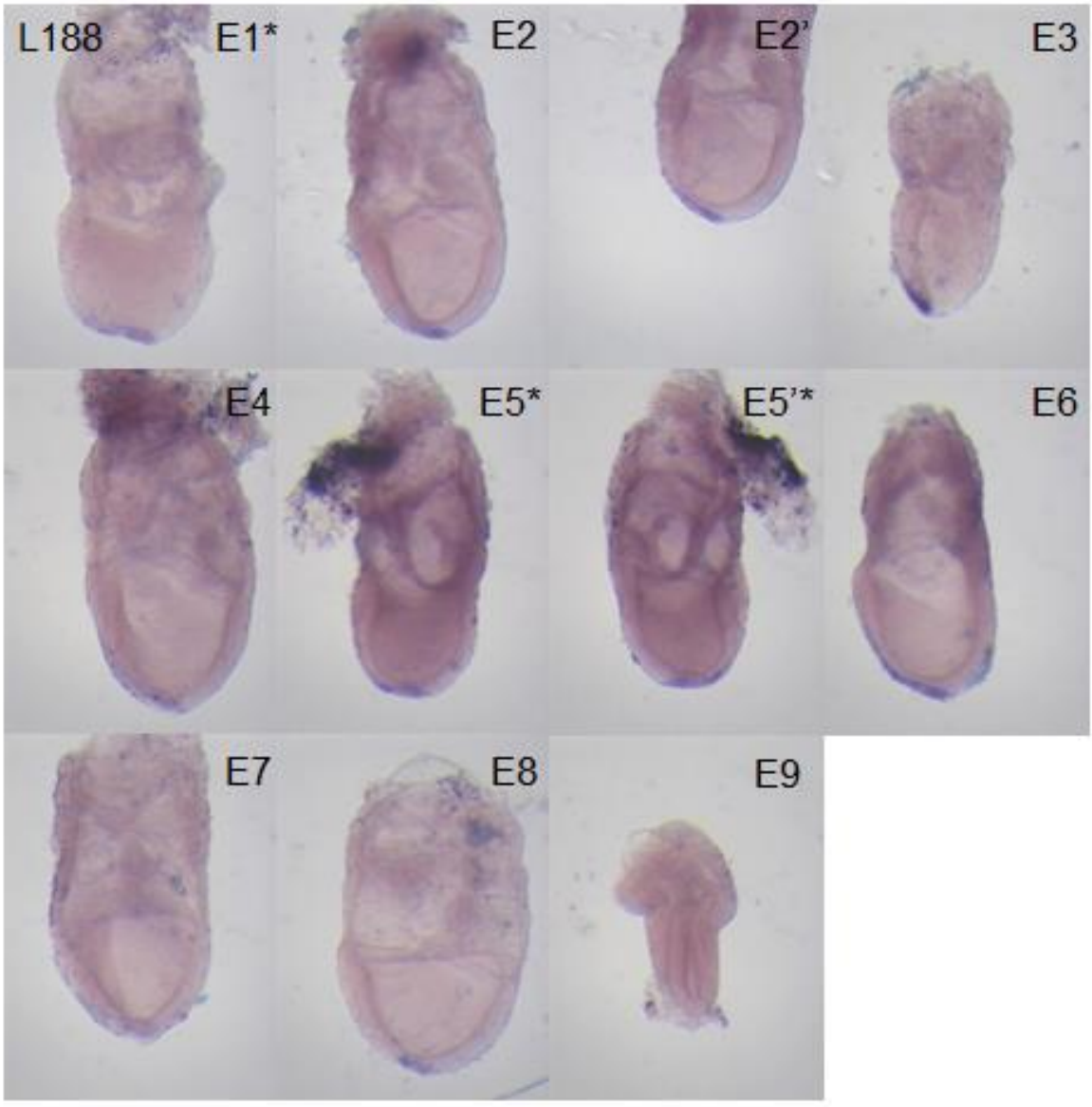

Supplementary Figure 18: *Foxa2 in situ* of *Pofut2 Sox2::Cre* Cross L188 at late E 7.5.
The asterisks represent *Pofut2* mutants as determined by morphology. PCR genotyping was unsuccessful in this litter.

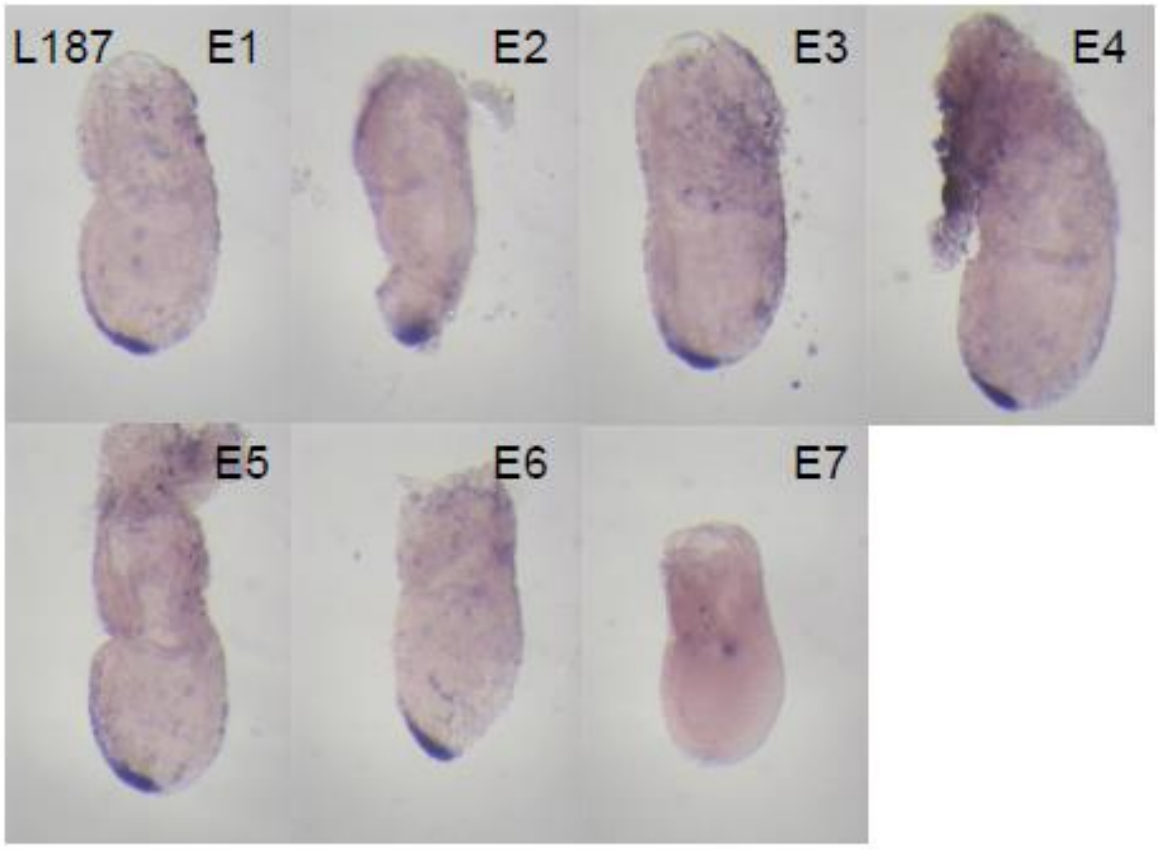

Supplementary Figure 19: *Foxa2 in situ* of *Pofut2 Sox2::Cre* Conditional Cross L187 at E 7.5.
There were no *Pofut2* mutants determined by morphology. PCR genotyping was unsuccessful in this litter.